

THE I.I. MECHNIKOV ODESSA NATIONAL UNIVERSITY  
The manuscript

Saidov Tamerlan Adamovich

UDC 524.83: 531.51: 530.145

THE COMPACTIFICATION PROBLEMS OF ADDITIONAL DIMENSIONS  
IN MULTIDIMENSIONAL COSMOLOGICAL THEORIES

01.04.02 - theoretical physics

The PhD thesis for  
physical and mathematical science

Scientific adviser  
Zhuk Alexander Ivanovich  
Dr. of phys.-math. sci., Professor

Odessa – 2011

You can't look forward with head down.

A.A. Cron

# CONTENT

<b>LIST OF ABBREVIATIONS</b>	<b>4</b>
<b>INTRODUCTION</b>	<b>5</b>
<b>CHAPTER 1. LITERATURE OVERVIEW</b>	<b>10</b>
<b>CHAPTER 2. ASYMPTOTICALLY AdS NONLINEAR GRAVITATIONAL MODELS</b>	<b>14</b>
2.1. General setup . . . . .	14
2.2. Stabilization of internal dimensions . . . . .	16
2.3. $R^{-1}$ model . . . . .	21
2.4. $R^2 + R^4$ model . . . . .	23
2.5. Case $D = 8$ - analytical solution . . . . .	28
<b>CHAPTER 3. MULTIDIMENSIONAL NONLINEAR MODELS WITH FORMS</b>	<b>34</b>
3.1. General equations . . . . .	35
3.2. $R^{-1}$ model with forms . . . . .	38
3.3. Case $\Lambda_{eff} = 0$ . . . . .	40
3.4. Decoupling of excitations: $d_1 = D_0$ . . . . .	44
3.5. Cosmic acceleration and domain walls . . . . .	47
<b>CHAPTER 4. INFLATION IN MULTIDIMENSIONAL COSMOLOGICAL MODELS</b>	<b>55</b>
4.1. Linear model . . . . .	55

4.2. Quadratic model . . . . .	60
4.3. Quartic model . . . . .	68
4.4. Bouncing inflation in $R^2 + R^4$ model . . . . .	80
4.4.1. The fitting procedure . . . . .	81
4.4.2. Dynamics of the Universe and scalaron in $R^2 + R^4$ model . .	84
4.4.3. Properties of the potential $U(\theta)$ . . . . .	87
4.4.4. Dynamical behavior of the Universe and field $\theta$ . . . . .	91
4.4.5. Branching points $\theta = \pi, 2\pi$ . . . . .	92
4.4.6. Monotonic points $\theta = 0, 3\pi$ . . . . .	94
<b>CONCLUSION</b>	<b>100</b>
<b>APPENDIXES</b>	<b>103</b>
Appendix 1. The critical dimensions in $f(\bar{R})$ theories . . . . .	103
Appendix 2. On the particular properties of potential $U_{eff}$ . . . . .	105
Appendix 3. Multi-component scalar field model . . . . .	106
Appendix 4. Bouncing inflation in the Brans-Dicke frame . . . . .	109
<b>LITERATURE</b>	<b>111</b>
<b>ACKNOWLEDGMENT</b>	<b>124</b>
<b>CURRICULUM VITAE</b>	<b>125</b>

## LIST OF ABBREVIATIONS

**ADD-model** – ADditional Dimensions model (or large extra dimensions model);

**AdS** – Anti de Sitter;

**BBN** – Big Bang Nucleosynthesis;

**$\Lambda$ CDM** – Cold Dark Matter with Lambda-term;

**CMB** – Cosmic Microwave Background;

**ETG** – Extended Theory of Gravitation;

**GR** – General Relativity;

**KK** – Kaluza-Klein;

**MCM** – Multidimensional Cosmological Model.

## INTRODUCTION

Latest observation of Ia type supernovas and CMB yields to following composition of the Universe: 4% of baryonic matter, 20% of dark matter and 76% of dark energy. The term "dark matter" is implemented for the unknown matter, which has an ability for clustering, but was not yet detected in lab-conditions. The "dark energy" is the energy not been detected yet, but also unable for clustering, as common energy does.

Most probably, the dark energy is responsible for the value of the cosmological constant. Recent experiments indicate the value of the cosmological constant to be too small if originated only by vacuum energy of common matter. This brings some difficulties for developing of corresponding theories. A few ways for interpretation of presents for the cosmological constant are known. Some of those are dynamical alternatives of dark energy.

In this Thesis the attention is focused on  $f(\bar{R})$  theory. This kind of gravitational theory is the result of the lagrangian generalization in the Hilbert-Einstein action. On the base of this theory a study will be undertaken on the problem of the effective cosmological constant, accelerated expansion of the Universe and the compactification (non-observation) of additional dimensions.

### **Topicality of the subject.**

Multidimensionality of our Universe is one of the most intriguing assumption in modern physics. It follows naturally from theories unifying different fundamental interactions with gravity, e.g. M/string theory [1, 2]. The idea has received a great deal of renewed attention over the last few years. However, it also brings a row of additional questions.

According to observations the internal space should be static or nearly static at least from the time of primordial nucleosynthesis, otherwise the fundamental physical constants would vary. This means that at the present

evolutionary stage of the Universe there are two possibilities: slow variation or compactification of internal space scale parameters [3].

in many recent studies the problem of extra dimensions stabilization was studied for so-called ADD (see e.g., Refs. [4–11]). Under these approaches a massive scalar fields (gravitons or radions) of external space-time can be presented as conformal excitations.

In above mentioned works it was assumed that multidimensional action to be linear with respect to curvature. Although as follows from string theory, the gravity action needs to be extended to nonlinear one. In order to investigate effects of nonlinearity, in this Thesis a multidimensional Lagrangian will be studied, having the form  $L = f(\bar{R})$ , where  $f(\bar{R})$  is an arbitrary smooth function of the scalar curvature.

### **Connection of the Thesis with scientific programs, plans and projects.**

The study under this Thesis was undertaken as part of the budget project of Odessa National Mechnikov University #519 "Compactification of space-time in quantum cosmology".

### **The target and the task of the study.**

The task of this study is an investigation of diverse non-linear cosmological models with respect to condition of additional dimensions compactification and an analysis of additional dimensions effect on the evolution of the Universe.

For that, several surveys have to be implemented: an analysis of non-linearity influence on the effective potential in the equivalent theory; capability of extrema for these potentials as result of additional dimensions non-observability condition. Stabilization and compactification of additional dimensions and their consistency with observations.

Hence, the attention is accumulated on the possibility to achieve models, in which external space (our 4D space-time) behaves as being observed Universe and internal space is stabilized and compactified on the Plank scales. These kind of models allow to build a bridge between observations, multi-

dimensionality and evolution of the Universe, proving by this the principal possibility for existence of additional dimensions.

### **The scientific novelty of obtained results.**

The multidimensional models of type  $\bar{R}^2 + \bar{R}^4$  for pure geometric action and of  $\bar{R}^{-1}$  with forms are studied for stabilization and compactification of additional dimensions.

It is shown, that for non-linearity of type  $\bar{R}^{-1}$  in multidimensional case with forms, the stabilization of internal spaces is independent on signatures of internal space curvature, multidimensional and effective cosmological constants. Moreover, effective cosmological constant may satisfy to observed densities of dark energy by applying fine tuning. First time for this kind of model, the capability for stable compactification of additional dimensions and accelerated expansion of the Universe is shown. When in case of pure geometrical model of  $\bar{R}^{-1}$  this two phenomena simultaneously are not obtainable.

The analysis of inflation is undertaken for linear, quadratic, quartic models with forms and for  $\bar{R}^2 + \bar{R}^4$  model with pure gravitational action.

A new type of inflation is found for  $\bar{R}^2 + \bar{R}^4$  model, called as bouncing inflation. For this type of inflation there is no need for original potential to have a minimum or to check the slowroll conditions. A necessary condition is the existence of the branching points. It is shown that this inflation takes place both in the Einstein and Brans-Dicke frames.

### **Practical value of obtained results.**

The obtained results have fundamental and theoretical value, giving possibility for assay of the Universe evolution, taking into account presence of additional dimensions for diverse non-linear models either pure gravitational or with forms. The parameters values obtained in the Thesis may become an object for further study and justification in experiments.

### **Approbation of the Thesis results.**

The main results of the study, present in the Thesis, were reported on



following conferences:

1. International conference "QUARQS 2008", May 23-26, Ser.-Pasad, Russia;
2. The 8-th G. Gamow Odessa International Astronomical Summer School, Astronomy and beyond: Astrophysics, Radio astronomy, Cosmology and Astrobiology, August 1-5, 2006, Odessa, Ukraine;
3. The 6-th G. Gamow Odessa International Astronomical Summer School, Astronomy and beyond: Astrophysics, Radio astronomy, Cosmology and Astrobiology, August 1-5, 2006, Odessa, Ukraine;
4. VI International Conference: Relativistic Astrophysics, Gravitation and Cosmology, May 24-26 2006, Kyiv, Ukraine;
5. Kyiv High Energy Astrophysics Semester (by ISDC, CERN), April 17 - May 12, 2006, Kiyv, Ukraine;
6. III International Symposium Fundamental Problems in Modern Quantum Theories and Experiments, September 2005, Kiyv-Sevastopol, Ukraine.

### **Publications.**

The main results of the study, present in the Thesis, were explained in following publications:

1. Saidov T.  $1/R$  multidimensional gravity with form-fields: Stabilization of extra dimensions, cosmic acceleration, and domain walls / Saidov T., Zhuk. A. // Phys. Rev. D. – 2007. – V. 75. – 084037, 10 p.
2. Saidov T. AdS Nonlinear Curvature-Squared and Curvature-Quartic Multidimensional ( $D=8$ ) Gravitational Models with Stabilized Extra Dimensions / Saidov T., Zhuk. A. // Gravitation and Cosmology. – 2006. – V. 12. – P. 253–261.
3. Saidov T. A non linear multidimensional gravitational model  $R + R^{-1}$  with form fields and stabilized extra dimensions / Saidov T., Zhuk. A. // Astronomical & Astrophysical Transactions. – 2006. – V. 25. – P. 447–453.
4. Saidov T. Problem of inflation in nonlinear multidimensional cosmological models / Saidov T., Zhuk. A. // Phys. Rev. D. – 2009. – V. 79. – 024025, 18 p.

5. Saidov T. Bouncing inflation in a nonlinear  $R^2 + R^4$  gravitational model  
/ Saidov T., Zhuk. A. // Phys. Rev. D. – 2010. – V. 81. – 124002, 13 p.

# CHAPTER 1

## LITERATURE OVERVIEW

The currently observed accelerated expansion of the Universe suggests that cosmic flow dynamics is dominated by some unknown form of dark energy characterized by a large negative pressure [12]. Most recent observations of CMB and Ia supernovas indicates that Universe consists of: 76% of dark energy, 20% of dark matter and 4% of baryonic matter [13–16]. Many approaches are known for distinguishing of dark matter and dark energy. Usually it is assumed that dark energy despite of dark matter is incapable for clustering and satisfies for Strong Energy Condition [17, 18]. Due to dark energy dominates over matter, it is responsible for late-time acceleration of the Universe (i.e. determines the value of effective cosmological constant), following after early-time acceleration as predicted with inflation paradigm [19–21]. In between these two stages, the period of decelerated expansion is needed to provide eras of radiation domination for BBN and matter domination for formation of Universe structure

As general approach, the standard Einstein’s General Relativity (GR) is used as paradigm (foundation) for developing of new theories, called as Extended Theories of Gravity (ETG). This allows to keep successful features of GR and apply extensions and corrections to Einstein’s theory. Usually by adding higher order curvature invariants and/or minimally or non-minimally coupled scalar fields to the dynamics; these corrections emerge from the effective action of quantum gravity [12, 22].

Among many, the simplest theory capable more or less to describe experimental data is so-called  $\Lambda$ CDM model. It gives appropriate qualitative picture of the observed Universe, but do not explain the inflation. Also, in different models well known problem of the cosmological constant magnitude arises being higher in 120 orders of magnitude than observed one [23].

As next step for modification of GR, one may apply Mach's principle, which states that the local inertial frame is determined by the average motion of distant astronomical objects [24]. This means that the gravitational coupling could be determined by the distant distribution of matter, and it can be scale-dependent and related to some scalar field. As a consequence, the concept of "inertia" and the Equivalence Principle have to be revised. Brans-Dicke theory [25] constituted the first consistent and complete theory alternative to Einstein's GR. Brans-Dicke theory incorporates a variable gravitational coupling strength whose dynamics are governed by a scalar field non-minimally coupled to the geometry, which implements Mach's principle in the gravitational theory [12, 25–27].

Nonlinear ETG models may arise either due to quantum fluctuations of matter fields including gravity [28], or as a result of compactification of extra spatial dimensions [29]. Compared, e.g., to others higher-order gravity theories,  $f(\bar{R})$  theories are free of ghosts and of Ostrogradski instabilities [30]. Recently, it was realized that these models can also explain the late time acceleration of the Universe. This fact resulted in a new wave of papers devoted to this topic (see e.g., recent reviews [12, 31, 32]).

Another intriguing assumption in modern physics is the multidimensionality of our Universe. It follows from theories which unify different fundamental interactions with gravity, such as M or string theory [1, 2], and which have their most consistent formulation in spacetimes with more than four dimensions. Thus, multidimensional cosmological models have received a great deal of attention over the last years.

Stabilization of additional dimensions near their present day values (dilation/geometrical moduli stabilization) is one of the main problems for any multidimensional theory because a dynamical behavior of the internal spaces results in a variation of the fundamental physical constants. Observations show that internal spaces should be static or nearly static at least from the time of recombination (in some papers arguments are given in favor of the assumption that variations of the fundamental constants are absent from the time of primordial nucleosynthesis [33]). In other words, from this time

the compactification scale of the internal space should either be stabilized and trapped at the minimum of some effective potential, or it should be slowly varying (similar to the slowly varying cosmological constant in the quintessence scenario). In both cases, small fluctuations over stabilized or slowly varying compactification scales (conformal scales/geometrical moduli) are possible.

Stabilization of extra dimensions (moduli stabilization) in models with large extra dimensions (ADD-type models) has been considered in a number of papers (see e.g., Refs. [4, 11]). In the corresponding approaches, a product topology of the  $(4 + D')$ -dimensional bulk spacetime was constructed from Einstein spaces with scale (warp) factors depending only on the coordinates of the external 4-dimensional component. As a consequence, the conformal excitations had the form of massive scalar fields living in the external spacetime. Within the framework of multidimensional cosmological models (MCM) such excitations were investigated in [34, 35] where they were called gravitational excitons. Later, since the ADD compactification approach these geometrical moduli excitations are known as radions [4, 6].

Most of the aforementioned papers are devoted to the stabilization of large extra dimensions in theories with a linear multidimensional gravitational action. String theory suggests that the usual linear Einstein-Hilbert action should be extended with higher order nonlinear curvature terms. In the papers [36, 37] a simplified model is considered with multidimensional Lagrangian of the form  $L = f(\bar{R})$ , where  $f(\bar{R})$  is an arbitrary smooth function of the scalar curvature. Without connection to stabilization of the extra-dimensions, such models (4-dimensional as well as multidimensional ones) were considered e.g. in Refs. [38–46]. There, it was shown that the nonlinear models are equivalent to models with linear gravitational action plus a minimally coupled scalar field with self-interaction potential. Similar approach was elaborated in Refs. [47] where the main attention was paid to a possibility of the late time acceleration of the Universe due to the nonlinearity of the model.

The most simple, and, consequently, the most studied models are polyno-

mials of  $\bar{R}$ :  $f(\bar{R}) = \sum_{n=0}^k C_n \bar{R}^n$  ( $k > 1$ ), e.g., quadratic  $\bar{R} + \bar{R}^2$  and quartic  $\bar{R} + \bar{R}^4$  ones. Active investigation of these models, which started in 80-th years of the last century [48–50], continues up to now [51, 52]. Obviously, the correction terms (to the Einstein action) with  $n > 1$  give the main contribution in the case of large  $\bar{R}$ , e.g., in the early stages of the Universe evolution. As it was shown first in [53] for the quadratic model, such modification of gravity results in early inflation. From the other hand, function  $f(\bar{R})$  may also contain negative degrees of  $\bar{R}$ . For example, the simplest model is  $\bar{R} + \bar{R}^{-1}$ . In this case the correction term plays the main role for small  $\bar{R}$ , e.g., at the late stage of the Universe evolution (see e.g. [37, 54] and numerous references therein). Such modification of gravity may result in the late-time acceleration of our Universe [55]. Nonlinear models with polynomial as well as  $\bar{R}^{-1}$ -type correction terms have also been generalized to the multidimensional case (see e.g., [37, 54, 56–61]).

In this Thesis several models of  $f(\bar{R})$ -theory are analyzed for pure gravitational case in chapter 2, and with forms in chapter 3, as well as inflation possibility is studied in chapter 4.

## CHAPTER 2

### ASYMPTOTICALLY AdS NONLINEAR GRAVITATIONAL MODELS

In this chapter the non-linear gravitational models with curvatures of type  $\bar{R}^{-1}$  and  $\bar{R}^2 + \bar{R}^4$  are studied. It is shown that for particular values of parameters, the stabilization and compactification of additional dimensions is achievable with negative constant curvature of internal space. In this case the 4-dimensional effective cosmological constant becomes negative. As result homogenous and isotropic external time-space appears to be  $\text{AdS}_4$ . The correlation between  $D$ -dimensional and 4-dimensional fundamental masses imposes restrictions on the parameters in the models.

#### 2.1. General setup

Let us consider a  $D = (4 + D')$ -dimensional nonlinear pure gravitational theory with action functional

$$S = \frac{1}{2\kappa_D^2} \int_M d^D x \sqrt{|\bar{g}|} f(\bar{R}) , \quad (2.1)$$

where  $f(\bar{R})$  is an arbitrary smooth function with mass dimension  $\mathcal{O}(m^2)$  ( $m$  has the unit of mass) of a scalar curvature  $\bar{R} = R[\bar{g}]$  constructed from the  $D$ -dimensional metric  $\bar{g}_{ab}$  ( $a, b = 1, \dots, D$ ).  $D'$  is the number of extra dimensions and  $\kappa_D^2$  denotes the  $D$ -dimensional gravitational constant which is connected with the fundamental mass scale  $M_{*(4+D')}$  and the surface area  $S_{D-1} = 2\pi^{(D-1)/2}/\Gamma[(D-1)/2]$  of a unit sphere in  $D-1$  dimensions by the relation [62]

$$\kappa_D^2 = 2S_{D-1}/M_{*(4+D')}^{2+D'} . \quad (2.2)$$

Before endowing the metric of the pure gravity theory (2.1) with explicit structure, let us recall that this  $\bar{R}$ -nonlinear theory is equivalent to a theory

which is linear in another scalar curvature  $R$  but which contains an additional self-interacting scalar field. According to standard techniques [38–46, 50], the corresponding  $R$ –linear theory has the action functional:

$$S = \frac{1}{2\kappa_D^2} \int_M d^D x \sqrt{|g|} [R[g] - g^{ab} \phi_{,a} \phi_{,b} - 2U(\phi)] , \quad (2.3)$$

where

$$f'(\bar{R}) = \frac{df}{d\bar{R}} := e^{A\phi} > 0 , \quad A := \sqrt{\frac{D-2}{D-1}} , \quad (2.4)$$

and where the self-interaction potential  $U(\phi)$  of the scalar field  $\phi$  is given by

$$\begin{aligned} U(\phi) &= \frac{1}{2} (f')^{-D/(D-2)} [\bar{R} f' - f] , \\ &= \frac{1}{2} e^{-B\phi} [\bar{R}(\phi) e^{A\phi} - f(\bar{R}(\phi))] , \quad B := \frac{D}{\sqrt{(D-2)(D-1)}} . \end{aligned} \quad (2.5)$$

This scalar field  $\phi$  carries the nonlinearity degrees of freedom in  $\bar{R}$  of the original theory, and for brevity will be called the nonlinearity field. The metrics  $g_{ab}$ ,  $\bar{g}_{ab}$  of the two theories (2.1) and (2.3) are conformally connected by the relations

$$g_{ab} = \Omega^2 \bar{g}_{ab} = [f'(\bar{R})]^{2/(D-2)} \bar{g}_{ab} . \quad (2.6)$$

Next, let us assume that the  $D$ -dimensional bulk space-time  $M$  undergoes a spontaneous compactification to a warped product manifold

$$M = M_0 \times M_1 \times \dots \times M_n \quad (2.7)$$

with metric

$$\bar{g} = \bar{g}_{ab}(X) dX^a \otimes dX^b = \bar{g}^{(0)} + \sum_{i=1}^n e^{2\bar{\beta}^i(x)} g^{(i)} . \quad (2.8)$$

The coordinates on the  $(D_0 = d_0 + 1)$ –dimensional manifold  $M_0$  (usually interpreted as our observable  $(D_0 = 4)$ –dimensional Universe) are denoted by  $x$  and the corresponding metric by

$$\bar{g}^{(0)} = \bar{g}_{\mu\nu}^{(0)}(x) dx^\mu \otimes dx^\nu . \quad (2.9)$$

For simplicity, the internal factor manifolds  $M_i$  are chosen as  $d_i$ –dimensional Einstein spaces with metrics  $g^{(i)} = g_{m_i n_i}^{(i)}(y_i) dy_i^{m_i} \otimes dy_i^{n_i}$ , so that the relations

$$R_{m_i n_i} [g^{(i)}] = \lambda^i g_{m_i n_i}^{(i)} , \quad m_i, n_i = 1, \dots, d_i \quad (2.10)$$



and

$$R \left[ g^{(i)} \right] = \lambda^i d_i \equiv R_i \quad (2.11)$$

hold. The specific metric ansatz (2.8) leads to a scalar curvature  $\bar{R}$  which depends only on the coordinates  $x$  of the external space:  $\bar{R}[\bar{g}] = \bar{R}(x)$ . Correspondingly, also the nonlinearity field  $\phi$  depends on  $x$  only:  $\phi = \phi(x)$ .

Passing from the  $\bar{R}$ -nonlinear theory (2.1) to the equivalent  $R$ -linear theory (2.3) the metric (2.8) undergoes the conformal transformation  $\bar{g} \mapsto g$  [see relation (2.6)]

$$g = \Omega^2 \bar{g} = \left( e^{A\phi} \right)^{2/(D-2)} \bar{g} := g^{(0)} + \sum_{i=1}^n e^{2\beta^i(x)} g^{(i)} \quad (2.12)$$

with

$$g_{\mu\nu}^{(0)} := \left( e^{A\phi} \right)^{2/(D-2)} \bar{g}_{\mu\nu}^{(0)}, \quad \beta^i := \bar{\beta}^i + \frac{A}{D-2} \phi. \quad (2.13)$$

## 2.2. Stabilization of internal dimensions

The main subject of subsequent considerations will be the stabilization of the internal space components. A strong argument in favor of stabilized or almost stabilized internal space scale factors  $\bar{\beta}^i(x)$ , at the present evolution stage of the Universe, is given by the intimate relation between variations of these scale factors and those of the fine-structure constant  $\alpha$  [63]. The strong restrictions on  $\alpha$ -variations in the currently observable part of the Universe [64–67] imply a correspondingly strong restriction on these scale factor variations [63]. For this reason, the derivation of criteria ensuring a freezing stabilization of the scale factors will be performed below.

In Ref. [35] it was shown that for models with a warped product structure (2.8) of the bulk spacetime  $M$  and a minimally coupled scalar field living on this spacetime, the stabilization of the internal space components requires a simultaneous freezing of the scalar field. Here a similar situation with simultaneous freezing stabilization of the scale factors  $\beta^i(x)$  and the nonlinearity field  $\phi(x)$  is expected. According to (2.13), this will also imply a stabilization of the scale factors  $\bar{\beta}^i(x)$  of the original nonlinear model.

In general, the model will allow for several stable scale factor configurations (minima in the landscape over the space of volume moduli). Let us choose one of them<sup>1</sup>, denote the corresponding scale factors as  $\beta_0^i$ , and work further on with the deviations

$$\hat{\beta}^i(x) = \beta^i(x) - \beta_0^i \quad (2.14)$$

as the dynamical fields. After dimensional reduction of the action functional (2.3) one passes from the intermediate Brans-Dicke frame to the Einstein frame via a conformal transformation

$$g_{\mu\nu}^{(0)} = \hat{\Omega}^2 \hat{g}_{\mu\nu}^{(0)} = \left( \prod_{i=1}^n e^{d_i \hat{\beta}^i} \right)^{-2/(D_0-2)} \hat{g}_{\mu\nu}^{(0)} \quad (2.15)$$

with respect to the scale factor deviations  $\hat{\beta}^i(x)$  [36, 37]. As result the following action is achieved

$$S = \frac{1}{2\kappa_{D_0}^2} \int_{M_0} d^{D_0}x \sqrt{|\hat{g}^{(0)}|} \left\{ \hat{R} [\hat{g}^{(0)}] - \bar{G}_{ij} \hat{g}^{(0)\mu\nu} \partial_\mu \hat{\beta}^i \partial_\nu \hat{\beta}^j - \hat{g}^{(0)\mu\nu} \partial_\mu \phi \partial_\nu \phi - 2U_{eff} \right\}, \quad (2.16)$$

which contains the scale factor offsets  $\beta_0^i$  through the total internal space volume

$$V_{D'} \equiv V_I \times v_0 \equiv \prod_{i=1}^n \int_{M_i} d^{d_i}y \sqrt{|g^{(i)}|} \times \prod_{i=1}^n e^{d_i \beta_0^i} \quad (2.17)$$

in the definition of the effective gravitational constant  $\kappa_{D_0}^2$  of the dimensionally reduced theory

$$\kappa_{(D_0=4)}^2 = \kappa_D^2 / V_{D'} = 8\pi / M_4^2 \implies M_4^2 = \frac{4\pi}{S_{D-1}} V_{D'} M_{*(4+D')}^{2+D'}. \quad (2.18)$$

Obviously, at the present evolution stage of the Universe, the internal space components should have a total volume which would yield a four-dimensional mass scale of order of the Planck mass  $M_{(4)} = M_{Pl}$ . The tensor components of the midisuperspace metric (target space metric on  $\mathbb{R}_T^n$ ) reads:  $\bar{G}_{ij} = d_i \delta_{ij} +$

---

<sup>1</sup>Although the toy model ansatz (2.1) is highly oversimplified and far from a realistic model, one can roughly think of the chosen minimum, e.g., as that one which is expected to correspond to current evolution stage of our observable Universe.

$d_i d_j / (D_0 - 2)$ , where  $i, j = (1, \dots, n)$ , see [68, 69]. The effective potential has the explicit form

$$U_{eff}(\hat{\beta}, \phi) = \left( \prod_{i=1}^n e^{d_i \hat{\beta}^i} \right)^{-\frac{2}{D_0-2}} \left[ -\frac{1}{2} \sum_{i=1}^n \hat{R}_i e^{-2\hat{\beta}^i} + U(\phi) \right], \quad (2.19)$$

where abbreviated

$$\hat{R}_i := R_i \exp(-2\beta_0^i). \quad (2.20)$$

A freezing stabilization of the internal spaces will be achieved if the effective potential has at least one minimum with respect to the fields  $\hat{\beta}^i(x)$ . Assuming, without loss of generality, that one of the minima is located at  $\beta^i = \beta_0^i \Rightarrow \hat{\beta}^i = 0$ , the extremum condition reads:

$$\left. \frac{\partial U_{eff}}{\partial \hat{\beta}^i} \right|_{\hat{\beta}=0} = 0 \implies \hat{R}_i = \frac{d_i}{D_0 - 2} \left( -\sum_{j=1}^n \hat{R}_j + 2U(\phi) \right). \quad (2.21)$$

From its structure (a constant on the l.h.s. and a dynamical function of  $\phi(x)$  on the r.h.s) it follows that a stabilization of the internal space scale factors can only occur when the nonlinearity field  $\phi(x)$  is stabilized as well. In the freezing scenario this will require a minimum with respect to  $\phi$ :

$$\left. \frac{\partial U(\phi)}{\partial \phi} \right|_{\phi_0} = 0 \iff \left. \frac{\partial U_{eff}}{\partial \phi} \right|_{\phi_0} = 0. \quad (2.22)$$

Hence, a stabilization problem is arrived, some of whose general aspects have been analyzed already in Refs. [34–37]. For brevity let us summarize the corresponding essentials as they will be needed for more detailed discussions in the next consideration.

1. Eq. (2.21) implies that the scalar curvatures  $\hat{R}_i$  and with them the compactification scales  $e^{\beta_0^i}$  [see relation (2.20)] of the internal space components are finely tuned

$$\frac{\hat{R}_i}{d_i} = \frac{\hat{R}_j}{d_j}, \quad i, j = 1, \dots, n. \quad (2.23)$$

2. The masses of the normal mode excitations of the internal space scale factors (gravitational excitons/radions) and of the nonlinearity field  $\phi$  near the minimum position are given as [35]:

$$m_1^2 = \dots = m_n^2 = -\frac{4}{D-2}U(\phi_0) = -2\frac{\hat{R}_i}{d_i} > 0, \quad (2.24)$$

$$m_\phi^2 := \left. \frac{d^2 U(\phi)}{d\phi^2} \right|_{\phi_0} > 0. \quad (2.25)$$

3. The value of the effective potential at the minimum plays the role of an effective 4D cosmological constant of the external (our) spacetime  $M_0$ :

$$\Lambda_{eff} := U_{eff} \Big|_{\substack{\hat{\beta}^i=0, \\ \phi=\phi_0}} = \frac{D_0-2}{D-2}U(\phi_0) = \frac{D_0-2}{2}\frac{\hat{R}_i}{d_i}. \quad (2.26)$$

4. Relation (2.26) implies

$$\text{sign } \Lambda_{eff} = \text{sign } U(\phi_0) = \text{sign } R_i. \quad (2.27)$$

Together with condition (2.24) this shows that in a pure geometrical model stable configurations can only exist for internal spaces with negative curvature<sup>2</sup>:

$$R_i < 0 \quad (i = 1, \dots, n). \quad (2.28)$$

Additionally, the effective cosmological constant  $\Lambda_{eff}$  as well as the minimum of the potential  $U(\phi)$  should be negative too:

$$\Lambda_{eff} < 0, \quad U(\phi_0) < 0. \quad (2.29)$$

Plugging the potential  $U(\phi)$  from Eq. (2.5) into the minimum conditions

---

<sup>2</sup>Negative constant curvature spaces  $M_i$  are compact if they have a quotient structure:  $M_i = H^{d_i}/\Gamma_i$ , where  $H^{d_i}$  and  $\Gamma_i$  are hyperbolic spaces and their discrete isometry group, respectively.

(2.22), (2.25) yields with the help of  $\partial_\phi \bar{R} = Af'/f''$  the conditions

$$\begin{aligned} \left. \frac{dU}{d\phi} \right|_{\phi_0} &= \frac{A}{2(D-2)} (f')^{-D/(D-2)} h \Big|_{\phi_0} = 0, \\ h &:= Df - 2\bar{R}f', \quad \implies \quad h(\phi_0) = 0, \end{aligned} \quad (2.30)$$

$$\begin{aligned} \left. \frac{d^2U}{d\phi^2} \right|_{\phi_0} &= \frac{1}{2} A e^{(A-B)\phi_0} [\partial_\phi \bar{R} + (A-B)\bar{R}]_{\phi_0} \\ &= \frac{1}{2(D-1)} (f')^{-2/(D-2)} \frac{1}{f''} \partial_{\bar{R}} h \Big|_{\phi_0} > 0, \end{aligned} \quad (2.31)$$

where the last inequality can be reshaped into the suitable form

$$f'' \partial_{\bar{R}} h|_{\phi_0} = f'' [(D-2)f' - 2\bar{R}f'']_{\phi_0} > 0. \quad (2.32)$$

Furthermore, from Eq. (2.30) follows

$$U(\phi_0) = \frac{D-2}{2D} (f')^{-\frac{2}{D-2}} \bar{R}(\phi_0) \quad (2.33)$$

so that (2.29) leads to the additional restriction

$$\bar{R}(\phi_0) < 0 \quad (2.34)$$

at the extremum.

Thus, to avoid the effective four-dimensional fundamental constant variation, it is necessary to provide the mechanism of the internal spaces stabilization. In these models, the scale factors of the internal spaces play the role of additional scalar fields (geometrical moduli/gravexcitons [34]). To achieve their stabilization, an effective potential should have minima with respect to all scalar fields (gravexcitons and scalaron). Previous analysis (see e.g. [35]) shows that for a model of the form (2.3) the stabilization is possible only for the case of negative minimum of the potential  $U(\phi)$ . According to the definition (2.4), the positive branch of  $f'(\bar{R}) > 0$  will be considered. Although the negative  $f' < 0$  branch can be considered as well (see e.g. Refs. [37, 50, 58]). However, negative values of  $f'(\bar{R})$  result in negative effective gravitational "constant"  $G_{eff} = \kappa_D^2/f'$ . Thus  $f'$  should be positive for the graviton to

carry positive kinetic energy (see e.g., [12]). From action (2.3) the equation of motion of scalaron field  $\phi$  can be obtained in the form:

$$\square\phi - \frac{\partial U}{\partial\phi} = 0. \quad (2.35)$$

Now, let us analyze the internal space stabilization conditions (2.23) - (2.29) and (2.30) - (2.34) on their compatibility with particular scalar curvature nonlinearity  $f(\bar{R})$ .

### 2.3. $R^{-1}$ model

Recently it has been shown in Refs. [70–78] that cosmological models with a nonlinear scalar curvature term of the type  $\bar{R}^{-1}$  can provide a possible explanation of the observed late-time acceleration of our Universe within a pure gravity setup. The equivalent linearized model contains an effective potential with a positive branch which can simulate a transient inflation-like behavior in the sense of an effective dark energy. The corresponding considerations have been performed mainly in four dimensions. Here these analyses are extended to higher dimensional models, assuming that the scalar curvature nonlinearity is of the same form in all dimensions. Starting from a nonlinear coupling of the type:

$$f(\bar{R}) = \bar{R} - \mu/\bar{R}, \quad \mu > 0, \quad (2.36)$$

in front of the  $\bar{R}^{-1}$ -term, the minus sign is chosen, because otherwise the potential  $U(\phi)$  will have no extremum.

With the help of definition (2.4), the scalar curvature  $\bar{R}$  can be expressed in terms of the nonlinearity field  $\phi$  and obtain two real-valued solution branches

$$\bar{R}_{\pm} = \pm\sqrt{\mu} (e^{A\phi} - 1)^{-1/2}, \quad \implies \quad \phi > 0 \quad (2.37)$$

of the quadratic equation  $f'(\bar{R}) = e^{A\phi}$ . The corresponding potentials

$$U_{\pm}(\phi) = \pm\sqrt{\mu} e^{-B\phi} \sqrt{e^{A\phi} - 1} \quad (2.38)$$

---

<sup>8</sup>A discussion of pro and contra of a higher dimensional origin of  $\bar{R}^{-1}$  terms can be found in Ref. [29].

have extrema for curvatures [see Eq. (2.30)]

$$\begin{aligned}\bar{R}_{0,\pm} &= \pm\sqrt{\mu}\sqrt{\frac{D+2}{D-2}} \\ e^{A\phi_0} &= \frac{2B}{2B-A} = \frac{2D}{D+2} > 1 \quad \text{for } D \geq 3\end{aligned}\quad (2.39)$$

and take for these curvatures the values

$$U_{\pm}(\phi_0) = \pm\sqrt{\mu}\sqrt{\frac{D-2}{D+2}} e^{-B\phi_0} = \pm\sqrt{\mu}\sqrt{\frac{D-2}{D+2}} \left(\frac{2D}{D+2}\right)^{-D/(D-2)}. \quad (2.40)$$

The stability defining second derivatives [Eq. (2.31)] at the extrema (2.39),

$$\begin{aligned}\partial_{\phi}^2 U_{\pm}|_{\phi_0} &= \mp\sqrt{\mu}\frac{D}{D-1}\sqrt{\frac{D+2}{D-2}} e^{B\phi_0} \\ &= \mp\sqrt{\mu}\frac{D}{D-1}\sqrt{\frac{D+2}{D-2}} \left(\frac{2D}{D+2}\right)^{-D/(D-2)},\end{aligned}\quad (2.41)$$

show that only the negative curvature branch  $\bar{R}_-$  yields a minimum with stable internal space components. The positive branch has a maximum with  $U_+(\phi_0) > 0$ . According to (2.27) it can provide an effective dark energy contribution with  $\Lambda_{eff} > 0$ , but due to its tachyonic behavior with  $\partial_{\phi}^2 U(\phi_0) < 0$  it cannot give stably frozen internal dimensions. This means that the simplest extension of the four-dimensional purely geometrical  $\bar{R}^{-1}$  setup of Refs. [70–78] to higher dimensions is incompatible with a freezing stabilization of the extra dimensions. A possible circumvention of this behavior could consist in the existence of different nonlinearity types  $f_i(\bar{R}_i)$  in different factor spaces  $M_i$  so that their dynamics can decouple one from the other. This could allow for a freezing of the scale factors of the internal spaces even in the case of a late-time acceleration with  $\Lambda_{eff} > 0$ . Another circumvention could consist in a mechanism which prevents the dynamics of the internal spaces from causing strong variations of the fine-structure constant  $\alpha$ . The question of whether one of these schemes could work within a physically realistic setup remains to be clarified.

Finally, in the minimum of the effective potential  $U_{eff}(\phi, \beta^i)$ , which is provided by the negative curvature branch  $\bar{R}(\phi)$ , one finds excitation masses

for the gravexcitons/radions and the nonlinearity field (see Eqs. (2.24), (2.40) and (2.41)) of order

$$m_1 = \dots = m_n \sim m_\phi \sim \mu^{1/4}. \quad (2.42)$$

For the four-dimensional effective cosmological constant  $\Lambda_{eff}$  defined in (2.26) one obtains in accordance with Eq. (2.40)  $\Lambda_{eff} \sim -\sqrt{\mu}$ .

## Summary

As stability condition the existence of a minimum of the effective potential of the dimensionally reduced theory is assumed, so that a late-time attractor of the system could be expected with freezing stabilization of the extra-dimensional scale factors and the nonlinearity field. It was shown in Refs. [57, 58], that for purely geometrical setups this is only possible for negative scalar curvatures, ( $\bar{R} < 0$ ), independently of the concrete form of the function  $f(\bar{R})$ .

Four-dimensional purely gravitational models with  $\bar{R}^{-1}$  curvature contributions have been proposed recently as possible explanation of the observed late-time acceleration (dark energy) of the Universe [70–78]. It is shown that higher dimensional models with the same  $\bar{R}^{-1}$  scalar curvature nonlinearity reproduce (after dimensional reduction) the two solution branches of the four-dimensional models. But due to their oversimplified structure these models cannot simultaneously provide a late-time acceleration of the external four-dimensional spacetime and a stabilization of the internal space. A late-time acceleration is only possible for one of the solution branches — for that which yields a positive maximum of the potential  $U(\phi)$  of the nonlinearity field. A stabilization of the internal spaces requires a negative minimum of  $U(\phi)$  as it can be induced by the other solution branch.

## 2.4. $R^2 + R^4$ model

In this section let us analyze a model with curvature-quadratic and curvature-quartic correction terms of the type

$$f(\bar{R}) = \bar{R} + \alpha \bar{R}^2 + \gamma \bar{R}^4 - 2\Lambda_D. \quad (2.43)$$



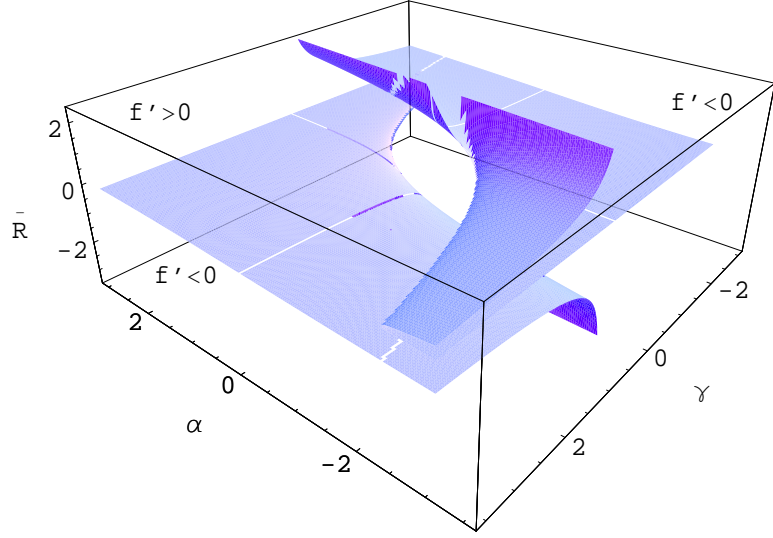


Figure 2.1: The surfaces  $f' = 0$  as a functions  $\bar{R} = \bar{R}(\alpha, \gamma)$  for the model (2.43).

According to eq. (2.4):

$$f' = e^{A\phi} = 1 + 2\alpha\bar{R} + 4\gamma\bar{R}^3. \quad (2.44)$$

The definition (2.4)  $f' = \exp(A\phi)$  clearly indicates that the positive branch  $f' > 0$  is chosen. For the given model (2.43), the surfaces  $f' = 0$  as a functions  $\bar{R} = \bar{R}(\alpha, \gamma)$  are given in Fig. 2.1. As it easily follows from Eq. (2.44), points where all three values  $\bar{R}$ ,  $\gamma$  and  $\alpha$  are positive correspond to the region  $f' > 0$ . Thus, this picture shows that there is one simply connected region  $f' > 0$  and two disconnected regions  $f' < 0$ .

Eq. (2.44) can be rewritten equivalently in the form:

$$\bar{R}^3 + \frac{\alpha}{2\gamma}\bar{R} - \frac{1}{4\gamma}X = 0, \quad (2.45)$$

$$\begin{aligned} X &\equiv e^{A\phi} - 1, & -\infty < \phi < +\infty \\ &\implies & -1 < X < +\infty. \end{aligned} \quad (2.46)$$

Eq. (2.45) has three solutions  $\bar{R}_{1,2,3}$ , where one or three of them are real-valued. Let

$$q := \frac{\alpha}{6\gamma}, \quad r := \frac{1}{8\gamma}X. \quad (2.47)$$

The sign of the discriminant

$$Q := r^2 + q^3 \quad (2.48)$$

defines the number of real solutions:

$$\begin{aligned} Q > 0 &\implies \Im \bar{R}_1 = 0, \quad \Im \bar{R}_{2,3} \neq 0, \\ Q = 0 &\implies \Im \bar{R}_i = 0 \quad \forall i, \quad \bar{R}_1 = \bar{R}_2, \\ Q < 0 &\implies \Im \bar{R}_i = 0 \quad \forall i. \end{aligned} \quad (2.49)$$

Physical scalar curvatures correspond to real solutions  $\bar{R}_i(X)$ . It is the most convenient to consider  $\bar{R}_i = \bar{R}_i(X)$  as solution family depending on the two additional parameters  $(\alpha, \gamma)$ :  $\text{sign}(\alpha) = \text{sign}(\gamma) \implies Q > 0$ ,  $\text{sign}(\alpha) \neq \text{sign}(\gamma) \implies Q \geq 0$ .

For  $Q > 0$  the single real solution  $\bar{R}_1$  is given as

$$\bar{R}_1 = \left[ r + Q^{1/2} \right]^{1/3} + \left[ r - Q^{1/2} \right]^{1/3} := z_1 + z_2, \quad (2.50)$$

where  $z_{1,2}$  is defined in the form:

$$\begin{aligned} z_{1,2}^3 &= p e^{\pm \theta}, \quad p^2 = r^2 - Q = -q^3, \\ \cosh(\theta) &= \frac{r}{\sqrt{-q^3}}. \end{aligned} \quad (2.51)$$

Taking into account eq. (2.47), the function  $X$  reads

$$X(\theta) = 8\gamma \sqrt{-q^3} \cosh(\theta). \quad (2.52)$$

The three real solutions  $\bar{R}_{1,2,3}(X)$  for  $Q < 0$  are given as

$$\begin{aligned} \bar{R}_1 &= s_1 + s_2, \\ \bar{R}_2 &= \frac{1}{2}(-1 + i\sqrt{3})s_1 + \frac{1}{2}(-1 - i\sqrt{3})s_2 \\ &= e^{i\frac{2\pi}{3}}s_1 + e^{-i\frac{2\pi}{3}}s_2, \\ \bar{R}_3 &= \frac{1}{2}(-1 - i\sqrt{3})s_1 + \frac{1}{2}(-1 + i\sqrt{3})s_2 \\ &= e^{-i\frac{2\pi}{3}}s_1 + e^{i\frac{2\pi}{3}}s_2, \end{aligned} \quad (2.53)$$

where one can fix the Riemann sheet of  $Q^{1/2}$  by setting in the definitions of  $s_{1,2}$

$$s_{1,2} := \left[ r \pm i|Q|^{1/2} \right]^{1/3}. \quad (2.54)$$

A simple Mathematica calculation gives for Vieta's relations from (2.53)

$$\begin{aligned}\bar{R}_1 + \bar{R}_2 + \bar{R}_3 &= 0, \\ \bar{R}_1\bar{R}_2 + \bar{R}_1\bar{R}_3 + \bar{R}_2\bar{R}_3 &= -3s_1s_2 = 3q, \\ \bar{R}_1\bar{R}_2\bar{R}_3 &= s_1^3 + s_2^3 = 2r.\end{aligned}\tag{2.55}$$

In order to work with explicitly real-valued  $\bar{R}_i$  let us rewrite  $s_{1,2}$  from (2.54) as follows

$$\begin{aligned}s_{1,2} &= |b|^{1/3}e^{\pm i\vartheta/3}, \\ |b|^2 &= r^2 + |Q| = r^2 - Q = -q^3, \\ \cos(\vartheta) &= \frac{r}{|b|} = \frac{r}{\sqrt{-q^3}}.\end{aligned}\tag{2.56}$$

and get via (2.53)

$$\begin{aligned}\bar{R}_1 &= s_1 + s_2 = 2|b|^{1/3}\cos(\vartheta/3), \\ \bar{R}_2 &= e^{i\frac{2\pi}{3}}s_1 + e^{-i\frac{2\pi}{3}}s_2 = 2|b|^{1/3}\cos(\vartheta/3 + 2\pi/3), \\ \bar{R}_3 &= e^{-i\frac{2\pi}{3}}s_1 + e^{i\frac{2\pi}{3}}s_2 = 2|b|^{1/3}\cos(\vartheta/3 - 2\pi/3)\end{aligned}\tag{2.57}$$

or

$$\begin{aligned}\bar{R}_k &= 2|b|^{1/3}\cos\left(\frac{\vartheta + 2\pi k}{3}\right) \\ &= 2\sqrt{-q}\cos\left(\frac{\vartheta + 2\pi k}{3}\right), \quad k = -1, 0, 1.\end{aligned}\tag{2.58}$$

In order to understand the qualitative behavior of these three real-valued solutions as part of the global solution picture let us first note that, according to (2.45), one may interpret  $X$  as single-valued function

$$X(\bar{R}) = 4\gamma\bar{R}^3 + 2\alpha\bar{R}\tag{2.59}$$

and look what is happening when  $(\alpha, \gamma)$  are changed. Obviously, the inverse function  $\bar{R}(X)$  has three real-valued branches when  $X(\bar{R})$  is not a monotonic function but instead has a minimum and a maximum, i.e. when

$$\partial_{\bar{R}}X := X' = 12\gamma\bar{R}^2 + 2\alpha = 0 \implies \bar{R}^2 = -\frac{\alpha}{6\gamma}\tag{2.60}$$

has two real solutions  $\bar{R}_\pm = \pm\sqrt{-\alpha/(6\gamma)}$  and corresponding extrema<sup>3</sup>

$$X(\bar{R}_\pm) = \frac{4}{3}\alpha\bar{R}_\pm. \quad (2.61)$$

It should hold  $\text{sign}(\alpha) \neq \text{sign}(\gamma)$  in this case, so that one find

$$\begin{aligned} \gamma > 0, \alpha < 0 : \quad & X_{max} = X(\bar{R}_-), \quad X_{min} = X(\bar{R}_+) \\ \gamma < 0, \alpha > 0 : \quad & X_{max} = X(\bar{R}_+), \quad X_{min} = X(\bar{R}_-). \end{aligned} \quad (2.62)$$

The transition from the three-real-solution regime to the one-real-solution regime occurs when maximum and minimum coalesce at the inflection point

$$\bar{R}_+ = \bar{R}_- = 0 \implies \alpha = 0, \quad \gamma \neq 0. \quad (2.63)$$

(The non-degenerate case  $\gamma \neq 0$  is considered here. Models with  $\gamma = 0$  are degenerated ones and are characterized by quadratic scalar curvature terms only.) Due to  $-1 \leq X \leq +\infty$  the limit  $X \rightarrow +\infty$  where in leading approximation may be considered:

$$4\gamma\bar{R}^3 \approx X \rightarrow +\infty \quad (2.64)$$

so that

$$\bar{R}(X \rightarrow \infty) \rightarrow \text{sign}(\gamma) \times \infty. \quad (2.65)$$

Leaving the restriction  $X \geq -1$  for a moment aside, it was found that for product  $\alpha\gamma < 0$  there exist three real solution branches  $\bar{\mathcal{R}}_{1,2,3}$ :

$$\begin{aligned} \gamma > 0 : \quad & -\infty \leq \bar{\mathcal{R}}_1 \leq \bar{R}_-, \quad -\infty \leq X \leq X_{max}, \\ & \bar{R}_- \leq \bar{\mathcal{R}}_2 \leq \bar{R}_+, \quad X_{max} \geq X \geq X_{min}, \\ & \bar{R}_+ \leq \bar{\mathcal{R}}_3 \leq +\infty, \quad X_{min} \leq X \leq +\infty, \\ \gamma < 0 : \quad & -\infty \leq \bar{\mathcal{R}}_1 \leq \bar{R}_-, \quad +\infty \geq X \geq X_{min}, \\ & \bar{R}_- \leq \bar{\mathcal{R}}_2 \leq \bar{R}_+, \quad X_{min} \leq X \leq X_{max}, \\ & \bar{R}_+ \leq \bar{\mathcal{R}}_3 \leq +\infty, \quad X_{max} \geq X \geq -\infty. \end{aligned} \quad (2.66)$$

---

<sup>3</sup>It is worth of noting that  $f''(\bar{R}_\pm) = X'(\bar{R}_\pm) = 0$ .

It remains for each of these branches to check which of the solutions  $\bar{R}_k$  from (2.58) can be fitted into this scheme. Finally, one will have to set the additional restriction  $X \geq -1$  on the whole picture.

To define the conditions for minima of the effective potential  $U_{eff}$ , first the extremum positions of the potential  $U(\phi)$  is to be obtained. The extremum condition (2.30) for the given particular model (2.43) reads:

$$\gamma \bar{R}_{(0)i}^4 \left( \frac{D}{2} - 4 \right) + \alpha \bar{R}_{(0)i}^2 \left( \frac{D}{2} - 2 \right) + \bar{R}_{(0)i} \left( \frac{D}{2} - 1 \right) - D\Lambda_D = 0, \quad (2.67)$$

## 2.5. Case $D = 8$ - analytical solution

In this part let us investigate the case of positive  $Q(\phi)$  that is equivalent to the condition

$$Q(\phi) > 0 \quad \Rightarrow \quad \text{sign } \alpha = \text{sign } \gamma. \quad (2.68)$$

The case  $\text{sign } \alpha \neq \text{sign } \gamma$  that corresponds to different signatures of the discriminant  $Q$  will be considered in chapter 4.

To define the conditions for minima of the effective potential  $U_{eff}$ , first let us obtain the extremum positions of the potential  $U(\phi)$ . The extremum condition (2.30) for the given particular model (2.43) reads:

$$\bar{R}_{(0)1}^4 \gamma \left( \frac{D}{2} - 4 \right) + \bar{R}_{(0)1}^2 \alpha \left( \frac{D}{2} - 2 \right) + \bar{R}_{(0)1} \left( \frac{D}{2} - 1 \right) - D\Lambda_D = 0, \quad (2.69)$$

where subscript "1" indicates seeking the extremum positions for the solution (2.50). Eq. (2.69) clearly shows that  $D = 8$  is the critical dimension for the model (2.43) in full agreement with the result of the appendix 1 (see (A1.4)). In what follows, that this critical case is investigated here. For  $D = 8$  eq. (2.69) is reduced to a quadratic one

$$\bar{R}_{(0)1}^2 + \frac{3}{2\alpha} \bar{R}_{(0)1} - \frac{4\Lambda_8}{\alpha} = 0; \quad \Lambda_8 \equiv \Lambda_{D=8} \quad (2.70)$$

with the following two roots:

$$\bar{R}_{(0)1}^{(\pm)} = -\frac{3}{4\alpha} \pm \sqrt{\left( \frac{3}{4\alpha} \right)^2 + \frac{4}{\alpha} \Lambda_8}. \quad (2.71)$$

These roots are real if parameters  $\alpha$  and  $\Lambda_8$  satisfy the following condition:

$$\left(\frac{3}{4\alpha}\right)^2 + \frac{4}{\alpha}\Lambda_8 \geq 0. \quad (2.72)$$

If  $\text{sign}(\alpha) = \text{sign}(\Lambda_8)$ , then condition (2.72) is automatically executed, else

$$|\Lambda_8| \leq \frac{9}{64|\alpha|}, \quad \text{sign}(\alpha) \neq \text{sign}(\Lambda_8). \quad (2.73)$$

To insure that roots (2.71) correspond to a minimum value of  $U(\phi)$ , they should satisfy the condition (2.32):

$$f'' [(D-2)f' - 2\bar{R}f'']_{\phi_0} > 0 \iff f''[3 + 4\alpha\bar{R}]_{\phi_0} > 0, \quad (2.74)$$

where

$$f'' = 2\alpha + 12\gamma\bar{R}^2. \quad (2.75)$$

Because for  $Q > 0$  eq. (2.50) is the single real solution of the cubic eq. (2.69), then  $\bar{R} = \bar{R}_1(\phi)$  is a monotonic function of  $\phi$ . Thus, the derivative  $\partial_\phi \bar{R}_1 = Af'/f''$  does not change its sign. Keeping in mind that the  $f' > 0$  branch is considered, the function  $\bar{R}_1(\phi)$  is a monotone increasing one for  $f'' > 0$ . As apparent from eq. (2.50), for increasing  $\bar{R}_1$  one should take  $\gamma > 0$ . In a similar manner, the function  $\bar{R}_1(\phi)$  is a monotone decreasing one for  $f'', \gamma < 0$ . Thus, for the minimum position  $\bar{R}_{(0)1}$ , inequality (2.74) leads to the following conditions (reminding that according to eq. (2.34) the minimum position  $\bar{R}_{(0)1}$  should be negative and according to eq. (2.68)  $\text{sign } \alpha = \text{sign } \gamma$ ):

**I.**  $f'', \gamma, \alpha > 0$  :

$$3 + 4\alpha\bar{R}_{(0)1}^\pm > 0 \iff |R_{(0)1}^\pm| < \frac{3}{4\alpha}. \quad (2.76)$$

**II.**  $f'', \gamma, \alpha < 0$  :

$$3 + 4\alpha\bar{R}_{(0)1}^\pm < 0 \iff -|R_{(0)1}^\pm| > \frac{3}{4|\alpha|}. \quad (2.77)$$

Obviously, inequality (2.77) is impossible and one arrives to the conclusion that the minimum of the effective potential  $U_{eff}$  is absent if  $\text{sign } \alpha = \text{sign } \gamma = -1$ .

Additionally, it can be easily seen that in the case

$$\text{sign } \alpha = \text{sign } \gamma = \text{sign } \Lambda_D = +1 \quad (2.78)$$

the effective potential  $U_{eff}$  has no minima also. This statement follows from the form of the potential  $U(\phi)$  for the model (2.43). According to eq. (2.5),  $U(\phi)$  reads:

$$U(\phi) = (1/2)e^{-B\phi} (\alpha \bar{R}^2 + 3\gamma \bar{R}^4 + 2\Lambda_D) . \quad (2.79)$$

Thus, this potential is always positive for parameters satisfying (2.78) and one arrives to the contradiction with the minimum condition (2.29). Therefore, the investigation carried above indicates that the internal space stable compactification is possible only if the parameters satisfy the following sign relation:

$$\alpha > 0, \gamma > 0, \Lambda_8 < 0 . \quad (2.80)$$

Let us investigate this case in more detail. For this choice of signs of the parameters, it can be easily seen that both extremum values  $\bar{R}_{(0)1}^{(\pm)}$  from eq. (2.71) satisfy the condition (2.34):  $\bar{R}_{(0)1}^{(\pm)} < 0$ . However, the expression

$$f' \left( \bar{R}_{(0)1}^{(\pm)} \right) = 1 + 2\alpha \bar{R}_{(0)1}^{(\pm)} + 4\gamma \bar{R}_{(0)1}^{(\pm)3} = -\frac{1}{2} \pm \sqrt{\frac{9}{4} - 16\alpha|\Lambda_8|} - 4\gamma \left| \bar{R}_{(0)1}^{(\pm)} \right|^3 \quad (2.81)$$

shows that only  $\bar{R}_{(0)1}^{(+)}$  can belong to  $f' > 0$  branch. To make  $f' \left( \bar{R}_{(0)1}^{(+)} \right)$  positive, parameter  $\gamma$  should satisfy the condition

$$\gamma < \frac{-\frac{1}{2} + \sqrt{\frac{9}{4} - 16\alpha|\Lambda_8|}}{4 \left| \bar{R}_{(0)1}^{(+)} \right|^3} . \quad (2.82)$$

As apparent from this equation, parameter  $\gamma$  remains positive if  $\Lambda_8$  belongs to the interval

$$\Lambda_8 \in \left( -\frac{1}{8\alpha}, 0 \right) . \quad (2.83)$$

For this values of  $\Lambda_8$ , the condition (2.73) is automatically satisfied. It should be noted, that for positive  $\alpha$  and negative  $\bar{R}_{(0)1}^{(+)}$  the condition (2.76) is also satisfied. Taking into account the interval (2.83), the corresponding allowed

interval for  $\gamma$  reads<sup>4</sup>

$$\gamma \in \left( 0, \frac{1}{4 \left| \bar{R}_{(0)1}^{(+)} \right|^3} \right) . \quad (2.84)$$

Thus, for any positive value of  $\alpha$ , Eqs. (2.83) and (2.84) define allowed intervals for parameters  $\Lambda_8$  and  $\gamma$  which ensure the existence of a global minimum of the effective potential  $U_{eff}$ . Here, the required stable compactification of the internal space is obtained. The position of the minimum  $(\beta_0^1, \phi_0)$  and its value can be easily found (via the root  $\bar{R}_{(0)1}^{(+)}$ ) with the help of Eq. (2.44). The Figs.(2.2), (2.3) demonstrate such minimum for a particular choice of the parameters:  $\alpha = 1, \gamma = 1, \Lambda_8 = -0.1$ . Moreover, the limit  $\Lambda_8 \rightarrow 0$  corresponds to  $\bar{R}_{(0)1}^{(+)} \rightarrow 0$  which results in the decompactification of the internal space  $\beta_0^1 \rightarrow \infty$ .

## Summary

In this section the model with curvature-quadratic and curvature-quartic correction terms of the type (2.43) was analyzed and it was shown that the stable compactification of the internal space takes place for the sign relation (2.80). Moreover, the parameters of the model should belong to the allowed intervals (regions of stability) (2.83) and (2.84). The former one can be rewritten in the form

$$\Lambda_8 = \frac{\xi}{8\alpha}, \quad \xi \in (-1, 0) . \quad (2.85)$$

Thus, for the root  $\bar{R}_{(0)1}^{(+)}$  and parameter  $\gamma$  one obtains respectively

$$\bar{R}_{(0)1}^{(+)} = \frac{\eta}{\alpha}, \quad \eta \equiv \frac{1}{4} \left( -3 + \sqrt{9 + 8\xi} \right) < 0 \quad (2.86)$$

and

$$\gamma = \frac{\zeta \alpha^3}{4 |\eta|^3}, \quad \zeta \in (0, 1) . \quad (2.87)$$

Eq. (2.86) shows that  $\bar{R}_{(0)1}^{(+)} \in \left( -\frac{1}{2\alpha}, 0 \right)$ .

---

<sup>4</sup>Similar interval for the allowed values of  $\gamma$  was also found in [37] for the curvature-quartic model.



It is of interest to estimate the masses of the gravitational excitons (2.24) and of the nonlinearity field  $\phi$  (2.25) as well as the effective cosmological constant (2.26). From Eqs. (2.85)-(2.87) follows that  $\bar{R}_{(0)1}^{(+)} \sim \Lambda_8 \sim -\alpha^{-1}$ ,  $\gamma \sim \alpha^3 \implies f'(\phi_0) \sim \mathcal{O}(1)$ ,  $f''(\phi_0) \sim \alpha$ ,  $U(\phi_0) \sim -\alpha^{-1}$ . Then, the corresponding estimates read:

$$-\Lambda_{eff} \sim m_1^2 \sim m_\phi^2 \sim \alpha^{-1}. \quad (2.88)$$

From other hand (see Eqs. (2.20) and (2.24))

$$U(\phi_0) \sim \exp(-2\beta_0^1) = b_{(0)1}^{-2}. \quad (2.89)$$

So, if the scale factor of the stabilized internal space is of the order of the Fermi length:  $b_{(0)1} \sim L_F \sim 10^{-17}\text{cm}$ , then  $\alpha \sim L_F^2$  and for the effective cosmological constant and masses one obtains:  $-\Lambda_{eff} \sim m_1^2 \sim m_\phi^2 \sim 1\text{TeV}^2$ .

The internal space stable compactification analysis was performed in the case  $Q(\phi) > 0 \implies \text{sign } \alpha = \text{sign } \gamma$ . In forthcoming chapters the extend of this investigation to the case of negative  $Q(\phi)$  is performed, where the function  $\bar{R}(\phi)$  has three real-valued branches.

For the visualization reasons, let us consider the model with one internal space and critical dimension  $D = 8$  (as usual, for the external spacetime  $D_0 = 4$ ). Then, the effective potential (2.19) reads:

$$U_{eff}(\hat{\beta}^1, \phi) = e^{-4\hat{\beta}^1} \left[ -\frac{1}{2} \hat{R}_1 e^{-2\hat{\beta}^1} + U(\phi) \right]. \quad (2.90)$$

To draw this effective potential, let us define  $\hat{R}_1$  via  $U(\phi_0)$  in Eq. (2.24). In its turn,  $U(\phi_0)$  is defined in Eq. (2.33) where  $\bar{R}(\phi_0) = \bar{R}_{(0)1}^{(+)}$  and  $f'(\bar{R}_{(0)1}^{(+)})$  can be found from (2.81). In Figs.(2.2), (2.3) the generic form of the  $U_{eff}$  is illustrated by a model with parameters  $\alpha = 1, \gamma = 1, \Lambda_8 = -0.1$  from the stability regions (2.83) and (2.84).

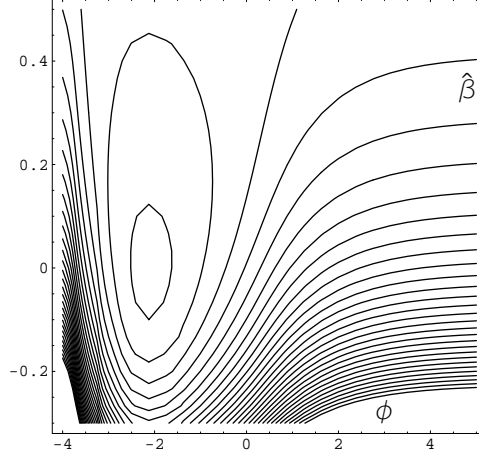


Figure 2.2: Typical contour plot of the effective potential  $U_{eff}(\hat{\beta}^1, \phi)$  given in Eq. (2.90) with parameters  $\alpha = 1, \gamma = 1, \Lambda_8 = -0.1$ .  $U_{eff}$  reaches the global minimum at  $(\hat{\beta}^1 = 0, \phi \approx -2.45)$ .

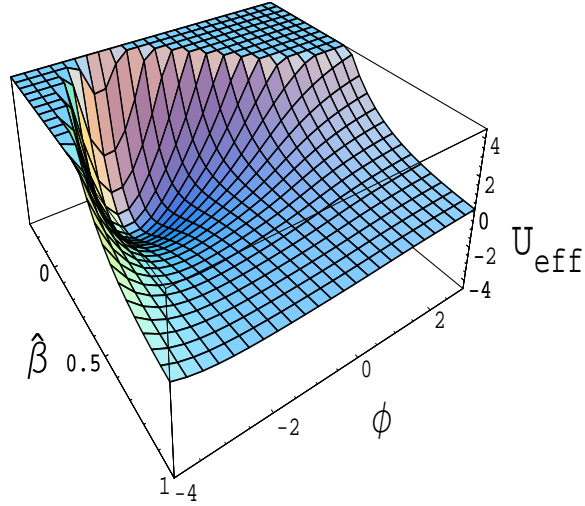


Figure 2.3: Typical form of the effective potential  $U_{eff}(\hat{\beta}^1, \phi)$  given in Eq. (2.90) with parameters  $\alpha = 1, \gamma = 1, \Lambda_8 = -0.1$ .

## CHAPTER 3

# MULTIDIMENSIONAL NONLINEAR MODELS WITH FORMS

In the present chapter, the nonlinear gravitational multidimensional cosmological model is considered with action of the type  $\bar{R} + 1/\bar{R}$  with form-fields as a matter source, including a bare cosmological term as an additional parameter of the theory. It is assumed that the corresponding higher-dimensional space-time manifold undergoes a spontaneous compactification to a manifold with warped product structure of the external and internal spaces. Each of spaces has its own scale factor. A model without form-fields and bare cosmological constant was considered in previous chapter, where the internal space freezing stabilization was achieved due to negative minimum of the effective potential. Thus, such model is asymptotically AdS without accelerating behavior of our Universe. It is well known that inclusion of usual matter can uplift potential to the positive values [58]. One of the main task of present investigations is to observe such uplifting due to the form-fields. Indeed, it is demonstrated that for certain parameter regions the late-time acceleration scenario in present model becomes reachable. However, it is not simple uplifting of the negative minimum of the theory (2.1) to the positive values. The presence of the form-fields results in much more rich structure of the effective potential than for (2.1). Here, additional branches are obtained with extremum points, and one of such extremum corresponds to the positive minimum of the effective potential. This minimum plays the role of the positive cosmological constant. With the corresponding fine tuning of the parameters, it can provide the late-time accelerating expansion of the Universe. Moreover, it is shown that for this branch of the effective potential there is also a saddle point. Thus, domain walls are obtained, which separate regions with different vacua. It is demonstrated that these domain walls do

not undergo inflation because the effective potential is not flat enough around the saddle point.

It is also worth of noting that the effective potential in this reduced model has a branchpoint. It gives very interesting possibility to investigate transitions from one branch to another by analogy with catastrophe theory or similar to phase transitions in statistical theory. This idea needs more detail investigation.

The chapter is structured as follows. First, a brief description of multi-dimensional models with scalar curvature nonlinearity  $f(\bar{R})$  and the form-fields as a matter source is given. Then, dimensional reduction is performed and effective four-dimensional action with effective potential is obtained. General formulas from this section are applied to the specific model  $f(\bar{R}) = \bar{R} - \mu/R - 2\Lambda_D$ . Then minimum conditions of the effective potential are obtained. These conditions are analyzed for the cases of zero and positive effective cosmological constants respectively. Furthermore, it is demonstrated that the positive minimum of the effective potential plays the role of the positive cosmological constant and can provide the late-time accelerating expansion. Additionally, this minimum is accompanied by a saddle point. It results in non-inflating domain walls in the Universe.

### 3.1. General equations

Let us consider a  $D = (D_0 + D')$ -dimensional nonlinear gravitational theory with action functional

$$\begin{aligned}
 S = & \frac{1}{2\kappa_D^2} \int_M d^D x \sqrt{|\bar{g}|} f(\bar{R}) \\
 & - \frac{1}{2} \int_M d^D x \sqrt{|\bar{g}|} \sum_{i=1}^n \frac{1}{d_i!} \left( F^{(i)} \right)^2,
 \end{aligned} \tag{3.1}$$

where  $f(\bar{R})$  is an arbitrary smooth function of a scalar curvature  $\bar{R} := R[\bar{g}]$  constructed from the  $D$ -dimensional metric  $\bar{g}_{ab}$  ( $a, b = 1, \dots, D$ ).  $D'$  is the number of extra dimensions.  $\kappa_D^2$  denotes the  $D$ -dimensional gravitational

constant. In action (3.1), a form field (flux)  $F$  has block-orthogonal structure consisting of  $n$  blocks. Each of these blocks is described by its own antisymmetric tensor field  $F^{(i)} (i = 1, \dots, n)$  of rank  $d_i$  ( $d_i$ -form field strength). Additionally, let us assume that for the sum of the ranks holds  $\sum_{i=1}^n d_i = D'$ .

Following Refs. [37, 79], it can be shown that the nonlinear gravitational theory (3.1) is equivalent to a linear theory  $R = R[g]$  with conformally transformed metric

$$g_{ab} = \Omega^2 \bar{g}_{ab} = [f'(\bar{R})]^{2/(D-2)} \bar{g}_{ab} \quad (3.2)$$

and an additional minimal scalar field  $\phi = \ln[f'(\bar{R})]/A$  coupled with fluxes. The scalar field  $\phi$  is the result and the carrier of the curvature nonlinearity of the original theory. Thus, for brevity, referring to the field  $\phi$  as nonlinearity scalar field, a self-interaction potential  $U(\phi)$  of the scalar field  $\phi$  reads

$$U(\phi) = \frac{1}{2} e^{-B\phi} [\bar{R}(\phi) e^{A\phi} - f(\bar{R}(\phi))] , \quad (3.3)$$

where

$$A = \sqrt{\frac{D-2}{D-1}}, \quad B = \frac{D}{\sqrt{(D-2)(D-1)}}. \quad (3.4)$$

Furthermore, let us assume that the multidimensional space-time manifold undergoes a spontaneous compactification

$$M \longrightarrow M = M_0 \times M_1 \times \dots \times M_n \quad (3.5)$$

in accordance with the block-orthogonal structure of the field strength  $F$ , and that the form fields  $F^{(i)}$ , each nested in its own  $d_i$ -dimensional factor space  $M_i$  ( $i = 1, \dots, n$ ), respect a generalized Freund-Rubin ansatz [80]. Here,  $(D_0 = 4)$ -dimensional space-time  $M_0$  is treated as our external Universe with metric  $g^{(0)}(x)$ .

This allows performing of a dimensional reduction of the model along the lines of Refs. [34–36, 69]. The factor spaces  $M_i$  are then Einstein spaces with metrics  $g^{(i)} \equiv e^{2\beta^i(x)} \gamma^{(i)}$  which depend only through the warp factors  $a_i(x) := e^{\beta^i(x)}$  on the coordinates  $x$  of the external space-time  $M_0$ . For the corresponding scalar curvatures holds  $R[\gamma^{(i)}] = \lambda^i d_i \equiv r_i$  (in the case of the constant curvature spaces  $\lambda^i = k_i(d_i - 1)$ ,  $k_i = 0, \pm 1$ ). The warped product

of Einstein spaces leads to a scalar curvature  $\bar{R}$  which depends only on the coordinate  $x$  of the  $D_0$ -dimensional external space-time  $M_0$ :  $\bar{R}[\bar{g}] = \bar{R}(x)$ . This implies that the nonlinearity field  $\phi$  is also a function only of  $x$ :  $\phi = \phi(x)$ . Additionally, it can be easily seen [37] that the generalized Freund-Rubin ansatz results in the following expression for the form-fields:  $(F^{(i)})^2 = f_i^2/a_i^{2d_i}$  where  $f^i = \text{const.}$

In general, the model will allow for several stable scale factor configurations (minima in the landscape over the space of volume moduli). Let us choose one of them (which is expected to correspond to current evolution stage of our observable Universe), denote the corresponding scale factors as  $\beta_0^i$ , and work further on with the deviations  $\hat{\beta}^i(x) = \beta^i(x) - \beta_0^i$ .

Without loss of generality<sup>5</sup>, one shall consider a model with only one  $d_1$ -dimensional internal space. After dimensional reduction and subsequent conformal transformation to the Einstein frame the action functional (3.1) reads<sup>6</sup>

$$S = \frac{1}{2\kappa_0^2} \int_{M_0} d^{D_0}x \sqrt{|\tilde{g}^{(0)}|} \left\{ R[\tilde{g}^{(0)}] - \tilde{g}^{(0)\mu\nu} \partial_\mu \varphi \partial_\nu \varphi - \tilde{g}^{(0)\mu\nu} \partial_\mu \phi \partial_\nu \phi - 2U_{eff}(\varphi, \phi) \right\}, \quad (3.6)$$

where  $\varphi := -\sqrt{d_1(D-2)/(D_0-2)} \hat{\beta}^1$  and  $\kappa_0^2 := \kappa_D^2/V_{d_1}$  denotes the  $D_0$ -dimensional (four-dimensional) gravitational constant.  $V_{d_1} \sim \exp(d_1\beta_0^1)$  is the volume of the internal space at the present time.

A stable compactification of the internal space  $M_1$  is ensured when its scale factor  $\varphi$  is frozen at the minimum of the effective potential

$$U_{eff} = e^{b\varphi} \left[ -\frac{1}{2} R_1 e^{a\varphi} + U(\phi) + h e^{c\phi} e^{ad_1\varphi} \right], \quad (3.7)$$

where  $R_1 := r_1 \exp(-2\beta_0^1)$  defines the curvature of the internal space at the present time and contribution of the form-field into the effective action

---

<sup>5</sup>The difference between a general model with  $n > 1$  internal spaces and the particular one with  $n = 1$  consists in an additional diagonalization of the geometrical moduli excitations.

<sup>6</sup>The equivalency between original higher dimensional and effective dimensionally reduced models was investigated in a number of papers (see e.g. [81–83]). The origin of this equivalence results from high symmetry of considered models (i.e. because of specific metric ansatz which is defined on the manifold consisting of direct product of the Einstein spaces).

is described by  $h := \kappa_D^2 f_1^2 \exp(-2d_1\beta_0^1) > 0$ . For brevity let us introduce notations

$$\begin{aligned} a : &= 2\sqrt{\frac{D_0 - 2}{d_1(D - 2)}} , \quad b : = 2\sqrt{\frac{d_1}{(D - 2)(D_0 - 2)}} , \\ c : &= \frac{2d_1 - D}{\sqrt{(D - 1)(D - 2)}} . \end{aligned} \quad (3.8)$$

### 3.2. $R^{-1}$ model with forms

In this section the conditions of the compactification are analyzed for a model with

$$f(\bar{R}) = \bar{R} - \frac{\mu}{\bar{R}} - 2\Lambda_D . \quad (3.9)$$

Then from the relation  $f'(\bar{R}) = \exp(A\phi)$  one obtains

$$\bar{R} = q\sqrt{\frac{|\mu|}{s(e^{A\phi} - 1)}} , \quad q = \pm 1 , \quad s = \text{sign}(\mu) . \quad (3.10)$$

Thus, the ranges of variation of  $\phi$  are  $\phi \in (-\infty, 0)$  for  $\mu < 0$  ( $s = -1$ ) and  $\phi \in (0, +\infty)$  for  $\mu > 0$  ( $s = +1$ ).

It is worth of noting that the limit  $\phi \rightarrow \pm 0$  ( $f' \rightarrow 1$ ) corresponds to the transition to a linear theory:  $f(\bar{R}) \rightarrow \bar{R} - 2\Lambda_D$  and  $R \rightarrow \bar{R}$ . This is general feature of all nonlinear models  $f(\bar{R})$ . For example, in the case (3.9) one obtains  $f(\bar{R}) = \bar{R}(2 - \exp(A\phi)) - 2\Lambda_D \rightarrow \bar{R} - 2\Lambda_D$  for  $\phi \rightarrow 0$ . From other hand, for particular model (3.9), eq. (3.10) shows that the point  $\phi = 0$  maps into infinity  $\bar{R}, R = \pm\infty$ . Thus, in this sense, one shall refer to the point  $\phi = 0$  as singularity.

For the model (3.9), potential (3.3)  $U(\phi)$  reads

$$U(\phi) = \frac{1}{2}e^{-B\phi} \left( 2qs\sqrt{|\mu|}\sqrt{se^{A\phi} - s} + 2\Lambda_D \right) . \quad (3.11)$$

It is well known (see e.g. [35, 36, 58]) that in order to ensure a stabilization and asymptotical freezing of the internal space  $M_1$ , the effective potential (3.7) should have a minimum with respect to both scalar fields  $\varphi$  and  $\phi$ . Let

us remind that the minimum position is chosen with respect to  $\varphi$  at  $\varphi = 0$ . Additionally, the eigenvalues of the mass matrix of the coupled  $(\varphi, \phi)$ -field system, i.e. the Hessian of the effective potential at the minimum position,

$$J := \left( \begin{array}{cc} \partial_{\varphi\varphi}^2 U_{eff} & \partial_{\varphi\phi}^2 U_{eff} \\ \partial_{\phi\varphi}^2 U_{eff} & \partial_{\phi\phi}^2 U_{eff} \end{array} \right) \bigg|_{extr} \quad (3.12)$$

should be positive definite (this condition ensures the positiveness of the mass squared of scalar field excitations). According to the Silvester criterion this is equivalent to the condition:

$$J_{11} > 0, \quad J_{22} > 0, \quad \det(J) > 0. \quad (3.13)$$

It is convenient in further consideration to introduce the following notations:

$$\phi_0 := \phi|_{extr}, \quad X := \sqrt{se^{A\phi_0} - s} > 0 \rightarrow X_{(s=-1)} < 1. \quad (3.14)$$

Then potentials  $U(\phi)$ ,  $U_{eff}(\varphi, \phi)$  and derivatives of the  $U_{eff}$  at an extremum (possible minimum) position ( $\varphi = 0, \phi_0$ ) can be rewritten as follows:

$$U_0 \equiv U|_{extr} = (1 + sX^2)^{-B/A} \left( qs\sqrt{|\mu|}X + \Lambda_D \right), \quad (3.15)$$

$$U_{eff}|_{extr} = -\frac{1}{2}R_1 + U_0(X) + h(1 + sX^2)^{c/A}, \quad (3.16)$$

$$\begin{aligned} \partial_{\varphi} U_{eff}|_{extr} &= -\frac{a+b}{2}R_1 + bU_0(X) \\ &+ (ad_1 + b)h(1 + sX^2)^{c/A} = 0, \end{aligned} \quad (3.17)$$

$$\begin{aligned} \partial_{\phi} U_{eff}|_{extr} &= ch(1 + sX^2)^{c/A} - BU_0(X) \\ &+ \frac{qA\sqrt{|\mu|}}{2X}(1 + sX^2)^{1-B/A} = 0, \end{aligned} \quad (3.18)$$

$$\begin{aligned} \partial_{\varphi\varphi}^2 U_{eff}|_{extr} &= -\frac{(a+b)^2}{2}R_1 + b^2U_0(X) \\ &+ (ad_1 + b)^2h(1 + sX^2)^{c/A}, \end{aligned} \quad (3.19)$$



$$\partial_{\varphi\phi}^2 U_{eff}|_{extr} = chad_1 (1 + sX^2)^{c/A} , \quad (3.20)$$

$$\begin{aligned} \partial_{\phi\phi}^2 U_{eff}|_{extr} &= ch(c - A + 2B) (1 + sX^2)^{c/A} \\ &+ B(A - B)U_0(X) \\ &- \frac{qs\sqrt{|\mu|}A^2}{4X^3} (1 + sX^2)^{2-B/A} . \end{aligned} \quad (3.21)$$

The most natural strategy for extracting detailed information about the location of stability region of parameters in which compactification is possible would consist in solving (3.18) for  $X$  with subsequent back-substitution of the found roots into the inequalities (3.13) and the equation (3.17). To get the main features of the model under consideration, it is sufficient to investigate two particular nontrivial situations. Both of these cases are easy to handle analytically.

### 3.3. Case $\Lambda_{eff} = 0$

It can be easily seen from eqs. (3.16) and (3.17) that condition  $\Lambda_{eff} = U_{eff}|_{extr} = 0$  results in relations

$$R_1 = 2d_1h (1 + sX^2)^{c/A} = \frac{2d_1}{d_1 - 1}U_0(X) , \quad d_1 \geq 2 , \quad (3.22)$$

which enables to get from eq. (3.18) quadratic equation for  $X$

$$(d_1 + 1)X^2 + qsd_1zX - s(d_1 - 1) = 0 , \quad z \equiv 2\Lambda_D/\sqrt{|\mu|} \quad (3.23)$$

with the following solutions:

$$\begin{aligned} X_p &= qs \frac{d_1}{2(d_1 + 1)} \left( -z + p \sqrt{z^2 + 4s \frac{d_1^2 - 1}{d_1^2}} \right) , \\ p &= \pm 1 . \end{aligned} \quad (3.24)$$

In the case  $s = -1$  parameter  $z$  should satisfy condition  $|z| \geq z_0 \equiv 2\sqrt{d_1^2 - 1}/d_1 < 2$  and for  $z = z_0$  two solutions  $X_p$  degenerate into one:  $X_p \equiv X_0 = -qs\sqrt{(d_1 - 1)/(d_1 + 1)}$ .

Because of conditions  $h \geq 0$  and  $e^{A\phi_0} = 1 + sX^2 > 0$ , the relations (3.22) show that parameters  $R_1$  and  $U_0(X)$  should be non-negative:  $R_1 \geq 0$ ,  $U_0(X) \geq 0$ . Obviously, only one of the solutions (3.24) corresponds to a minimum of the effective potential. With respect to this solution let us define parameters in the relation (3.22). Therefore, one must distinguish now which of  $X_p$  corresponds to the minimum of  $U_{eff}$ . Let us investigate solutions (3.24) for the purpose of their satisfactions to conditions  $e^{A\phi_0} > 0$ ,  $U_0(X) \geq 0$  and  $X_p \geq 0$ .

**The condition  $e^{A\phi_0} = 1 + sX_p^2 > 0$ :**

Simple analysis shows that solutions  $X_p$  satisfy this inequality for the following combinations of parameters:

$\mu > 0$ ( $s = +1$ )	$p = \pm 1 : z \in (-\infty, +\infty)$	(3.25)
$\mu < 0$ ( $s = -1$ )	$p = +1 : z \in (-2, -z_0) \cup (z_0, +\infty)$ $p = -1 : z \in (-\infty, -z_0) \cup (z_0, 2)$ $z = z_0$	

**The condition  $U_0(X) \geq 0$ :**

As appears from eq. (3.15), this condition takes place if  $X_p$  satisfies inequality  $2qsX_p + z \geq 0$  which leads to the conditions:

$\mu > 0$ ( $s = +1$ )	$p = +1 : z \in (-\infty, +\infty)$	(3.26)
$\mu < 0$ ( $s = -1$ )	$p = +1 : z \in (z_0, +\infty)$ $p = -1 : z \in (z_0, 2]$ $z = z_0$	

**The condition  $X_p > 0$ :**

This condition is satisfied for the combinations:

$\mu > 0$ $(s = +1)$	$q = +1 :$ $q = -1 :$	$\left\{ \begin{array}{ll} z < 0 : & X_+ > 0 \quad X_- < 0 \\ z > 0 : & X_+ > 0 \quad X_- < 0 \\ z < 0 : & X_+ < 0 \quad X_- > 0 \\ z > 0 : & X_+ < 0 \quad X_- > 0 \end{array} \right.$	(3.27)
$\mu < 0$ $(s = -1)$	$q = +1 :$ $q = -1 :$	$\left\{ \begin{array}{ll} z < 0 : & X_+ < 0 \quad X_- < 0 \\ z > 0 : & X_+ > 0 \quad X_- > 0 \\ z < 0 : & X_+ > 0 \quad X_- > 0 \\ z > 0 : & X_+ < 0 \quad X_- < 0 \end{array} \right.$	

The comparison of (3.25), (3.26) and (3.27) shows that they are simultaneously satisfied only for the following combinations:

$\mu > 0$ $(s = +1)$	$p = +1 : \quad q = +1 : \quad z \in (-\infty, +\infty)$	(3.28)
$\mu < 0$ $(s = -1)$	$p = +1 : \quad q = +1 : \quad z \in (z_0, +\infty)$ $p = -1 : \quad q = +1 : \quad z \in (z_0, 2)$ $q = +1 : \quad z = z_0$	

Additionally, the extremum solutions  $X_p$  should correspond to the minimum of  $U_{eff}$ . The inequalities (3.13) are the sufficient and necessary conditions for that. Let us analyze them in the case of four-dimensional external space  $D_0 = 4$ . Taking into account definitions (3.4), (3.8), (3.19)-(3.21) and relations (3.22), for  $J_{11}$ ,  $J_{22}$  and  $J_{21}$  one gets respectively:

$$J_{11} = \frac{8}{d_1 + 2} U_0(X_p), \quad (3.29)$$

$$J_{22} = -\sqrt{|\mu|} \left[ \frac{6d_1(2qsX_p + z)(1 + sX_p^2)^{-\frac{d_1+4}{d_1+2}}}{(d_1 - 1)(d_1 + 2)(d_1 + 3)} + \frac{qs(d_1 + 2)}{4X_p^3(d_1 + 3)} (1 + sX_p^2)^{\frac{d_1}{d_1+2}} \right], \quad (3.30)$$

$$J_{21} = -\sqrt{|\mu|} \left[ \frac{(d_1 - 4)(2qsX_p + z)}{(d_1 - 1)(d_1 + 2)} \times \sqrt{\frac{2}{d_1(d_1 + 3)}} (1 + sX_p^2)^{-\frac{d_1+4}{d_1+2}} \right]. \quad (3.31)$$

It is supposed in these equations that each of  $X_p$  can define zero minimum of  $U_{eff}$ . In what follows, one shall check this assumption for every  $X_p$  with corresponding combinations of signs of the parameters  $s$  and  $q$  in accordance with the table (3.28).

According to the Sylvester criterion (3.13),  $J_{11}$  should be positive. Thus eqs. (3.22) and (3.29) result in the following conclusions: the potential  $U_0$  should be positive  $U_0 > 0$ , the internal space should have positive curvature  $R_1 > 0$  (hence,  $d_1 > 1$ ) and its stabilization (with zero minimum  $\Lambda_{eff} = 0$ ) takes place only in the present of form-field ( $h > 0$ ). Transition from the non-negativity condition  $U_0 \geq 0$  to the positivity one  $U_0 > 0$  corresponds to the only substitution in (3.26)  $(z_0, 2] \rightarrow (z_0, 2)$  for the case  $s = -1$ ,  $p = -1$ . Exactly this interval  $(z_0, 2)$  appears in concluding table (3.28). Therefore,  $J_{11}$  is positive for all  $X_p$  from the table (3.28).

Concerning expressions  $J_{22}$  and  $\det(J) = J_{11}J_{22} - J_{12}^2$ , graphical plotting (see Fig.3.4 and Fig.3.5) demonstrates that they are negative for  $s = +1$ ,  $p = +1$ ,  $q = +1$  and  $s = -1$ ,  $p = -1$ ,  $q = +1$  but positive in the case  $s = -1$ ,  $p = +1$ ,  $q = +1$ . For this latter combination  $z \in (z_0, \infty)$ . The case  $s = -1$ ,  $q = +1$  and  $z = z_0$  should be investigated separately. Here,  $X_p \equiv X_0 = \sqrt{(d_1 - 1)/(d_1 + 1)}$  and for  $J_{22}$  and  $J_{21}$  one obtains:

$$J_{22} = - \sqrt{|\mu|} X_0^{-3} (1 + sX_0^2)^{-\frac{d_1+4}{d_1+2}} \times \left( \frac{12(d_1 - 1) - (d_1 + 2)^2}{(d_1 + 1)^2(d_1 + 2)(d_1 + 3)} \right), \quad (3.32)$$

$$J_{21} = - \sqrt{|\mu|} X_0^{-3} (1 + sX_0^2)^{-\frac{d_1+4}{d_1+2}} \times \left( \frac{2\sqrt{2}(d_1 - 4)(d_1 - 1)}{(d_1 + 1)^2(d_1 + 2)\sqrt{d_1(d_1 + 3)}} \right). \quad (3.33)$$

It can be easily seen from eqs. (3.32) and (3.33) that  $J_{22} > 0$  for  $d_1 \neq 4$  and  $J_{22} = J_{21} = 0$  for  $d_1 = 4$ . Additionally,  $\det(J) > 0$  for  $d_1 \neq 4$ .

Thus, it can finally concluded that zero minimum of the effective potential  $U_{eff}$  takes place either for  $s = -1$ ,  $q = +1$ ,  $z \in (z_0, \infty)$ ,  $\forall d_1 > 1$  (position of this minimum is defined by solution (3.24) with  $p = +1$ ) or for  $s = -1$ ,  $q =$

$+1$ ,  $z = z_0, \forall d_1 \neq 4$ . Concerning the signs of parameters, one obtains that  $\mu < 0$  and  $\Lambda_D > 0$ .

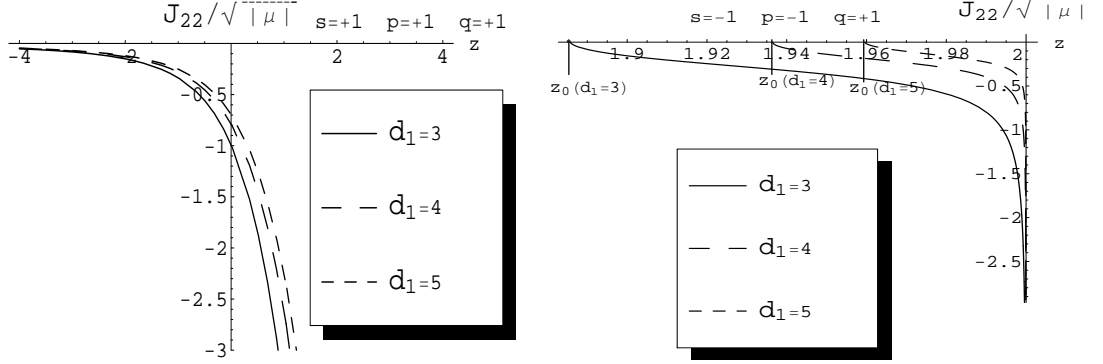


Figure 3.4: Typical form of  $J_{22}/\sqrt{|\mu|}$  (eq. (3.30)) for parameters  $s = +1$ ,  $q = +1$ ,  $p = +1$  (left) and  $s = -1$ ,  $q = +1$ ,  $p = -1$  (right). For both of these combinations of the parameters,  $J_{22} < 0$ .

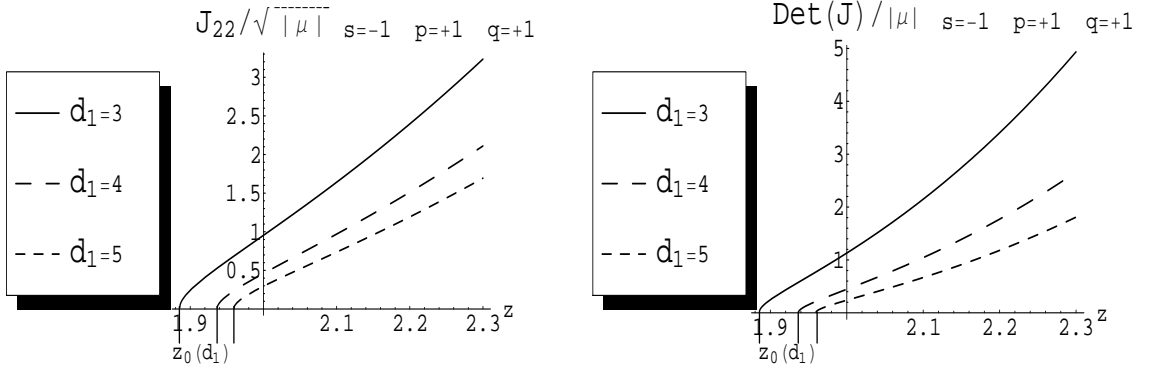


Figure 3.5: Typical form of  $J_{22}/\sqrt{|\mu|}$  (left) and  $\det(J)/|\mu|$  (right) (see eqs. (3.29)-(3.31)) for parameters  $s = -1$ ,  $q = +1$ ,  $p = +1$ . For this combination of the parameters,  $J_{22} > 0$  and  $\det J > 0$ .

### 3.4. Decoupling of excitations: $d_1 = D_0$

It can be easily seen from eq. (3.8) that in the case  $d_1 = D_0$  parameter  $c = 0$  that leads to condition  $\partial_{\varphi\phi}^2 U_{eff}|_{extr} = 0$  (see eq. (3.20)). Thus, the Hessian (3.12) is diagonalized. It means that the excitations of the fields  $\varphi$  and  $\phi$  near the extremum position are decoupled from each other<sup>7</sup>.

<sup>7</sup>In the vicinity of a minimum of the effective potential, squared masses of these excitations are  $m_\varphi^2 = J_{11}$  and  $m_\phi^2 = J_{22}$ .

Dropping the  $h$  term in eq. (3.18) (because of  $c = 0$ ) and taking into account eq. (3.15), one obtains quadratic equation for  $X$

$$(D + 2)X^2 + DqsX - (D - 2)s = 0, \quad (3.34)$$

which for  $D_0 = d_1$  exactly coincides with eq. (2.43). Thus, in spite of the fact that the condition  $\Lambda_{eff} = 0$  is not applied directly, one obtains in the case  $d_1 = D_0$  precisely the same solutions (3.24). However, parameters  $R_1, U_0$  and  $h$  satisfy now relations different from (3.22). For example, for the most physically interesting case  $D_0 = d_1 = 4$ , eqs. (3.16) and (3.17) result in the following relations:

$$R_1 = 4 \left[ \frac{1}{3}U_0(X) + h \right], \quad \Lambda_{eff}(X) = \frac{1}{3}U_0(X) - h. \quad (3.35)$$

Nonzero components of the Hessian read

$$\begin{aligned} J_{11} &= \frac{2}{3} [9h - U_0(X)], \\ J_{22} &= -\sqrt{|\mu|} \left[ \frac{4(z + 2qsX_p)}{21(1 + sX_p^2)^{4/3}} + \frac{3qs(1 + sX_p^2)^{2/3}}{14X_p^3} \right]. \end{aligned} \quad (3.36)$$

Now, let us to look for a positive minimum of the effective potential. It means that  $\Lambda_{eff} > 0$ ,  $J_{11} > 0$  and  $J_{22} > 0$ . From the positivity of  $J_{11}$  and  $\Lambda_{eff}$  follows respectively<sup>8</sup>:

$$J_{11} > 0 : \quad 16h > R_1 > 16U_0(X)/9 > 8\Lambda_{eff} \quad (3.37)$$

and

$$\Lambda_{eff} > 0 : \quad h > R_1/16 > U_0(X)/9 > h/3 > 0. \quad (3.38)$$

These inequalities show that for the considered model positive minimum of the effective potential is possible only in the case of positive curvature of the internal space  $R_1 > 0$  and in the presence of the form field ( $h > 0$ ).

To realize which combination of parameters  $s, p$  and  $q$  ensures the minimum of the effective potential, one should perform analysis as in the previous

---

<sup>8</sup>It is interesting to note that (in the case  $D_0 = d_1 = 4$ ) relations (3.34),  $J_{11}$  in (3.36) and inequalities (3.37), (3.38) coincide with the analogous expressions in paper [58] with quadratic nonlinear model. This is not surprising because they do not depend on the form of nonlinearity  $f(\bar{R})$  (and, consequently, on the form of  $U(\phi)$ ). However, the expressions for  $J_{22}$  are different because here the exact form of  $U(\phi)$  is used.

case with  $\Lambda_{eff} = 0$ . However, there is no need to perform such analysis here because solutions of eq. (3.34) coincides with (3.24) and all conditions for  $X_p$  and  $U_0$  are the same as in the previous section. Thus, one obtains concluding table of the form (3.28). Additionally, it can be easily seen that expressions of  $J_{22}$  in (3.36) and (3.30) exactly coincide with each other if one put  $d_1 = 4$  in the latter equation<sup>9</sup>. Hence, Fig.3.4 and Fig.3.5 can be used (for the lines with  $d_1 = 4$ ) for analyzing the sign of  $J_{22}$ . With the help of these pictures as well as keeping in the mind that  $J_{22}(d_1 = 4, z = z_0) = 0$ , follows that the only combination which ensures the positive minimum of  $U_{eff}$  is:  $s = -1$ ,  $p = +1$ ,  $q = +1$  and  $z \in (z_0 = 1.936, +\infty)$ . It is clear that potential  $U_0(X)$  in eqs. (3.35)-(3.38) is defined by solution of eq. (3.34) (i.e. (3.24) for  $d_1 = 4$ ) with this combination of the parameters. Because  $s = -1$  and  $z > 0$ , the parameters  $\mu$  and  $\Lambda_D$  should have the following signs:  $\mu < 0$  and  $\Lambda_D > 0$ .

Additionally, it is easy to verify that second solution of eq. (3.24)  $X_-$  (with  $p = -1$  and  $s = -1$ ,  $q = +1$ ) does not correspond to the maximum of the effective potential  $U_{eff}$ . Indeed, in this case  $\partial_\phi U_{eff}(X_-) = 0$  but  $\partial_\varphi U_{eff}(X_-) \neq 0$ .

Fig. 3.6 demonstrates the typical profile  $\varphi = 0$  of the effective potential  $U_{eff}(\varphi, \phi)$  in the case of positive minimum of  $U_{eff}$  considered in the present section. This picture is in good concordance with the table (3.28). According to this table, positive extrema of  $U_{eff}$  are possible only for the branch  $q = +1$  of the solution (3.10) (solid lines in Fig. 3.6). It is obvious that for  $z_0 < z < 2$  one can have 3 such extrema: one for positive  $\mu > 0 \rightarrow s = +1$  and two for negative  $\mu < 0 \rightarrow s = -1$ . These investigations show that in the left half plane (i.e. for  $\mu < 0$ ) the right extremum ( $p = +1$  in eq. (3.24)) is the local minimum<sup>10</sup> and the left maximum ( $p = -1$ ) is not the extremum of  $U_{eff}$  because here  $\partial_\varphi U_{eff} \neq 0$ . Analogously, maximum in the right half plane

---

<sup>9</sup>It follows from the fact that in (3.30)  $D_0 = 4$ . Although in this equation the relation (3.22) between  $h$  and  $U_0$  is used, it enters here in the combination which is proportional to  $c$ . Thus, this combination does not contribute if additionally  $d_1 = 4$ .

<sup>10</sup>It can be easily seen for the branch  $q = +1$ ,  $s = -1$  that  $U(\phi \rightarrow -\infty) \rightarrow +\infty$  for  $z \geq 2$  and  $U(\phi \rightarrow -\infty) \rightarrow -\infty$  for  $z < 2$ . Thus, for  $z \geq 2$  this minimum becomes global one.

$\mu > 0$  (which corresponds to  $(p = +1)$ -solution (3.24)) is not the extremum of  $U_{eff}$ . For completeness of picture, lines corresponding to the branch  $q = -1$  (dashed lines in Fig. 3.6) are also included. The minimum of the right dashed line (for  $X_p$  with  $s = +1$ ,  $p = -1$ ,  $q = -1$ ) does not describe the extremum of  $U_{eff}$  because again  $\partial_\phi U_{eff} \neq 0$ .

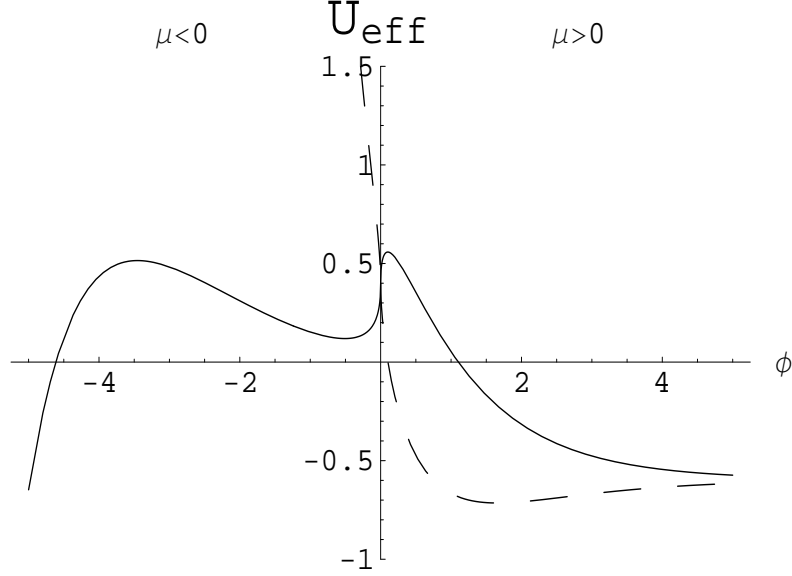


Figure 3.6: Profile  $\varphi = 0$  of the effective potential  $U_{eff}(\varphi, \phi)$  for parameters  $z = 1.99$  ( $\Lambda_D = 1.99/2$ ,  $|\mu| = 1$ ),  $D_0 = d_1 = 4$  and  $h = U_0/6$ . The rest of parameters can be found from relations (3.35). Solid and dashed lines describe branches  $q = +1$  and  $q = -1$  respectively. For the solid line, there is only one local minimum of  $U_{eff}$  which is defined by solution  $X_p$  with the following parameters:  $s = -1$ ,  $p = +1$ ,  $q = +1$ . Left ( $s = -1$ ,  $p = -1$ ,  $q = +1$ ) and right ( $s = +1$ ,  $p = +1$ ,  $q = +1$ ) maxima are not extrema of  $U_{eff}$  because in these points  $\partial_\phi U_{eff} = 0$  but  $\partial_\varphi U_{eff} \neq 0$ . Analogously, for right dashed line the solution  $X_p$  (with  $s = +1$ ,  $p = -1$ ,  $q = -1$ ) does not correspond to the extremum of  $U_{eff}$ .

### 3.5. Cosmic acceleration and domain walls

Let us consider again the model with  $d_1 = D_0 = 4$  in order to define stages of the accelerating expansion of our Universe. It was proven that for certain conditions (see (3.35)-(3.38)) the effective potential  $U_{eff}$  has local (for  $z_0 < z < 2$ ) or global (for  $z \geq 2$ ) positive minimum. The position of this minimum is  $(\varphi = 0, \phi = (1/A) \ln(1 + sX_p^2))$  where  $s = -1$ ,  $p = +1$ ,  $q = +1$  and  $z \in (z_0, +\infty)$ . Obviously, positive minimum of the effective potential



plays the role of the positive cosmological constant. Therefore, the Universe undergoes the accelerating expansion in this position. Thus, one can "kill two birds with one stone": to achieve the stable compactification of the internal space and to get the accelerating expansion of our external space.

Let us associate this acceleration with the late-time accelerating expansion of our Universe. As it follows from eqs. (3.35) and (3.38), positive minimum takes place if the parameters are positive and the same order of magnitude:  $\Lambda_{eff} \sim R_1 \sim U(X) \sim h > 0$ . On the other hand, in KK models the size of extra dimensions at present time should be  $b_{(0)1} \lesssim 10^{-17}\text{cm} \sim 1\text{TeV}^{-1}$ . In this case  $R_1 \gtrsim b_{(0)1}^{-2} \sim 10^{34}\text{cm}^{-2}$ . Thus, for the TeV scale of  $b_{(0)1} \sim 1\text{TeV}$  one gets that  $\Lambda_{eff} \sim R_1 \sim U(X) \sim h \sim 1\text{TeV}^2$ . Moreover, in the case of natural condition  $\Lambda_D \sim \sqrt{|\mu|}$  it follows that the masses of excitations  $m_\varphi \sim m_\phi \sim 1\text{TeV}$ . The above estimates clearly demonstrate the typical problem of the stable compactification in multidimensional cosmological models because for the effective cosmological constant one obtains a value which is in many orders of magnitude greater than observable at the present time dark energy  $\sim 10^{-57}\text{cm}^{-2}$ . The necessary small value of the effective cosmological constant can be achieved only if the parameters  $R_1, U(X), h$  are extremely fine tuned with each other to provide the observed small value from equation  $\Lambda_{eff}(X) = U_0(X)/3 - h$ . Two possibilities to avoid this problem can be seen. Firstly, the inclusion of different form-fields/fluxes may result in a big number of minima (landscape) [84, 85] with sufficient large probability to find oneself in a dark energy minimum. Secondly, the restriction  $R_1 \sim b_{(0)1}^{-2} \sim 10^{34}\text{cm}^{-2}$  can be avoided if the internal space is Ricci-flat:  $R_1 = 0$ . For example, the internal factor-space  $M_1$  can be an orbifold with branes in fixed points (see corresponding discussion in [86]).

The WMAP three year data as well as CMB data are consistent with wide range of possible inflationary models (see e.g. [13]). Therefore, it is of interest to get the stage of early inflation in the given model. It is well known that it is rather difficult to construct inflationary models from multidimensional cosmological models and string theories. The main reason of it consists in the form of the effective potential which is a combination of exponential functions

(see e.g. eq. (3.7)). Usually, degrees of these exponents are too large to result in sufficiently small slow-roll parameters (see e.g. [37]). Nevertheless, there is a possibility that in the vicinity of maximum or saddle points the effective potential is flat enough to produce the topological inflation [87–94]. Let us investigate this possibility for the given model.

As stated above, the value  $\varphi = 0$  corresponds to the internal space value at the present time. Following this statement, the minimum of the effective potential at this value of  $\varphi$  is found. Obviously, the effective potential can also have extrema at  $\varphi \neq 0$ . Let us investigate this possibility for the model with  $d_1 = D_0 = 4$ , i.e. for  $c = 0$ . In this case, the extremum condition of the effective potential reads

$$\begin{aligned} \partial_\varphi U_{eff}|_{\varphi_0, \phi_0} &= -\frac{1}{2}R_1(a+b)e^{(a+b)\varphi_0} + bU_0e^{b\varphi_0} \\ &+ (ad_1 + b)he^{(ad_1+b)\varphi_0} = 0 \end{aligned} \quad (3.39)$$

and

$$\partial_\phi U_{eff}|_{\varphi_0, \phi_0} = e^{b\varphi_0} \frac{\partial U}{\partial \phi} \Big|_{\phi_0} = 0 ; \implies \frac{\partial U}{\partial \phi} \Big|_{\phi_0} = 0 . \quad (3.40)$$

Here,  $\varphi_0$  and  $\phi_0$  define the extremum position. It clearly follows from eq. (3.40) that  $\phi_0$  is defined by equation  $\partial U / \partial \phi = 0$  which does not depend on  $\varphi$ . Therefore, extrema of the effective potential may take place only for  $\phi_0$  which correspond to the solutions  $X_p$  of eq. (3.34) and different possible extrema should lie on the sections  $X_p = \text{const}$ . So, let us take  $X_+$  (with  $s = -1$  and  $q = +1$ ) which defines the minimum of  $U_{eff}$  in the previous section. Hence,  $U_0$  in eq. (3.39) is the same as for eq. (3.35).

Let us define now  $\varphi_0$  from eq. (3.39). With the help of inequalities (3.37) and (3.38) one can write  $h = nU_0$  where  $n \in (1/9, 1/3)$ . Taking also into account relations (3.35), eq. (3.39) can be written as

$$y^4 - \left(1 + \frac{1}{3n}\right)y + \frac{1}{3n} = 0 , \quad (3.41)$$

where the definition is done  $y \equiv \exp(a\varphi_0) = \exp(\varphi_0/\sqrt{3})$  and put  $d_1 = D_0 = 4$ . Because  $y = 1$  is the solution of eq. (3.41), the remaining three solutions

satisfy the following cubic equation:

$$y^3 + y^2 + y - \frac{1}{3n} = 0. \quad (3.42)$$

It can be easily verified that the only real solution of this equation is

$$y_0 = \frac{1}{3} \left( -1 - 2\nu + \frac{1}{\nu} \right), \quad (3.43)$$

where

$$\begin{aligned} \nu &= \frac{2^{1/3}n}{(9n^2 + 7n^3 + 3\sqrt{9n^4 + 14n^6 + 9n^6})^{1/3}}; \\ n &\in \left( \frac{1}{9}, \frac{1}{3} \right). \end{aligned} \quad (3.44)$$

Thus  $\varphi_0(y_0)$  and  $\phi_0(X_+)$  define new extremum of  $U_{eff}$ . To clarify the type of this extremum one should check signs of the second derivatives of the effective potential in this point. First of all let us remind that in the case  $c = 0$  mixed second derivative disappears. Concerning second derivative with respect to  $\phi$ , one obtains

$$J_{22} \equiv \left. \frac{\partial^2 U_{eff}}{\partial \phi^2} \right|_{\varphi_0, \phi_0} = e^{b\varphi_0} \left. \frac{\partial^2 U}{\partial \phi^2} \right|_{\phi_0} > 0 \quad (3.45)$$

because in previous section was obtained  $\partial^2 U / \partial \phi^2|_{\phi_0(X_+)} > 0$ . Second derivative with respect to  $\varphi$  reads

$$\begin{aligned} J_{11} &\equiv \left. \frac{\partial^2 U_{eff}}{\partial \varphi^2} \right|_{\varphi_0, \phi_0} = y_0^2 U_0 \left[ -6 \left( \frac{1}{3} + n \right) y_0 + \frac{4}{3} \right. \\ &\quad \left. + 12ny_0^4 \right] = 2y_0^2 U_0 \left[ (3n + 1)y_0 - \frac{4}{3} \right], \end{aligned} \quad (3.46)$$

where eq. (3.41) is taken into account. Simple analysis shows that  $(3n + 1)y_0 < 4/3$  for  $n \in (1/9, 1/3)$ . Keeping in mind that  $U_0 > 0$  one obtains  $J_{11} < 0$ . Therefore, the extremum is the saddle surface<sup>11</sup>. Figure 3.7 demonstrates contour plot of the effective potential in the vicinity of the local minimum and the saddle point.

---

<sup>11</sup> Similar analysis performed for the branch with  $s = +1$ ,  $q = -1$  (right dashed line in the Fig. 3.6) shows the existence of the global negative minimum with  $\varphi \neq 0$  along the section  $X_- = const$ .

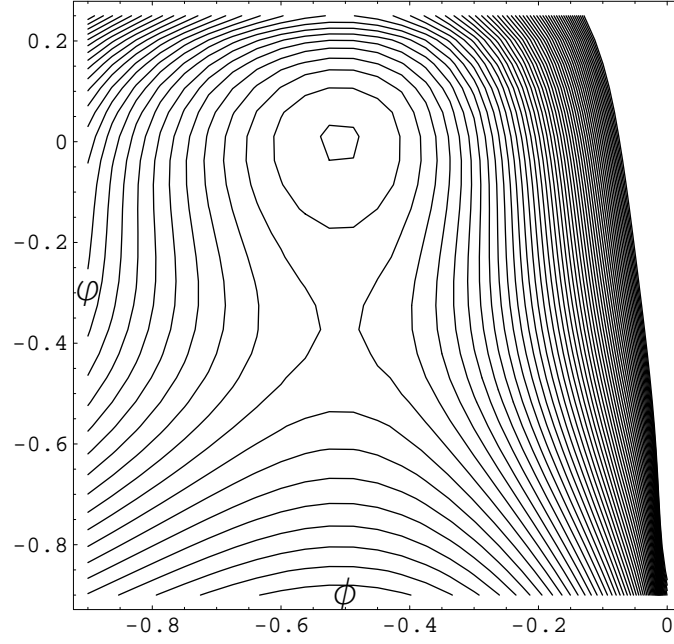


Figure 3.7: Contour plot of the effective potential  $U_{eff}(\varphi, \phi)$  for parameters  $z = 1.99$  ( $\Lambda_D = 1.99/2$ ,  $|\mu| = 1$ ),  $D_0 = d_1 = 4$  and  $h = U_0/6$ . The rest of parameters follows from relations (3.35). The branch corresponding to  $s = -1$ ,  $q = +1$  is chosen. This plot clearly shows the minimum and the saddle points of the effective potential.

Therefore, very interesting possibility become possible for the production of an inflating domain wall in the vicinity of the saddle point. The mechanism for the production of the domain walls is the following [87, 88]. If the scalar field  $\varphi$  is randomly distributed, some part of the Universe will roll down to  $\varphi = 0$ , while in others parts it will run away to infinity. Between any two such regions there will appear domain walls. In Ref. [89], it was shown for the case of a double-well potential  $V_{dw}(\varphi) = (\lambda/4)(\varphi^2 - \xi^2)^2$  that a domain wall will undergo inflation if the distance  $\xi$  between the minimum and the maximum of  $V_{dw}$  exceeds a critical value  $\xi_{cr} = 0.33M_{Pl} \rightarrow \kappa_0\xi_{cr} = 1.65$ . In this case it means that the distance  $|\varphi_0|$  between the local minimum and the saddle point should be greater than  $\xi_{cr}$ :  $|\varphi_0| \geq 1.65$ . Unfortunately, for this model  $\varphi_0(n) < 1.65$  if  $n \in (1/9, 1.3)$ . For example, in the most interesting case  $n \rightarrow 1/3$  (where  $\Lambda_{eff} \rightarrow 0$  (see eq. (3.35))) one obtains  $|\varphi_0| \rightarrow 1.055$  which is less than  $\xi_{cr}$ . Moreover, the domain wall is not thick enough in comparison with the Hubble radius. The ration of the characteristic thickness of the wall to the

horizon scale is given by  $r_w H \approx |U_{eff}/3\partial_{\varphi\varphi}U_{eff}|_{\varphi_0,\phi(X_+)}^{1/2} \rightarrow 0.454$  for  $n \rightarrow 1/3$  which is less than the critical value 0.48 for a double-well potential. Thus, here there is no a sufficiently large (for inflation) quasi-homogeneous region of the energy density. And the given potential is too steep. Obviously, the slow roll parameter  $\epsilon \approx (1/2) (\partial_{\varphi}U_{eff}/U_{eff})_{\varphi_0,\phi_0}^2$  is equal to zero in the saddle point. However, another slow roll parameter  $\eta \approx |\partial_{\varphi\varphi}^2 U_{eff}/U_{eff}|_{\varphi_0,\phi_0} \rightarrow -1.617$  for  $n \rightarrow 1/3$ . Therefore, the domain walls do not inflate in contrast to the case  $R^4$  in Ref. [90–94].

In Fig. 3.8 the comparison is presented between the potential (solid line) and a double-well potential (dashed line) in the case  $n = (1 - 0.001)/3$ . It is shown that the given potential is flatter than a double-well potential around the saddle point. However, calculations show that it is not enough for inflation.

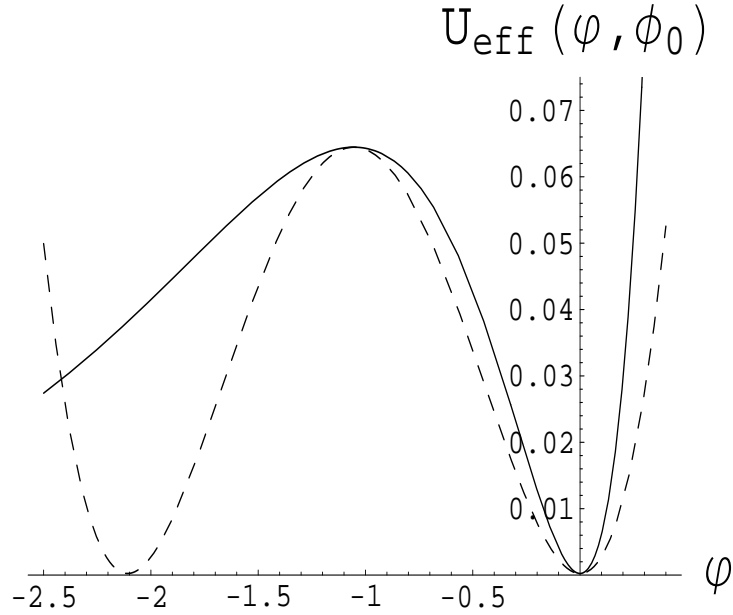


Figure 3.8: Comparison of the potential  $U_{eff}(\varphi, \phi_0)$  with a double well potential for parameters  $z = 1.99$  ( $\Lambda_D = 1.99/2$ ,  $|\mu| = 1$ ),  $D_0 = d_1 = 4$  and  $n = (1 - 0.001)/3$ .

## Summary

It was shown that positive minimum of the effective potential plays the double role in this model. Firstly, it provides the freezing stabilization of

the internal spaces which enables to avoid the problem of the fundamental constant variation in multidimensional models [95, 96]. Secondly, it ensures the stage of the cosmic acceleration. However, to get the present-day accelerating expansion, the parameters of the model should be fine tuned. Maybe, this problem can be resolved with the help of the idea of landscape of vacua [84, 85].

It was additionally found that given effective potential has the saddle point. It results in domain walls which separates regions with different vacua in the Universe. These domain walls do not undergo inflation because the effective potential is not flat enough around the saddle point.

It is worth of noting that minimum in Fig. 3.6 (left solid line) is metastable. In other words, classically it is stable but there is a possibility for quantum tunnelling both in  $\phi$  and in  $\varphi$  directions (see Fig. 3.7). One can avoid this problem in  $\phi$  direction in the case of parameters  $z \geq 2$  (see footnote 10). However, tunnelling in  $\varphi$  direction (through the saddle) is still valid because  $U_{eff}(\varphi, \phi_0) \approx e^{b\varphi} U(\phi_0) \rightarrow 0$  for  $\varphi \rightarrow -\infty$  which is less than any positive  $\Lambda_{eff}$ . It may result in the materialization of bubbles of the new phase in the metastable one (see e.g. [97]). Thus, late-time acceleration is possible only if characteristic lifetime of the metastable stage is greater than the age of the Universe. Careful investigation of this problem (including gravitational effects) is rather laborious task which needs a separate consideration. As it was mentioned in footnote 11, there is also the global negative minimum for right dashed line in Fig. 3.6 (it corresponds to the point  $(\varphi = 0.67, \phi = 1.66)$  for parameters taken in Fig. 3.7). This minimum is stable both in classical and quantum limits. However, the acceleration is absent because of its negativity.

Another very interesting feature of the model under consideration consists in multi-valued form of the effective potential. As it can be easily seen from eqs. (3.7) and (3.11), for each choice of parameter  $\mu$  potential  $U(\phi)$  (and consequently  $U_{eff}$ ) has two branches ( $q = \pm 1$ ) which joint smoothly with each other at  $\phi = 0$  (see Fig. 3.6). It gives very interesting possibility to investigate transitions from one branch to another one by analogy with

catastrophe theory or similar to the phase transitions in statistical theory. However, as it was mentioned above, in this particular model the point  $\phi = 0$  corresponds to the singularity  $\bar{R}, R \rightarrow \pm\infty$ . Thus, the analog of the second order smooth phase transition through the point  $\phi = 0$  is impossible in this model. Nevertheless, there is still a possibility for the analog of the first order transition via quantum jumps from one branch to another one.

To complete, let us investigate some limiting cases. Firstly, the limit  $h \rightarrow 0$  (for arbitrary  $D_0$  and  $d_1$ ) where the form-fields are absent. From eqs. (3.15) - (3.21) one obtains the following system of equations:

$$R_1 = \frac{2b}{a+b}U_0(X), \quad U_{eff}|_{extr} = \frac{a}{a+b}U_0(X) \quad (3.47)$$

and

$$\begin{aligned} J_{11} &= -abU_0(X), \quad J_{21} = 0, \\ J_{22} &= \left[ B(A-B) - \frac{sAB}{2X^2}(1+sX^2) \right] U_0(X). \end{aligned} \quad (3.48)$$

Since for minimum should hold true the condition  $J_{11} > 0$ , one arrives at the conclusion:  $R_1, U_0, U_{eff} < 0$ . Consequently, the minimum of the effective potential as well as the effective cosmological constant is negative and accelerating expansion is absent in this limit. Therefore, the presence of the form-fields is the necessary condition for the acceleration of the Universe in the position of the freezing stabilization of the internal spaces. Additionally, it can be easily seen that the extremum position equation takes the same form as (3.34). Simple analysis show that minimum takes place for the branch:  $s = +1$  (i.e.  $\mu > 0$ ),  $p = -1$ ,  $q = -1$  and  $z \in (-\infty, +\infty)$ . If additionally is imposed that  $z \rightarrow 0$  (i.e.  $\Lambda_D \rightarrow 0$  and  $\mu$  is fixed) then the results of Ref. [37] are reproduced.

## CHAPTER 4

### INFLATION IN MULTIDIMENSIONAL COSMOLOGICAL MODELS

In this chapter, a multidimensional cosmological models are considered with linear, nonlinear quadratic  $\bar{R}^2$  and quartic  $\bar{R}^4$  actions with a monopole form field as a matter source; and pure gravitational model with  $\bar{R}^2 + \bar{R}^4$  nonlinearities. The inflation is investigated in these models. It is shown that  $\bar{R}^2$  and  $\bar{R}^4$  models can have up to 10 and 22 e-foldings, respectively. These values are not sufficient to solve the homogeneity and isotropy problem but big enough to explain the recent CMB data. Additionally,  $\bar{R}^4$  model can provide conditions for eternal topological inflation. However, the main drawback of the given inflationary models consists in a value of spectral index  $n_s$  which is less than observable now  $n_s \approx 1$ . For example, in the case of  $\bar{R}^4$  model one finds  $n_s \approx 0.61$ .

For the model  $\bar{R}^2 + \bar{R}^4$ , the effective scalar degree of freedom  $\phi$  (scalaron) has a multi-valued potential  $U(\phi)$  consisting of a number of branches. These branches are fitted with each other in the branching and monotonic points. In the case of four-dimensional space-time, it is shown that the monotonic points are penetrable for scalaron while in the vicinity of the branching points scalaron has the bouncing behavior and cannot cross these points. Moreover, there are branching points where scalaron bounces an infinite number of times with decreasing amplitude and the Universe asymptotically approaches the de Sitter stage. Such accelerating behavior is called bouncing inflation. For this accelerating expansion there is no need for original potential  $U(\phi)$  to have a minimum or to check the slow-roll conditions. A necessary condition for such inflation is the existence of the branching points. This is a new type of inflation. It is shown that bouncing inflation takes place both in the Einstein and Brans-Dicke frames.



### 4.1. Linear model

To start with, let us define the topology of the given models and consider a factorizable  $D$ -dimensional metric

$$g^{(D)} = g^{(0)}(x) + L_{Pl}^2 e^{2\beta^1(x)} g^{(1)}, \quad (4.1)$$

which is defined on a warped product manifold  $M = M_0 \times M_1$ .  $M_0$  describes external  $D_0$ -dimensional space-time (usually  $D_0 = 4$ ) and  $M_1$  corresponds to  $d_1$ -dimensional internal space which is a flat orbifold<sup>12</sup> with branes in fixed points. Scale factor of the internal space depends on coordinates  $x$  of the external space-time:  $a_1(x) = L_{Pl} e^{\beta^1(x)}$ , where  $L_{Pl}$  is the Planck length.

First, let us consider the linear model  $f(R) = R$  with  $D$ -dimensional action of the form

$$S = \frac{1}{2\kappa_D^2} \int_M d^D x \sqrt{|g^{(D)}|} \left\{ R[g^{(D)}] - 2\Lambda_D \right\} + S_m + S_b. \quad (4.2)$$

$\Lambda_D$  is a bare cosmological constant<sup>13</sup>. In the spirit of Universal Extra Dimension models [98–102], the Standard Model fields are not localized on the branes but can move in the bulk. The compactification of the extra dimensions on orbifolds has a number of very interesting and useful properties, e.g. breaking (super)symmetry and obtaining chiral fermions in four dimensions (see e.g. paper by H.-C. Cheng et al in [98–102]). The latter property gives a possibility to avoid famous no-go theorem of KK models (see e.g. [103, 104]). Additional arguments in favor of UED models are listed in [105].

Following a generalized Freund-Rubin ansatz [80] to achieve a spontaneous compactification  $M \rightarrow M = M_0 \times M_1$ , one endows the extra dimensions with real-valued solitonic form field  $F^{(1)}$  with an action:

$$S_m = -\frac{1}{2} \int_M d^D x \sqrt{|g^{(D)}|} \frac{1}{d_1!} \left( F^{(1)} \right)^2, \quad (4.3)$$

<sup>12</sup>For example,  $S^1/Z_2$  and  $T^2/Z_2$  which represent circle and square folded onto themselves due to  $Z_2$  symmetry.

<sup>13</sup>Such cosmological constant can originate from  $D$ -dimensional form field which is proportional to the  $D$ -dimensional world-volume:  $F^{MN\dots Q} = (C/\sqrt{|g^{(D)}|})\epsilon^{MN\dots Q}$ . In this case the equations of motion gives  $C = \text{const}$  and  $F^2$  term in action is reduced to  $(1/D!)F_{MN\dots Q}F^{MN\dots Q} = -C^2$ .

This form field is nested in  $d_1$ -dimensional factor space  $M_1$ , i.e.  $F^{(1)}$  is proportional to the world-volume of the internal space. In this case  $(1/d_1!) (F^{(1)})^2 = \bar{f}_1^2/a_1^{2d_1}$ , where  $\bar{f}_1$  is a constant of integration [58].

Branes in fixed points contribute in action functional (4.2) in the form [86]:

$$S_b = \sum_{\substack{\text{fixed} \\ \text{points}}} \int_{M_0} d^4x \sqrt{|g^{(0)}(x)|} \left. L_b \right|_{\substack{\text{fixed} \\ \text{point}}}, \quad (4.4)$$

where  $g^{(0)}(x)$  is induced metric (which for the given geometry (4.1) coincides with the metric of the external space-time in the Brans-Dicke frame) and  $L_b$  is the matter Lagrangian on the brane. In what follows, that the case where branes are only characterized by their tensions  $L_{b(k)} = -\tau_{(k)}$ ,  $k = 1, 2, \dots, m$  is considered, where  $m$  is the number of branes.

Let  $\beta_0^1$  be the internal space scale factor at the present time and  $\bar{\beta}^1 = \beta^1 - \beta_0^1$  describes fluctuations around this value. Then after dimensional reduction of the action (4.1) and conformal transformation to the Einstein frame  $g_{\mu\nu}^{(0)} = (e^{d_1 \bar{\beta}^1})^{-2/(D_0-2)} \tilde{g}_{\mu\nu}^{(0)}$ , one arrives at effective  $D_0$ -dimensional action of the form

$$\begin{aligned} S_{eff} &= \frac{1}{2\kappa_0^2} \int_{M_0} d^{D_0}x \sqrt{|\tilde{g}^{(0)}|} \left\{ R[\tilde{g}^{(0)}] \right. \\ &\quad \left. - \tilde{g}^{(0)\mu\nu} \partial_\mu \varphi \partial_\nu \varphi - 2U_{eff}(\varphi) \right\}, \end{aligned} \quad (4.5)$$

where scalar field  $\varphi$  is defined by the fluctuations of the internal space scale factor:

$$\varphi \equiv \sqrt{\frac{d_1(D-2)}{D_0-2}} \bar{\beta}^1 \quad (4.6)$$

and  $G := \kappa_0^2/8\pi := \kappa_D^2/(8\pi V_{d_1})$  ( $V_{d_1}$  is the internal space volume at the present time) denotes the  $D_0$ -dimensional gravitational constant. The effective potential  $U_{eff}(\varphi)$  reads (hereafter  $D_0 = 4$ ):

$$\begin{aligned} U_{eff}(\varphi) &= e^{-\sqrt{\frac{2d_1}{d_1+2}} \varphi} \left[ \Lambda_D + f_1^2 e^{-2\sqrt{\frac{2d_1}{d_1+2}} \varphi} \right. \\ &\quad \left. - \lambda e^{-\sqrt{\frac{2d_1}{d_1+2}} \varphi} \right], \end{aligned} \quad (4.7)$$

where  $f_1^2 \equiv \kappa_D^2 \bar{f}_1^2 / a_{(0)1}^{2d_1}$  and  $\lambda \equiv -\kappa_0^2 \sum_{k=1}^m \tau_{(k)}$ .

Now, this potential should be investigated from the point of the external space inflation and the internal space stabilization. First, it is clear that internal space is stabilized if  $U_{eff}(\varphi)$  has a minimum with respect to  $\varphi$ . The position of minimum should correspond to the present day value  $\varphi = 0$ . Additionally, it needs to be demanded that the value of the effective potential in the minimum position is equal to the present day dark energy value  $U_{eff}(\varphi = 0) \sim \Lambda_{DE} \sim 10^{-57} \text{cm}^{-2}$ . However, it results in very flat minimum of the effective potential which in fact destabilizes the internal space [86]. To avoid this problem, the case of zero minimum  $U_{eff}(\varphi = 0) = 0$  shall be considered.

The extremum condition  $dU_{eff}/d\varphi|_{\varphi=0} = 0$  and zero minimum condition  $U_{eff}(\varphi = 0) = 0$  result in a system of equations for parameters  $\Lambda_D, f_1^2$  and  $\lambda$  which has the following solution:

$$\Lambda_D = f_1^2 = \lambda/2. \quad (4.8)$$

For the mass of scalar field excitations (gravexcitons/radions) one obtains:  $m^2 = d^2U_{eff}/d\varphi^2|_{\varphi=0} = (4d_1/(d_1 + 2))\Lambda_D$ . In Fig. 4.9 the effective potential (4.7) is presented in the case  $d_1 = 3$  and  $\Lambda_D = 10$ . It is worth of noting that usually scalar fields in the present paper are dimensionless<sup>14</sup> and  $U_{eff}, \Lambda_D, f_1^2, \lambda$  are measured in  $M_{Pl}^2$  units.

Let us turn now to the problem of the external space inflation. As far as the external space corresponds to our Universe, the metric  $\tilde{g}^{(0)}$  is taken in the spatially flat Friedmann-Robertson-Walker form with scale factor  $a(t)$ . Scalar field  $\varphi$  depends also only on the synchronous/cosmic time  $t$  (in the Einstein frame).

It can be easily seen that for  $\varphi \gg 0$  (more precisely, for  $\varphi > \varphi_{max} = \sqrt{(d_1 + 2)/2d_1} \ln 3$ ) the potential (4.7) behaves as

$$U_{eff}(\varphi) \approx \Lambda_D e^{-\sqrt{q}\varphi}, \quad (4.9)$$

with

$$q := \frac{2d_1}{d_1 + 2}. \quad (4.10)$$

---

<sup>14</sup>To restore dimension of scalar fields one should multiply their dimensionless values by  $M_{Pl}/\sqrt{8\pi}$ .

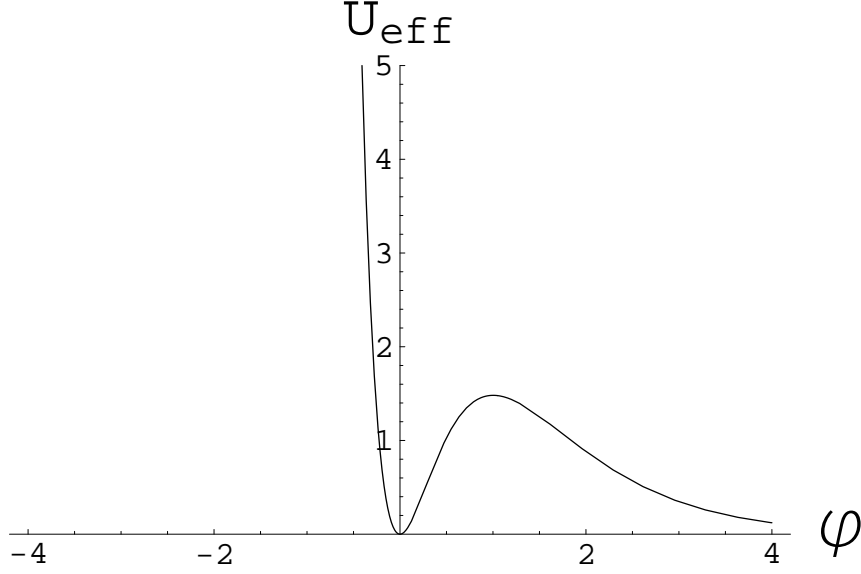


Figure 4.9: The form of the effective potential (4.7) in the case  $d_1 = 3$  and  $\Lambda_D = f_1^2 = \lambda/2 = 10$ .

It is well known (see e.g. [106–109]) that for such exponential potential scale factor has the following asymptotic form:

$$a(t) \sim t^{2/q}. \quad (4.11)$$

Thus, the Universe undergoes the power-law inflation if  $q < 2$ . Precisely this condition holds for eq. (4.10) if  $d_1 \geq 1$ .

It can be easily verified that  $\varphi > \varphi_{max}$  is the only region of the effective potential where inflation takes place. Indeed, in the region  $\varphi < 0$  the leading exponents are too large, i.e. the potential is too steep. The local maximum of the effective potential  $U_{eff}|_{max} = (4/27)\Lambda_D$  at  $\varphi_{max} = \sqrt{(d_1 + 2)/2d_1} \ln 3$  is also too steep for inflation because the slow-roll parameter  $\eta_{max} = \frac{1}{U_{eff}} \frac{d^2 U_{eff}}{d\varphi^2} \Big|_{max} = -\frac{3d_1}{d_1 + 2} \Rightarrow 1 \leq |\eta_{max}| < 3$  and does not satisfy the inflation condition  $|\eta| < 1$ . Topological inflation is also absent here because the distance between global minimum and local maximum  $\varphi_{max} = \sqrt{(d_1 + 2)/2d_1} \ln 3 \leq 1.35$  is less than critical value  $\varphi_{cr} \geq 1.65$  (see [54, 56, 89]). It is worth of noting that  $\eta_{max}$  and  $\varphi_{max}$  depend only on the number of dimensions  $d_1$  of the internal space and do not depend on the height of the local maximum (which is proportional to  $\Lambda_D$ ).

Therefore, there are two distinctive regions in this model. In the first

region, at the left of the maximum in the vicinity of the minimum, scalar field undergoes the damped oscillations. These oscillations have the form of massive scalar fields in our Universe (in [110] these excitations were called gravitational excitons and later (see e.g. [111]) these geometrical moduli oscillations were also named radions). Their life-time with respect to the decay  $\varphi \rightarrow 2\gamma$  into radiation is [63, 112, 113]  $\tau \sim (M_{Pl}/m)^3 T_{Pl}$ . For example, in given case one obtains  $\tau \sim 10\text{ s}, 10^{-2}\text{ s}$  for  $m \sim 10\text{ TeV}, 10^2\text{ TeV}$  correspondingly, where  $m^2 = (4d_1/(d_1+2))\Lambda_D$ . Therefore, this is the graceful exit region. Here, the internal space scale factor, after decay its oscillations into radiation, is stabilized at the present day value and the effective potential vanishes due to zero minimum. In second region, at the right of the maximum of the potential, our Universe undergoes the power-low inflation. However, it is impossible to transit from the region of inflation to the graceful exit region because given inflationary solution satisfies the following condition  $\dot{\varphi} > 0$ . There is also serious additional problem connected with obtained inflationary solution. The point is that for the exponential potential of the form (4.9), the spectral index reads [106, 108]<sup>15</sup>:

$$n_s = \frac{2 - 3q}{2 - q}. \quad (4.12)$$

In the case (4.10), it results in  $n_s = 1 - d_1$ . Obviously, for  $d_1 \geq 1$  this value is very far from observable data  $n_s \approx 1$ . Therefore, it is necessary to generalize given linear model.

## 4.2. Quadratic model

One of possible ways for generalizing of the effective potential making it more complicated and having more reach structure is an introduction of an additional minimal scalar field  $\phi$ . It is possible to do "by hand", inserting

---

<sup>15</sup>With respect to conformal time, solution (4.11) reads  $a(\eta) \sim \eta^{1+\beta}$  where  $\beta = -(4-q)/(2-q)$ . It was shown in [114] that for such inflationary solution (with  $q < 2$ ) the spectral index of density perturbation is given by  $n_s = 2\beta + 5$  resulting again in (4.12).

minimal scalar field  $\phi$  with a potential  $U(\phi)$  in linear action (4.2)<sup>16</sup>. Then, effective potential takes the form

$$U_{eff}(\varphi, \phi) = e^{-\sqrt{\frac{2d_1}{d_1+2}}\varphi} \left[ U(\phi) + f_1^2 e^{-2\sqrt{\frac{2d_1}{d_1+2}}\varphi} - \lambda e^{-\sqrt{\frac{2d_1}{d_1+2}}\varphi} \right], \quad (4.13)$$

where  $\Lambda_D = 0$  in (4.2).

However, it is well known that scalar field  $\phi$  can naturally originate from the nonlinearity of higher-dimensional models where the Hilbert-Einstein linear lagrangian  $\bar{R}$  is replaced by nonlinear one  $f(\bar{R})$ . These nonlinear theories are equivalent to the linear ones with a minimal scalar field (which represents additional degree of freedom of the original nonlinear theory). It is not difficult to verify (see e.g. [57, 58]) that nonlinear model

$$\begin{aligned} S &= \frac{1}{2\kappa_D^2} \int_M d^D x \sqrt{|\bar{g}^{(D)}|} f(\bar{R}) \\ &- \frac{1}{2} \int_M d^D x \sqrt{|g^{(D)}|} \frac{1}{d_1!} \left( F^{(1)} \right)^2 \\ &- \sum_{k=1}^m \int_{M_0} d^4 x \sqrt{|g^{(0)}(x)|} \tau_{(k)} \end{aligned} \quad (4.14)$$

is equivalent to a linear one with conformally related metric

$$g_{ab}^{(D)} = e^{2A\phi/(D-2)} \bar{g}_{ab}^{(D)} \quad (4.15)$$

plus minimal scalar field  $\phi = \ln[df/d\bar{R}]/A$  with a potential

$$U(\phi) = \frac{1}{2} e^{-B\phi} [\bar{R}(\phi) e^{A\phi} - f(\bar{R}(\phi))] , \quad (4.16)$$

where

$$\begin{aligned} A &= \sqrt{\frac{(D-2)}{(D-1)}} = \sqrt{\frac{(d_1+2)}{d_1+3}}; \\ B &= \frac{D}{\sqrt{(D-2)(D-1)}} = A \frac{(d_1+4)}{(d_1+2)}. \end{aligned} \quad (4.17)$$

---

<sup>16</sup>If such scalar field is the only matter field in these models, it is known (see e.g. [57, 115]) that the effective potential can has only negative minimum. i.e. the models are asymptotical AdS. To uplift this minimum to nonnegative values, it is necessary to add form-fields [58].

After dimensional reduction of this linear model, one obtains an effective  $D_0$ -dimensional action of the form

$$S_{eff} = \frac{1}{2\kappa_0^2} \int_{M_0} d^{D_0}x \sqrt{|\tilde{g}^{(0)}|} \left[ R[\tilde{g}^{(0)}] - \tilde{g}^{(0)\mu\nu} \partial_\mu \varphi \partial_\nu \varphi - \tilde{g}^{(0)\mu\nu} \partial_\mu \phi \partial_\nu \phi - 2U_{eff}(\varphi, \phi) \right], \quad (4.18)$$

with effective potential exactly of the form (4.13). It is worth to note that it is supposed that matter fields are coupled to the metric  $g^{(D)}$  of the linear theory (see also analogous approach in [116]). Because in all considered below models both fields  $\varphi$  and  $\phi$  are stabilized in the minimum of the effective potential, such convention results in a simple redefinition/rescaling of the matter fields and effective four-dimensional fundamental constants. After such stabilization, the Einstein and Brans-Dicke frames are equivalent each other (metrics  $g^{(0)}$  and  $\tilde{g}^{(0)}$  coincide with each other), and linear  $g^{(D)}$  and nonlinear  $\bar{g}^{(D)}$  metrics in (4.15) are related via constant prefactor (models became asymptotically linear)<sup>17</sup>.

Let us consider first the quadratic theory

$$f(\bar{R}) = \bar{R} + \xi \bar{R}^2 - 2\Lambda_D. \quad (4.19)$$

For this model the scalar field potential (4.16) reads:

$$U(\phi) = \frac{1}{2} e^{-B\phi} \left[ \frac{1}{4\xi} (e^{A\phi} - 1)^2 + 2\Lambda_D \right]. \quad (4.20)$$

It was proven [115] that the internal space is stabilized if the effective potential (4.13) has a minimum with respect to both fields  $\varphi$  and  $\phi$ . It can be easily seen from the form of  $U_{eff}(\varphi, \phi)$  that minimum  $\phi_0$  of the potential  $U(\phi)$  coincides with the minimum of  $U_{eff}(\varphi, \phi) : dU/d\phi|_{\phi_0} = 0 \rightarrow \partial_\phi U_{eff}|_{\phi_0} = 0$ . For minimum  $U(\phi_0)$  one obtains [57]:

$$U(\phi_0) = \frac{1}{8\xi} x_0^{\frac{-D}{D-2}} [(x_0 - 1)^2 + 8\xi\Lambda_D], \quad (4.21)$$

where the denotation  $x_0 := \exp(A\phi_0)$  is applied, taking into account that  $\exp(A\phi_0) = \left( A - B + \sqrt{A^2 + (2A - B)8sB\xi\Lambda_D} \right) / (2A - B)$ . It is the

---

<sup>17</sup>However, small quantum fluctuations around the minimum of the effective potential distinguish these metrics.

global minimum and the only extremum of  $U(\phi)$ . Nonnegative minimum of the effective potential  $U_{eff}$  takes place for positive  $\xi, \Lambda_D > 0$ . If  $\xi, \Lambda_D > 0$ , the potential  $U(\phi)$  has asymptotic behavior  $U(\phi) \rightarrow +\infty$  for  $\phi \rightarrow \pm\infty$ .

The relations (4.8), where one should make the substitution  $\Lambda_D \rightarrow U(\phi_0)$ , are the necessary and sufficient conditions of the zero minimum of the effective potential  $U_{eff}(\varphi, \phi)$  at the point  $(\varphi = 0, \phi = \phi_0)$ . Thus, if parameters of the quadratic models satisfy the conditions  $U(\phi_0) = f_1^2 = \lambda/2$ , one arrives at zero global minimum:  $U_{eff}(0, \phi_0) = 0$ .

It is clear that profile  $\phi = \phi_0$  of the effective potential  $U_{eff}$  has a local maximum in the region  $\varphi > 0$  because  $U_{eff}(\varphi, \phi = \phi_0) \rightarrow 0$  if  $\varphi \rightarrow +\infty$ . Such profile has the form shown in Fig. 4.9. Thus, the effective potential  $U_{eff}$  has a saddle point  $(\varphi = \varphi_{max}, \phi = \phi_0)$  where  $\varphi_{max} = \sqrt{(d_1 + 2)/2d_1} \ln 3$ . At this point  $U_{eff}|_{max} = (4/27)U(\phi_0)$ . The Figure 4.10 demonstrates the typical contour plot of the effective potential (4.13) with the potential  $U(\phi)$  of the form (4.20) in the vicinity of the global minimum and the saddle point.

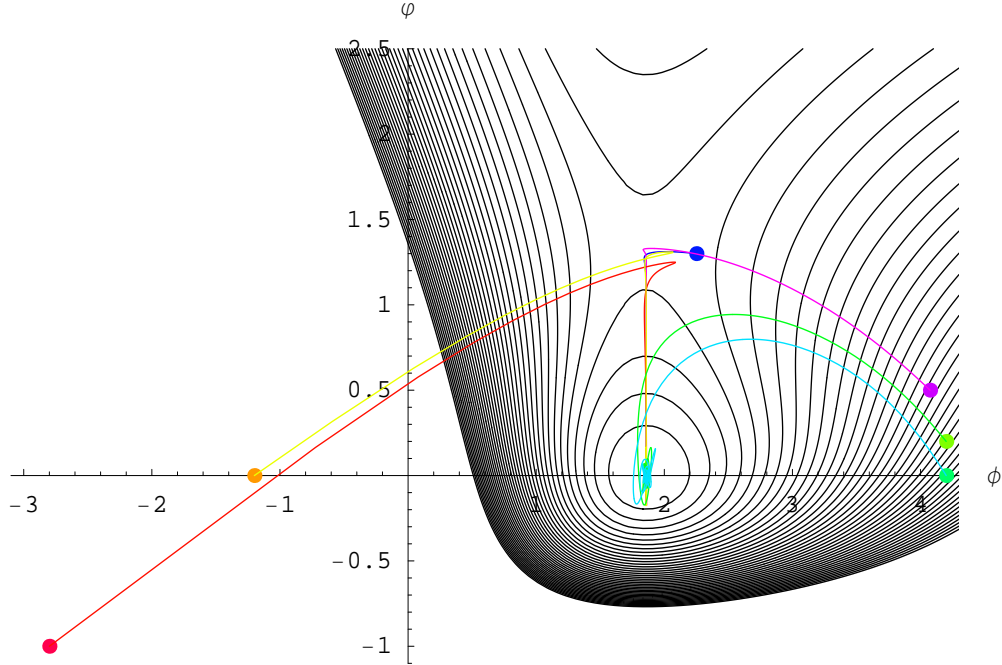


Figure 4.10: Contour plot of the effective potential  $U_{eff}(\varphi, \phi)$  (4.13) with potential  $U(\phi)$  of the form (4.20) for parameters  $d_1 = 1, \xi\Lambda_D = 1$  and relations  $U(\phi_0) = f_1^2 = \lambda/2$ . This plot clearly shows the global minimum and the saddle. The colored lines describe trajectories for scalar fields starting at different initial conditions.



Let us discuss now a possibility of the external space inflation in this model. It can be easily realized that for all models of the form (4.13) in the case of local zero minimum at  $(\varphi = 0, \phi_0)$ , the effective potential will also have a saddle point at  $(\varphi = \varphi_{max}, \phi_0)$  with  $\varphi_{max} = \sqrt{(d_1 + 2)/2d_1} \ln 3 < \varphi_{cr} = 1.65$  and the slow-roll parameter  $|\eta_\varphi|$  in this point cannot be less than 1:  $|\eta_\varphi| = 3d_1/(d_1 + 2) \geq 1$ . Therefore, such saddles are too steep (in the section  $\phi = \phi_0$ ) for the slow-roll and topological inflations. However, as one shall see below, a short period of de-Sitter-like inflation is possible if one start not precisely at the saddle point but first move in the vicinity of the saddle along the line  $\varphi \approx \varphi_{max}$  with subsequent turn into zero minimum along the line  $\phi \approx \phi_0$ . Similar situation happens for trajectories from different regions of the effective potential which can reach this saddle and spend here a some time (moving along the line  $\varphi \approx \varphi_{max}$ ).

Let us consider now regions where the following conditions take place:

$$U(\phi) \gg f_1^2 e^{-2\sqrt{\frac{2d_1}{d_1+2}}\varphi}, \quad \lambda e^{-\sqrt{\frac{2d_1}{d_1+2}}\varphi}. \quad (4.22)$$

For the potential (4.20) these regions exist both for negative and positive  $\phi$ . In the case of positive  $\phi$  with  $\exp(A\phi) \gg \max \{1, (8\xi\Lambda_D)^{1/2}\}$  one obtains

$$U_{eff} \approx \frac{1}{8\xi} e^{-\sqrt{q}\varphi} e^{\sqrt{q_1}\phi}, \quad (4.23)$$

where  $q$  is defined by Eq. (4.10),  $q_1 := (2A - B)^2 = d_1^2/[(d_1 + 2)(d_1 + 3)]$  and  $q > q_1$ . For potential (4.23) the slow-roll parameters are<sup>18</sup>:

$$\epsilon \approx \eta_1 \approx \eta_2 \approx \frac{q}{2} + \frac{q_1}{2} \quad (4.24)$$

and satisfy the slow-roll conditions  $\epsilon, \eta_1, \eta_2 < 1$ . As far as it is known, there are no analytic solutions for such two-scalar-field potential. Anyway, from the form of the potential (4.23) and condition  $q > q_1$  one can get an estimation  $a \approx t^s$  with  $s \gtrsim 2/q$  (e.g.  $2/q = 3, 2, 5/3$  for  $d_1 = 1, 2, 3$ , respectively).

<sup>18</sup>In the case of  $n$  scalar fields  $\varphi_i$  ( $i = 1, \dots, n$ ) with a flat ( $\sigma$ -model) target space, the slow-roll parameters for the spatially flat Friedmann Universe read (see e.g. [57, 115]):  $\epsilon \equiv \frac{2}{H^2} \sum_{i=1}^n (\partial_i H)^2 \approx \frac{1}{2} |\partial U|^2 / U^2$ ;  $\eta_i \equiv -\ddot{\varphi}_i / (H\dot{\varphi}_i) = 2\partial_{ii}^2 H / H \approx -\epsilon + \sum_{j=1}^n \partial_{ij}^2 U \partial_j U / (U \partial_i U)$ , where  $\partial_i := \partial / \partial \varphi_i$  and  $|\partial U|^2 = \sum_{i=1}^n (\partial_i U)^2$ . In some papers (see e.g. [117–119]) it was introduced a "cumulative" parameter  $\eta \equiv -\sum_{i=1}^n \ddot{\varphi}_i \dot{\varphi}_i / (H|\dot{\varphi}|^2) \approx -\epsilon + \sum_{i,j=1}^n (\partial_{ij}^2 U)(\partial_i U)(\partial_j U) / (U|\partial U|^2)$ , where  $|\dot{\varphi}|^2 = \sum_{i=1}^n \dot{\varphi}_i^2$ . One can easily find that for the potential (4.23) parameter  $\eta$  coincides exactly with parameters  $\eta_1$  and  $\eta_2$ .

Thus, in these regions it is possible to achieve a period of power-law inflation. In spite of a rude character of these estimates, one shall see below that external space scale factors undergo power-law inflation for trajectories passing through these regions.

Now, let us investigate dynamical behavior of scalar fields and the external space scale factor in more detail. There are no analytic solutions for considered model. So, let us use numerical calculations with applying of a Mathematica package proposed in [120], adjusting it to given models and notations (see appendix 3).

The colored lines on the contour plot of the effective potential in Fig. 4.10 describe trajectories for scalar fields  $\varphi$  and  $\phi$  with different initial values (the colored dots). The time evolution of these scalar fields<sup>19</sup> is drawn in Fig. 4.11. Here, the time  $t$  is measured in the Planck times and classical evolution starts at  $t = 1$ . For given initial conditions, scalar fields approach the global minimum of the effective potential along spiral trajectories.

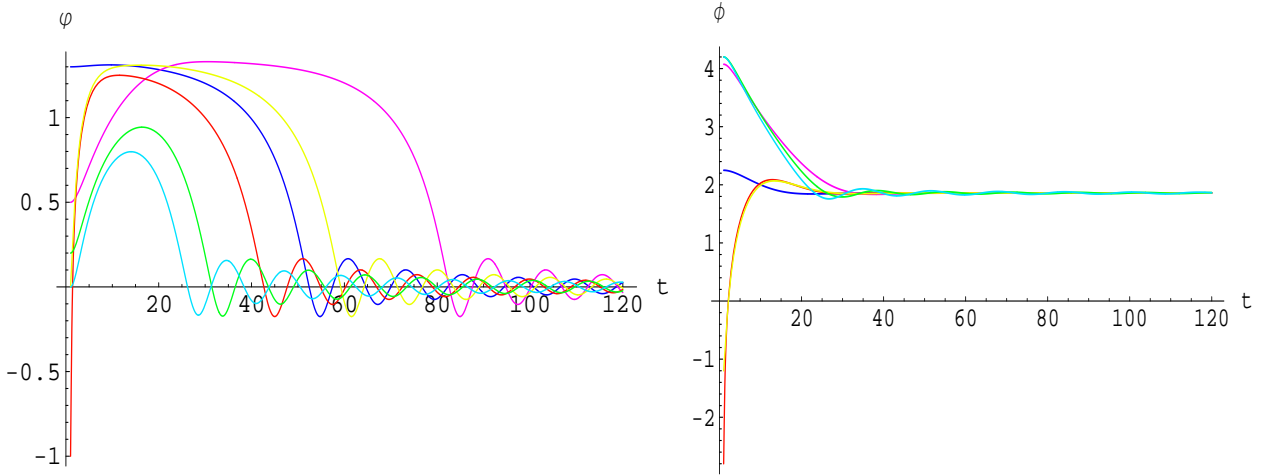


Figure 4.11: Dynamical behavior of scalar fields  $\varphi$  (left panel) and  $\phi$  (right panel) with corresponding initial values denoted by the colored dots in Fig. 4.10.

In Figure 4.12 the evolution of the logarithms of the scale factor  $a(t)$  (left panel) and the evolution of the Hubble parameter  $H(t)$  (right panel) are presented and in Fig. 4.13 the evolution of the parameter of acceleration  $q(t)$ .

<sup>19</sup>Let us remind that  $\varphi$  describes fluctuations of the internal space scale factor and  $\phi$  reflects the additional degree of freedom of the original nonlinear theory.

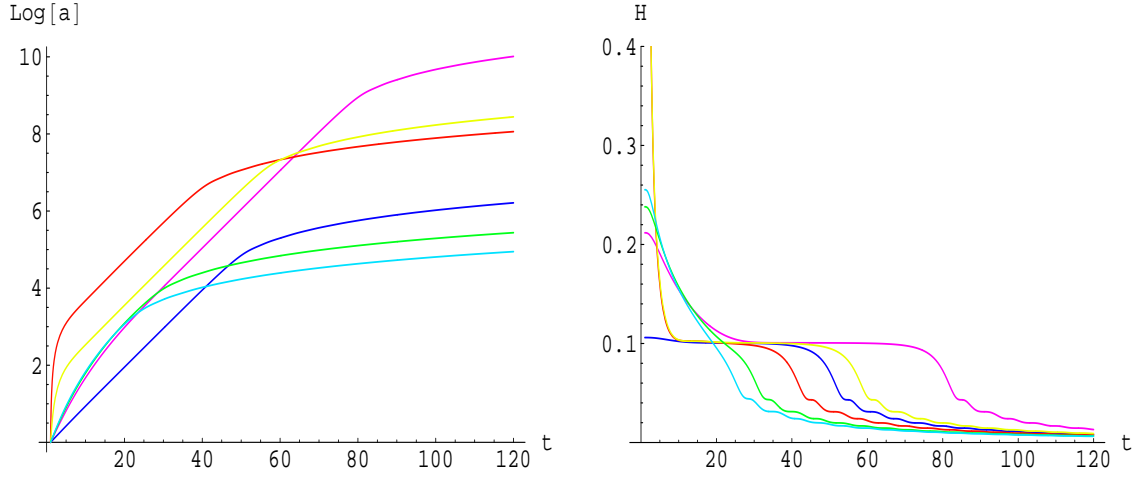


Figure 4.12: The number of e-folds (left panel) and the Hubble parameter (right panel) for the corresponding trajectories.

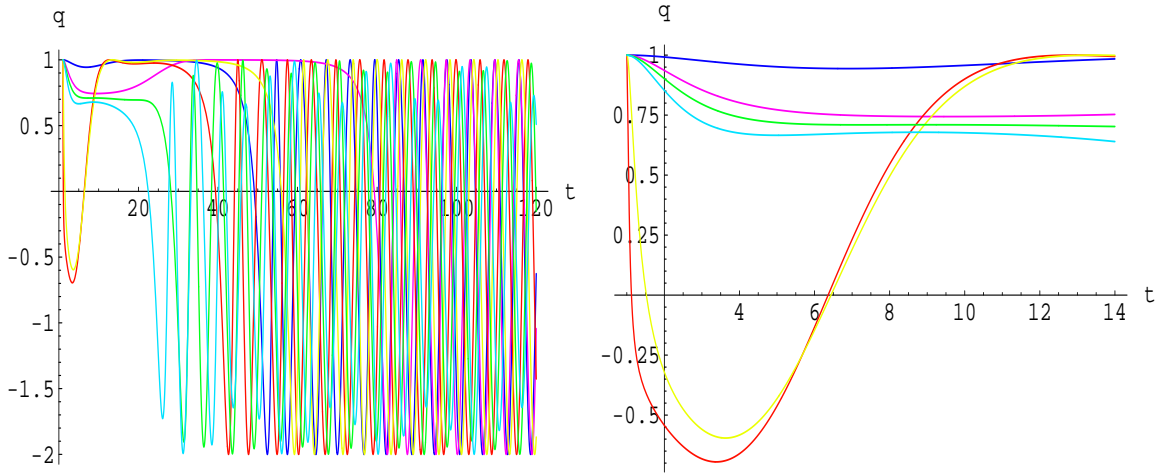


Figure 4.13: The parameter of acceleration (left panel) and its magnification for early times (right panel). There are two different form of acceleration with  $q \approx 1$  (De Sitter-like inflation) and  $q \approx 0.75$  (power-law inflation with  $s \approx 4$ ) accordingly. The averaging of  $q$  over a few periods of oscillations results in  $\bar{q} = -0.5$  which corresponds to the matter dominated decelerating Universe.

Because for initial condition the value  $a(t = 1) = 1$  (in the Planck units) is used, then  $\log a(t)$  gives the number of e-folds:  $\log a(t) = N(t)$ . The Figure 4.12 shows that for considered trajectories one can reach the maximum of e-folds of the order of 10. Clearly, 10 e-folds is not sufficient to solve the horizon and flatness problems but it can be useful to explain a part of the modern CMB data. For example, the Universe inflates by  $\Delta N \approx 4$  during the period that wavelengths corresponding to the CMB multipoles  $2 \leq l \leq 100$  cross the Hubble radius [121, 122]. However, to have the inflation which is long enough for all modes which contribute to the CMB to leave the horizon, it is usually supposed that  $\Delta N \geq 15$  [123].

The Figure 4.12 for the evolution of the Hubble parameter (right panel) demonstrates that the red, yellow, dark blue and pink lines have a plateau  $H \approx \text{const}$ . It means that the scale factor  $a(t)$  has a stage of the De Sitter expansion on these plateaus. Clearly, it happens because these lines reach the vicinity of the effective potential saddle point and spend there some time.

The Fig. 4.13 for the acceleration parameter defined in (A3.6) confirms also the above conclusions. According to Eq. (A3.8),  $q = 1$  for the De Sitter-like behavior. Indeed, all these 4 lines have stages  $q \approx 1$  for the same time intervals when  $H$  has a plateau. Additionally, the magnification of this picture at early times (the right panel of the Figure 4.13) shows that pink, green and blue lines have also a period of time when  $q$  is approximately constant less than one:  $q \approx 0.75$ . In accordance with Eq. (A3.8), it means that during this time the scale factor  $a(t)$  undergoes the power-law inflation  $a(t) \propto t^s$  with  $s \approx 4$ . This result confirms rude estimates made above for the trajectories which go through the regions where the effective potential has the form (4.23). After stages of the inflation, the acceleration parameter starts to oscillate. Averaging  $q$  over a few periods of oscillations, one obtains  $\bar{q} = -0.5$ . Therefore, the scale factor behaves as for the matter dominated Universe:  $a(t) \propto t^{2/3}$ . Clearly, it corresponds to the times when the trajectories reach the vicinity of the effective potential global minimum and start to oscillate there. It is worth of noting, that there is no need to plot dynamical behavior for the equation of state parameter  $\omega(t)$  because it is linearly connected with

$q$  (see Eq. (A3.7)) and its behavior can be easily understood from the pictures for  $q(t)$ .

As it is shown above for considered quadratic model, the maximal number of e-folds is near 10. Can this number be increased? To answer this question, let us consider a new model with a higher degree of nonlinearity, i.e. the nonlinear quartic model.

### 4.3. Quartic model

In this section let us consider the nonlinear quartic model

$$f(\bar{R}) = \bar{R} + \gamma \bar{R}^4 - 2\Lambda_D. \quad (4.25)$$

For this model the scalar field potential (4.16) reads [37]:

$$U(\phi) = \frac{1}{2}e^{-B\phi} \left[ \frac{3}{4}(4\gamma)^{-1/3}(e^{A\phi} - 1)^{4/3} + 2\Lambda_D \right]. \quad (4.26)$$

Here, the scalar curvature  $\bar{R}$  and scalar field  $\phi$  are connected as follows:  $e^{A\phi} \equiv f' = 1 + 4\gamma\bar{R}^3 \Leftrightarrow \bar{R} = [(e^{A\phi} - 1)/4\gamma]^{1/3}$ .

Let us look for a solution which has a nonnegative minimum of the effective potential  $U_{eff}(\varphi, \phi)$  (4.13) where potential  $U(\phi)$  is given by Eq. (4.26). If  $\phi_0$  corresponds to this minimum, then, as it was mentioned above (see also [86]),  $U(\phi_0)$ ,  $\lambda$  and  $f_1^2$  should be positive. To get zero minimum of the effective potential, these positive values should satisfy the relation of the form of (4.8):  $U(\phi_0) = f_1^2 = \lambda/2$ .

Additionally, it is important to note that positiveness of  $U(\phi_0)$  results in positive expression for  $\bar{R}(\phi_0) > 0$  [37].

Eq. (4.26) shows that potential  $U(\phi)$  has the following asymptotes for positive  $\gamma$  and  $\Lambda_D$ <sup>20</sup>:  $\phi \rightarrow -\infty \Rightarrow U(\phi) \approx \frac{1}{2}e^{-B\phi} \left[ \frac{3}{4}(4\gamma)^{-1/3} + 2\Lambda_D \right] \rightarrow +\infty$  and  $\phi \rightarrow +\infty \Rightarrow U(\phi) \approx \frac{3}{8}(4\gamma)^{-1/3}e^{(-B+4A/3)\phi} \rightarrow +0$ . For the latter

---

<sup>20</sup>Negative values of  $\Lambda_D$  and  $\gamma$  may lead either to negative minima, resulting in asymptotically AdS Universe, or to infinitely large negative values of  $U_{eff}$  [37]. In the present consideration let us to avoid both of these possibilities. Therefore, one shall consider the case of  $\Lambda_D, \gamma > 0$ . See also footnote 22.

asymptote  $-B + 4A/3 = (D - 8)/3\sqrt{(D - 2)(D - 1)} < 0$  is to be taken into account for  $D < 8$ . Obviously, the total number of dimensions  $D = 8$  plays the critical role in quartic nonlinear theories (see [37, 59, 124]) and investigations for  $D < 8$ ,  $D = 8$  and  $D > 8$  should be performed separately. Now, let us consider the case  $D < 8$  (i.e.  $d_1 = 1, 2, 3$ ).

It is worth of noting that for considered signs of parameters, the effective potential  $U_{eff}(\varphi, \phi)$  (4.13) acquires negative values when  $\phi \rightarrow +\infty$  (and  $U(\phi) \rightarrow 0$ ). For example, if  $U(\phi_0) = f_1^2 = \lambda/2$  (the case of zero minimum of the effective potential), the effective potential  $U_{eff}(\varphi, \phi \rightarrow \infty) < 0$  for  $0 < e^{-b\varphi} < 2$  and the lowest negative asymptotic value  $U_{eff}|_{min} \rightarrow -(16/27)\lambda$  takes place along the line  $e^{-b\varphi} = 4/3$ . Therefore, zero minimum of  $U_{eff}$  is local<sup>21</sup>.

As it was mentioned above, extremum positions  $\phi_i$  of the potential  $U(\phi)$  coincide with extremum positions of  $U_{eff}(\varphi, \phi) : dU/d\phi|_{\phi_i} = 0 \rightarrow \partial_\phi U_{eff}|_{\phi_i} = 0$ . The condition of extremum for the potential  $U(\phi)$  reads:

$$\frac{dU}{d\phi} = 0 \implies \bar{R}^4 - \frac{(2 + d_1)}{\gamma(4 - d_1)}\bar{R} + 2\Lambda_D \frac{(4 + d_1)}{\gamma(4 - d_1)} = 0. \quad (4.27)$$

For positive  $\gamma$  and  $\Lambda_D$  this equation has two real roots:

$$\bar{R}_{0(1)} = \frac{\Lambda_D}{2} \left( -\sqrt{\frac{2(2 + d_1)}{(4 - d_1)k\sqrt{M}}} - M + \sqrt{M} \right), \quad (4.28)$$

$$\bar{R}_{0(2)} = \frac{\Lambda_D}{2} \left( \sqrt{\frac{2(2 + d_1)}{(4 - d_1)k\sqrt{M}}} - M + \sqrt{M} \right), \quad (4.29)$$

where a dimensionless parameter  $k$  is introduces as

$$k := \gamma\Lambda_D^3, \quad (4.30)$$

---

<sup>21</sup>It is not difficult to show that the thin shell approximation is valid for considered model and a tunnelling probability from the zero local minimum to this negative  $U_{eff}$  region is negligible.

which is positive for positive  $\gamma$  and  $\Lambda_D$ , and quantities  $M$ ,  $\omega$  read

$$M \equiv -2^{10/3} \frac{(4 + d_1)}{\omega^{1/3}} - \frac{1}{3 \cdot 2^{1/3} k} \frac{\omega^{1/3}}{(4 - d_1)}, \quad (4.31)$$

$$\begin{aligned} \omega \equiv & k \left[ -27(4 - d_1)(2 + d_1)^2 \right. \\ & \left. + \sqrt{27^2(4 - d_1)^2(2 + d_1)^4 - 4 \cdot 24^3 k (16 - d_1^2)^3} \right]. \end{aligned} \quad (4.32)$$

It can be easily seen that for  $k > 0$  follows  $\omega < 0$  and  $M \geq 0$ . To have real  $\omega$ , parameter  $k$  should satisfy the following condition

$$k \leq \frac{27^2(4 - d_1)^2(2 + d_1)^4}{4 \cdot 24^3(16 - d_1^2)^3} \equiv k_0. \quad (4.33)$$

It is not difficult to verify that roots  $\bar{R}_{0(1,2)}$  are real and positive if  $0 < k \leq k_0$  and they degenerate for  $k \rightarrow k_0$  :  $\bar{R}_{0(1,2)} \rightarrow (\Lambda_D/2)\sqrt{M}$ . In this limit the minimum and maximum of  $U(\phi)$  merge into an inflection point. Now, let us define which of these roots corresponds to minimum of  $U(\phi)$  and which to local maximum. The minimum condition

$$\left. \frac{d^2 U(\phi)}{d\phi^2} \right|_{\phi_0} > 0 \implies \gamma [(d_1 + 2) - 4\gamma \bar{R}_0^3(4 - d_1)] > 0 \quad (4.34)$$

results in the following inequality<sup>22</sup>:

$$\gamma > 0 : \quad (d_1 + 2) - 4\gamma \bar{R}_0^3(4 - d_1) > 0. \quad (4.35)$$

Thus, the root  $\bar{R}_0$  which corresponds to the minimum of  $U(\phi)$  should satisfy the following condition:

$$0 < \bar{R}_0 < \left( \frac{d_1 + 2}{4\gamma(4 - d_1)} \right)^{1/3}. \quad (4.36)$$

Numerical analysis shows that  $\bar{R}_{0(1)}$  satisfies these conditions and corresponds to the minimum. For  $\bar{R}_{0(2)}$  one obtains that  $\bar{R}_{0(2)} > \left( \frac{d_1 + 2}{4\gamma(4 - d_1)} \right)^{1/3}$  and corresponds to the local maximum of  $U(\phi)$ . In what follows one shall use the

---

<sup>22</sup>As it was already mentioned above, the condition  $U(\phi_0) > 0$  leads to the inequality  $\bar{R}(\phi_0) > 0$  [37]. Taking into account the condition  $d_1 < 4$ , it is obvious that inequality  $(d_1 + 2) + 4|\gamma|\bar{R}_0^3(4 - d_1) < 0$  for  $\gamma < 0$  cannot be realized. This is an additional argument in favor of positive sign of  $\gamma$ .

notations:

$$\phi_{min} = \frac{1}{A} \ln \left[ 1 + 4\gamma \bar{R}_{0(1)}^3 \right], \quad (4.37)$$

$$\phi_{max} = \frac{1}{A} \ln \left[ 1 + 4\gamma \bar{R}_{0(2)}^3 \right] \quad (4.38)$$

and  $U(\phi_{min}) \equiv U_{min}$ ,  $U(\phi_{max}) \equiv U_{max}$ . Let us note that  $\phi_{min}$ ,  $\phi_{max}$  and the ratio  $U_{max}/U_{min}$  depend on the combination  $k$  (4.30) rather than on  $\gamma$  and  $\Lambda_D$  taken separately.

Obviously, because potential  $U(\phi)$  has two extrema at  $\phi_{min}$  and  $\phi_{max}$ , the effective potential  $U_{eff}(\varphi, \phi)$  may have points of extrema only on the lines  $\phi = \phi_{min}$  and  $\phi = \phi_{max}$  where  $\partial U_{eff}/\partial \phi|_{\phi_{min}, \phi_{max}} = 0$ . To find these extrema of  $U_{eff}$ , it is necessary to consider the second extremum condition  $\partial U_{eff}/\partial \varphi = 0$  on each line separately:

$$\frac{\partial U_{eff}}{\partial \varphi} = 0 \implies \begin{cases} -U_{min} - 3f_1^2 \chi_1^2 + 2\lambda \chi_1 = 0, \\ -U_{max} - 3f_1^2 \chi_2^2 + 2\lambda \chi_2 = 0, \end{cases} \quad (4.39)$$

where  $\chi_1 \equiv \exp \left( -\sqrt{2d_1/(d_1+2)} \varphi_1 \right) > 0$  and  $\chi_2 \equiv \exp \left( -\sqrt{2d_1/(d_1+2)} \varphi_2 \right) > 0$ ;  $\varphi_1$  and  $\varphi_2$  denote positions of extrema on the lines  $\phi = \phi_{min}$  and  $\phi = \phi_{max}$ , respectively. These equations have solutions

$$\begin{aligned} \chi_{1(\pm)} &= \alpha \pm \sqrt{\alpha^2 - \beta}, \\ \alpha &\geq \sqrt{\beta} \equiv \alpha_1; \end{aligned} \quad (4.40)$$

$$\begin{aligned} \chi_{2(\pm)} &= \alpha \pm \sqrt{\alpha^2 - \beta \frac{U_{max}}{U_{min}}}, \\ \alpha &\geq \sqrt{\beta \frac{U_{max}}{U_{min}}} \equiv \alpha_2 > \alpha_1; \end{aligned} \quad (4.41)$$

where  $\alpha \equiv \lambda/(3f_1^2)$  and  $\beta \equiv U_{min}/(3f_1^2)$ . These equations show that there are 5 different possibilities which are listed in the Table 1.

To clarify which of solutions (4.40) and (4.41) correspond to minima of the effective potential (with respect to  $\varphi$ ) one should consider the minimum condition

$$\left. \frac{\partial^2 U_{eff}}{\partial^2 \varphi} \right|_{min} > 0 \implies U_{extr} + \chi^2 9f_1^2 - 4\lambda \chi > 0, \quad (4.42)$$



Table 1: The number of extrema of the effective potential  $U_{eff}$  depending on the relation between parameters.

$0 < \alpha < \alpha_1$	$\alpha = \alpha_1$	$\alpha_1 < \alpha < \alpha_2$	$\alpha = \alpha_2$	$\alpha > \alpha_2$
<b>no extrema</b>	<b>one extremum</b> (point of inflection on the line $\phi = \phi_{min}$ )	<b>two extrema</b> (one minimum and one saddle on the line $\phi = \phi_{min}$ )	<b>three extrema</b> (minimum and saddle on the line $\phi = \phi_{min}$ , inflection on the line $\phi = \phi_{max}$ )	<b>four extrema</b> (minimum and saddle on the line $\phi = \phi_{min}$ maximum and saddle on the line $\phi = \phi_{max}$ )

where  $U_{extr}$  is either  $U_{min}$  or  $U_{max}$  and  $\chi$  denotes either  $\chi_1$  or  $\chi_2$ . Taking into account relations (4.39), one obtains

$$\chi^2 3f_1^2 - \chi\lambda > 0 \quad \implies \quad \chi > \frac{\lambda}{3f_1^2} = \alpha. \quad (4.43)$$

Thus, roots  $\chi_{1,2(+)}$  define the positions of local minima of the effective potential with respect to the variable  $\varphi$  and  $\chi_{1,2(-)}$  correspond to local maxima (in the direction of  $\varphi$ ).

Now, let us fix the minimum  $\chi_{1(+)}$  at the point  $\varphi = 0$ . It means that in this local minimum the internal space scale factor is stabilized at the present day value. In this case

$$\chi_{1(+)}|_{\varphi=0} = 1 = \alpha + \sqrt{\alpha^2 - \beta} \quad \implies \quad \alpha = \frac{1 + \beta}{2}. \quad (4.44)$$

Obviously, one can do it only if<sup>23</sup>  $\alpha < 1 \Rightarrow \beta \in [0, 1)$ . For  $\chi_{1(-)}$  follows:  $\chi_{1(-)} = \beta$ .

Additionally, the local minimum of the effective potential at the point  $(\varphi = 0, \phi = \phi_{min})$  should play the role of the nonnegative four-dimensional

---

<sup>23</sup>Particular value  $\alpha = 1$  corresponds to the case  $\alpha = \alpha_1 = 1$  where the only extremum is the inflection point with  $\chi_{1(-)} = \chi_{1(+)} = \alpha = 1$ . Here,  $\lambda = U_{min} = 3f_1^2$  and  $U_{eff}(\varphi = 0, \phi = \phi_{min}) = -\lambda + U_{min} + f_1^2 > 0$ .

effective cosmological constant. Thus, the following conditions appear:

$$\begin{aligned}
\Lambda_{eff} &\equiv U_{eff}(\varphi = 0, \phi = \phi_{min}) \\
&= -\lambda + U_{min} + f_1^2 \geq 0 \\
&\implies -\alpha + \beta + \frac{1}{3} \geq 0.
\end{aligned} \tag{4.45}$$

From the latter inequality and equation (4.44) takes place  $\beta \in [\frac{1}{3}, 1)$ . It can be easily seen that  $\beta = 1/3$  (and, correspondingly,  $\alpha = 2/3$ ) results in  $\Lambda_{eff} = 0$  and one obtains the mentioned above relations:  $U_{min} = f_1^2 = \lambda/2$ . In general, it is possible to demand that  $\Lambda_{eff}$  coincides with the present day dark energy value  $10^{-57}\text{cm}^{-2}$ . However, it leads to very flat local minimum which means the decompactification of the internal space [86]. In what follows, the case of zero  $\Lambda_{eff}$  is to be mainly considered although all obtained results are trivially generalized to  $\Lambda_{eff} = 10^{-57}\text{cm}^{-2}$ .

Summarizing results, in the most interesting case of  $\alpha > \alpha_2$  the effective potential has four extrema: local minimum at  $(\varphi|_{\chi_{1(+)}} = 0, \phi_{min})$ , local maximum at  $(\varphi|_{\chi_{2(-)}}, \phi_{max})$  and two saddle-points at  $(\varphi|_{\chi_{1(-)}}, \phi_{min})$ , and  $(\varphi|_{\chi_{2(+)}} , \phi_{max})$  (see Fig. 4.15).

Let us pay particular attention to the case of zero local minimum, when  $U_{eff}(\varphi|_{\chi_{1(+)}} = 0, \phi_{min}) = 0$  and where  $\beta = 1/3 \implies \alpha = (1 + \beta)/2 = 2/3$ . To satisfy the four-extremum condition  $\alpha > \alpha_2$ , next condition has to be satisfied

$$\frac{U_{max}}{U_{min}} < \frac{4}{3}. \tag{4.46}$$

The fraction  $U_{max}/U_{min}$  is the function of  $k$  and depends parametrically only on the internal space dimension  $d_1$ . Inequality (4.46) provides the lower bound on  $k$  and numerical analysis (see Fig. 4.14) gives  $\tilde{k}(d_1 = 1) \approx 0.000625$  ;  $\tilde{k}(d_1 = 2) \approx 0.00207$  ;  $\tilde{k}(d_1 = 3) \approx 0.0035$ . Therefore, effective potentials with zero local minimum will have four extrema if  $k \in (\tilde{k}, k_0)$  (where  $k_0$  is defined by Eq. (4.33)). The limit  $k \rightarrow \tilde{k}$  results in merging  $\chi_{2(-)} \leftrightarrow \chi_{2(+)}$  and the limit  $k \rightarrow k_0$  results in merging  $\chi_{1(-)} \leftrightarrow \chi_{2(-)}$  and  $\chi_{1(+)} \leftrightarrow \chi_{2(+)}$ . Such merging results in transformation of corresponding extrema into inflection points. For example, from Fig. 4.14 follows that

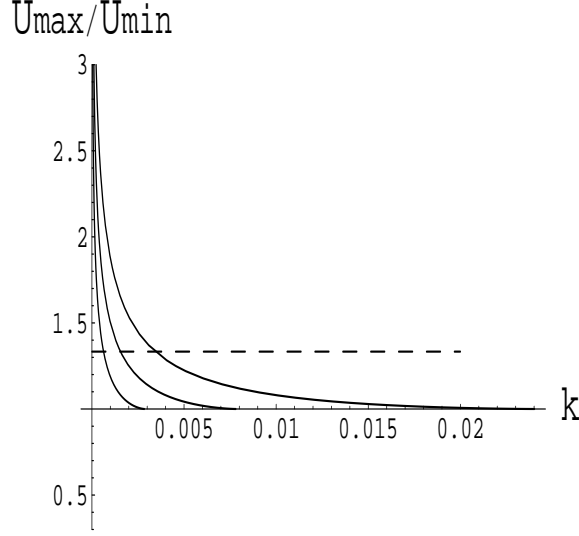


Figure 4.14: The form of  $U_{max}/U_{min}$  as a function of  $k \in (0, k_0]$  for  $d_1 = 1, 2, 3$  from left to right, respectively. Dashed line corresponds to  $U_{max}/U_{min} = 4/3$ .

$U_{max}/U_{min} \rightarrow 1$  for  $k \rightarrow k_0$ .

The typical contour plot of the effective potential with four extrema in the case of zero local minimum is drawn in Fig. 4.15. Here, for  $d_1 = 3$  it is taken  $k = 0.004 \in (\tilde{k}, k_0)$  which gives  $\alpha_2 \approx 0.655$ . Thus,  $\alpha = 2/3 \approx 0.666 > \alpha_2$ .

Let us investigate now a possibility of inflation for considered potential. First of all, taking into account the comments in previous section (see Eq. (4.22)), it is clear that topological inflation in the saddle point  $\chi_{1(-)}$  as well as the slow rolling from there in the direction of the local minimum  $\chi_{1(+)}$  are absent. It is not difficult to verified that the generalized power-low inflation discussed in the case of the nonlinear quadratic model is also absent here. Indeed, from Eqs. (4.13) and (4.26) follows that nonlinear potential  $U(\phi)$  can play the leading role in the region  $\phi \rightarrow -\infty$  (because  $U(\phi) \rightarrow 0$  for  $\phi \rightarrow +\infty$ ). In this region  $U_{eff} \propto \exp(-\sqrt{q}\phi) \exp(-\sqrt{q_2}\phi)$  where  $q = 2d_1/(d_1 + 2)$  and  $q_2 = B^2 = (d_1 + 4)^2/[(d_1 + 2)(d_1 + 3)]$ . For these values of  $q$  and  $q_2$  the slow-roll conditions are not satisfied:  $\epsilon \approx \eta_1 \approx \eta_2 \approx q/2 + q_2/2 > 1$ . However, there are two promising regions where the stage of inflation with subsequent stable compactification of the internal space may take place. These are the local maximum  $\chi_{2(-)}$  and the saddle  $\chi_{2(+)}$  (see Fig. 4.15). Let us estimate the slow roll parameters for these regions.

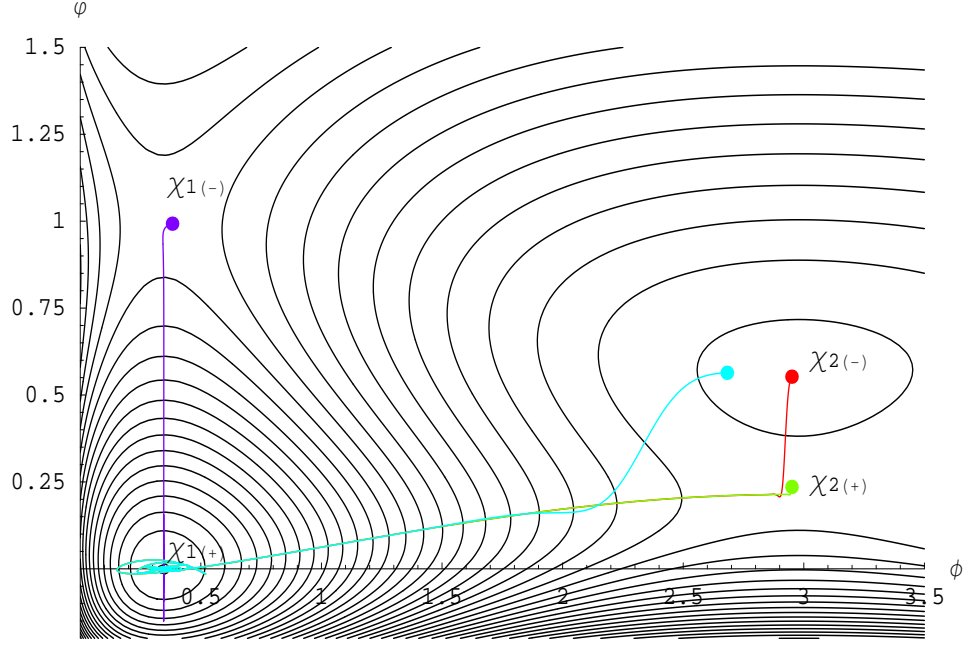


Figure 4.15: Contour plot of the effective potential  $U_{eff}(\varphi, \phi)$  (4.13) with potential  $U(\phi)$  of the form (4.26) for parameters  $\beta = 1/3$ ,  $d_1 = 3$  and  $k = 0.004$ . This plot shows the local zero minimum, local maximum and two saddles. The colored lines describe trajectories for scalar fields starting at different initial conditions.

First the local maximum  $\chi_{2(-)}$ . It is obvious that the parameter  $\epsilon$  is equal to zero here. Additionally, from the form of the effective potential (4.13) it is clear that the mixed second derivatives are also absent in extremum points. Thus, the slow roll parameters  $\eta_1$  and  $\eta_2$ , defined in the footnote (18), coincide exactly with  $\eta_\varphi$  and  $\eta_\phi$ . In Fig. 4.16 a typical form of these parameters is presented as functions of  $k \in (\tilde{k}, k_0)$  in the case  $\beta = 1/3$  and  $d_1 = 1, 2, 3$ . These plots show that, for considered parameters, the slow roll inflation in this region is possible for  $d_1 = 1, 3$ .

The vicinity of the saddle point  $\chi_{2(+)}$  is another promising region. Obviously, if one starts from this point, a test particle will roll mainly along direction of  $\phi$ . That is why it makes sense to draw only  $|\eta_\phi|$ . In Fig. 4.17 typical form of  $|\eta_\phi|$  is plotted in the case  $\beta = 1/3$  and  $d_1 = 1, 2, 3$ . Left panel represents general behavior for the whole range of  $k \in (\tilde{k}, k_0)$  and right panel shows detailed behavior in the most interesting region of small  $k$ . It shows that  $d_1 = 3$  is the most promising case in this region.

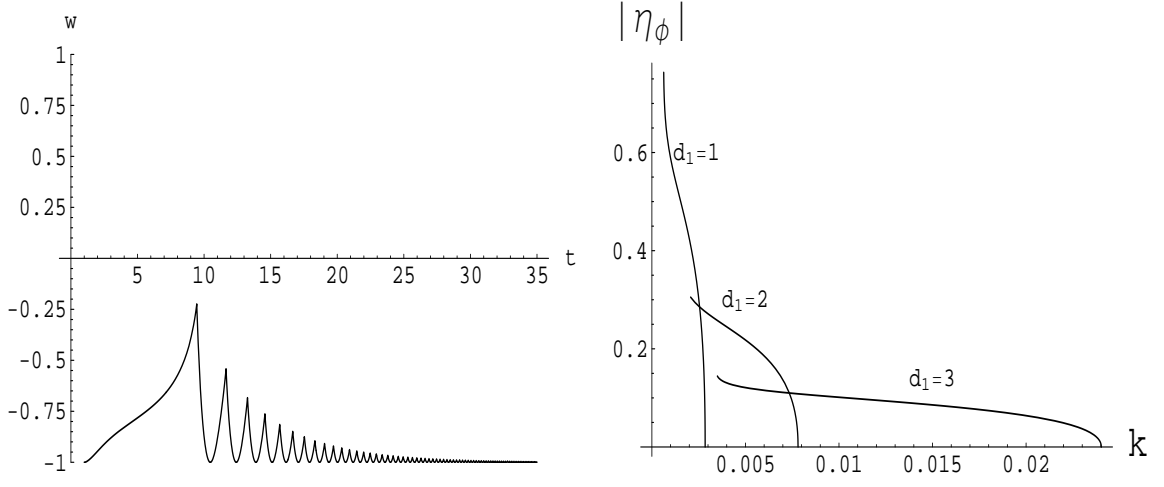


Figure 4.16: Graphs of  $|\eta_\phi|$  (left panel) and  $|\eta_\phi|$  (right panel) as functions of  $k \in (\tilde{k}, k_0)$  for local maximum  $\chi_{2(-)}$  and parameters  $\beta = 1/3$  and  $d_1 = 1, 2, 3$ .

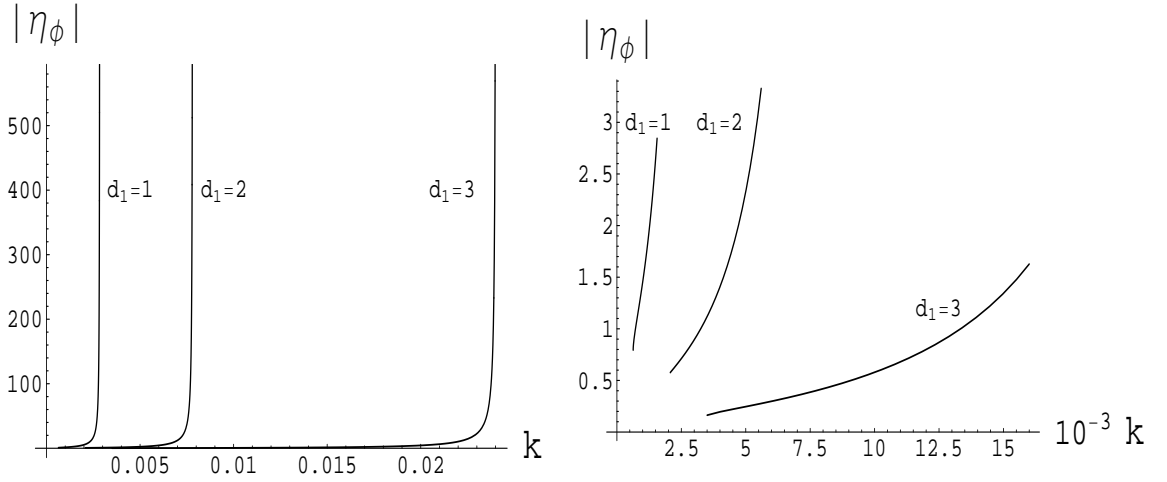


Figure 4.17: Graphs of  $|\eta_\phi|$  as functions of  $k$  for saddle point  $\chi_{2(+)}$  and parameters  $\beta = 1/3$  and  $d_1 = 1, 2, 3$ . Left panel demonstrates the whole region of variable  $k \in (\tilde{k}, k_0)$  and right panel shows detailed behavior for small  $k$ .

Now, let us investigate numerically the dynamical behavior of scalar fields and the external space scale factor for trajectories which start from the regions  $\chi_{1(-)}$ ,  $\chi_{2(-)}$  and  $\chi_{2(+)}$ . All numerical calculations perform for  $\beta = 1/3$ ,  $d_1 = 3$  and  $k = 0.004$ . The colored lines on the contour plot of the effective potential in Fig. 4.15 describe trajectories for scalar fields  $\varphi$  and  $\phi$  with different initial values (the colored dots) in the vicinity of these extrema points. The time evolution of these scalar fields is drawn in Fig. 4.18. For given initial conditions, scalar fields approach the local minimum  $\chi_{1(+)}$  of the effective potential along the spiral trajectories.

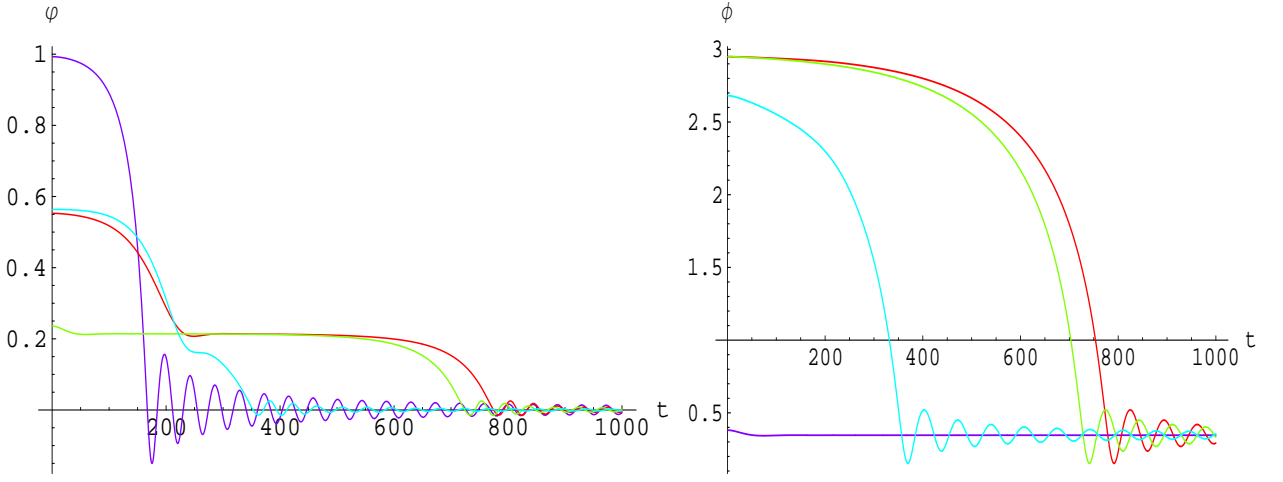


Figure 4.18: Dynamical behavior of scalar fields  $\varphi$  (left panel) and  $\phi$  (right panel) with corresponding initial values denoted by the colored dots in Fig. 4.15.

In Figure 4.19 the evolution of the logarithm of the scale factor  $a(t)$  (left panel) is plotted, which gives directly the number of e-folds and the evolution of the Hubble parameter  $H(t)$  (right panel) and in Fig. 4.20 the evolution of the parameter of acceleration  $q(t)$ .

The Figure 4.19 shows that for considered trajectories the maximum of e-folds that can be reached is of the order of 22 which is long enough for all modes which contribute to the CMB to leave the horizon.

The Figure 4.19 for the evolution of the Hubble parameter (right panel) demonstrates that all lines have plateaus  $H \approx \text{const.}$  However, the red, yellow and blue lines which pass in the vicinity of the saddle  $\chi_{2(+)}$  have bigger value of the Hubble parameter with respect to the dark blue line which starts from

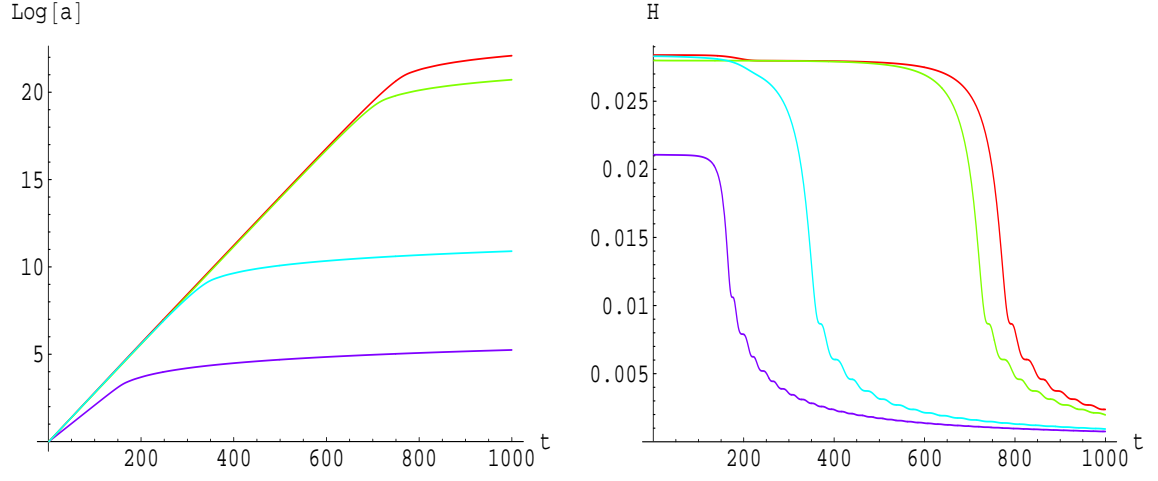


Figure 4.19: The number of e-folds (left panel) and the Hubble parameter (right panel) for the corresponding trajectories.

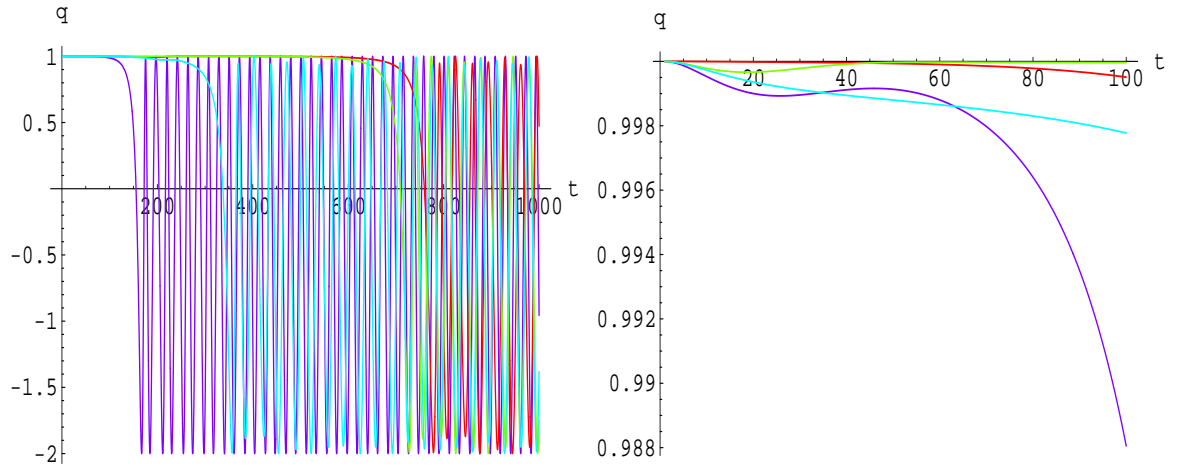


Figure 4.20: The parameter of acceleration (left panel) and its magnification for early times (right panel).

the  $\chi_{1(-)}$  region. Therefore, the scale factor  $a(t)$  has stages of the De Sitter-like expansion corresponding to these plateaus which last approximately from 100 (dark blue line) up to 800 (red line) Planck times.

The Fig. 4.20 for the acceleration parameter confirms also the above conclusions. All 4 lines have stages  $q \approx 1$  for the same time intervals when  $H$  has plateaus. After stages of inflation, the acceleration parameter starts to oscillate. Averaging  $q$  over a few periods of oscillations, one obtains  $\bar{q} = -0.5$ . Therefore, the scale factor behaves as for the matter dominated Universe:  $a(t) \propto t^{2/3}$ . Clearly, it corresponds to the times when the trajectories reach the vicinity of the effective potential local minimum  $\chi_{1(+)}$  and start to oscillate there.

Let us investigate now a possibility of the topological inflation [125, 126] if scalar fields  $\varphi, \phi$  stay in the vicinity of the saddle point  $\chi_{2(+)}$ . As it was mentioned before, topological inflation in the case of the double-well potential takes place if the distance between a minimum and local maximum bigger than  $\Delta\phi_{cr} = 1.65$ . In this case domain wall is thick enough in comparison with the Hubble radius. The critical ratio of the characteristic thickness of the wall to the horizon scale in local maximum is  $r_w H \approx |U/3\partial U_{\phi\phi}|^{1/2} \approx 0.48$  [89] and for topological inflation it is necessary to exceed this critical value. Therefore, the saddle  $\chi_{2(+)}$  should be checked from the point of these criteria.

In Fig. 4.21 (left panel) the difference  $\Delta\phi = \phi_{max} - \phi_{min}$  is drawn for the profile  $\varphi = \varphi|_{\chi_{2(+)}}$  as a functions of  $k \in (\tilde{k}, k_0)$  in the case  $\beta = 1/3$  for dimensions  $d_1 = 1, 2, 3$ . This picture shows that this difference can exceed the critical value if the number of the internal dimensions is  $d_1 = 2$  and  $d_1 = 3$ . Right panel of Fig. 4.21 confirms this conclusion. Here the case  $\beta = 1/3$ ,  $k = 0.004$  and  $d_1 = 3$  is considered. For chosen values of the parameters,  $\Delta\phi = 2.63$  which is considerably bigger than the critical value 1.65 and the ratio of the thickness of the wall to the horizon scale is 1.30 which again bigger than the critical value 0.48. Therefore, topological inflation can happen for considered model. Moreover, due to quantum fluctuations of scalar fields, inflating domain wall will have fractal structure: it will contain many other inflating domain walls and each of these domain walls again will



contain new inflating domain walls and so on [125]. Thus, from this point, such topological inflation is the eternal one.

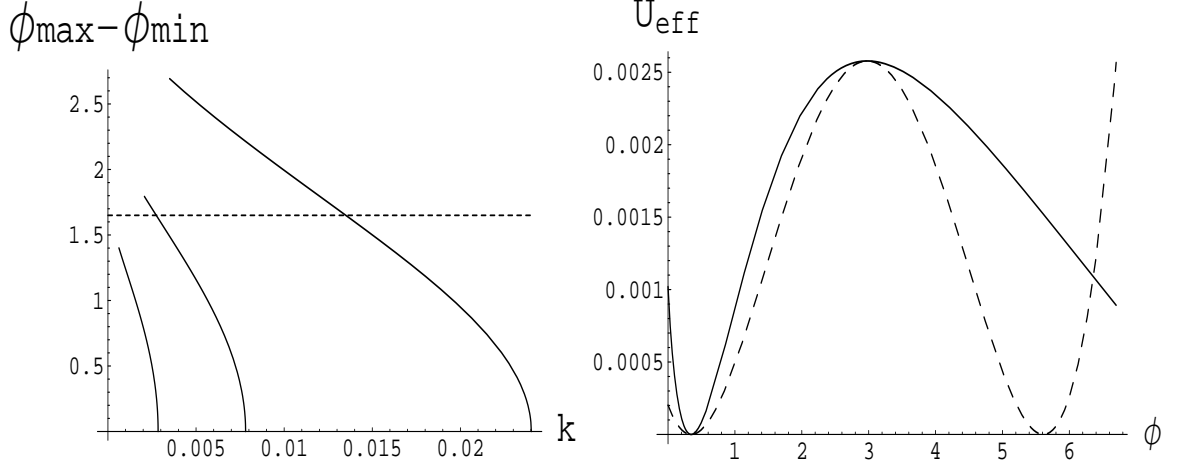


Figure 4.21: Left panel demonstrates the difference  $\phi_{\max} - \phi_{\min}$  (for the profile  $\varphi = \varphi|_{\chi_{2(+)}}$ ) as a functions of  $k \in (\tilde{k}, k_0)$  for parameters  $\beta = 1/3$ , and  $d_1 = 1, 2, 3$  (from left to right respectively). Dashed line corresponds to  $\phi_{\max} - \phi_{\min} = 1.65$ . Right panel shows the comparison of the potential  $U_{\text{eff}}(\varphi|_{\chi_{2(+)}} , \phi)$  with a double-well potential for parameters  $\beta = 1/3, k = 0.004$  and  $d_1 = 3$ .

To conclude this section, let us draw the attention to one interesting feature of the given model. From above consideration follows that in the case of zero minimum of the effective potential the positions of extrema are fully determined by the parameters  $k$  and  $d_1$ , and for fixed  $k$  and  $d_1$  do not depend on the choice of  $\Lambda_D$ . The same takes place for the slow roll parameters. On the other hand, if  $k$  and  $d_1$  are kept, the hight of the effective potential is defined by  $\Lambda_D$  (see Appendix 2). Therefore, the hight of extrema can be changed with the help of  $\Lambda_D$  but preserve the conditions of inflation for given  $k$  and  $d_1$ .

However, the dynamical characteristics of the model (drawn in Figures 4.18 - 4.20) depend on variations of  $\Lambda_D$  by the self-similar manner. It means that the change of hight of the effective potential via transformation  $\Lambda_D \rightarrow c\Lambda_D$  ( $c$  is a constant) with fixed  $k$  and  $d_1$  results in rescaling of Figures 4.18 - 4.20 in  $1/\sqrt{c}$  times along the time axis.

## 4.4. Bouncing inflation in $R^2 + R^4$ model

### 4.4.1. The fitting procedure

Here let us continue the investigation of the quadratic-quartic model started in section 2.4 for an arbitrary number of dimensions  $D$ , but in the most particular examples  $D = 4$  will be used (unless stated otherwise). First of all, let us define the relation between the scalar curvature  $\bar{R}$  and the scalaron field  $\phi$ .

Starting by considering a concrete example, for definiteness, let us assume  $\gamma > 0, \alpha < 0$ . The pairwise fitting of the various solution branches should be performed at points where  $Q = 0$  and different branches of the three-solution sector are fitted with each other or to the branches of the one-solution sector. The points with  $Q = 0$  correspond to the  $X$ -values  $X_{min}$  and  $X_{max}$ . Explicitly from (2.61) follows

$$X(\bar{R}_{\pm}) = \frac{4}{3}\alpha\bar{R}_{\pm} = \pm\frac{4}{3}\alpha\sqrt{-\frac{\alpha}{6\gamma}} \quad (4.47)$$

and for the concrete configuration  $\gamma > 0, \alpha < 0$

$$\begin{aligned} X_{max} &= X(\bar{R}_{-}) = -\frac{4}{3}\alpha\sqrt{-\frac{\alpha}{6\gamma}} \geq 0, \\ X_{min} &= X(\bar{R}_{+}) = \frac{4}{3}\alpha\sqrt{-\frac{\alpha}{6\gamma}} \leq 0. \end{aligned} \quad (4.48)$$

Next, from the defining equation (2.56) for the angle  $\vartheta$  that at  $Q = 0$  holds

$$\cos(\vartheta) = \frac{r}{|b|} = \frac{r}{|r|} \quad (4.49)$$

so that

$$\begin{aligned} X_{max} \geq 0 &\implies r > 0 \implies \cos(\vartheta) = 1 \\ &\implies \vartheta = 2\pi m, \quad m \in \mathbb{Z}, \\ X_{min} \leq 0 &\implies r < 0 \implies \cos(\vartheta) = -1 \\ &\implies \vartheta = \pi + 2\pi n, \quad n \in \mathbb{Z}. \end{aligned} \quad (4.50)$$

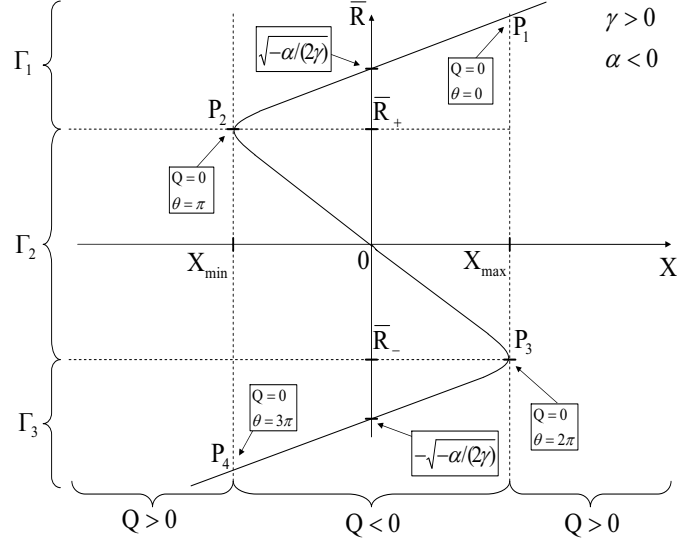


Figure 4.22: The schematic drawing of the real solution branches and the matching points  $P_{1,2,3,4}$ . This figure shows that points  $P_{2,3}$  (correspondingly,  $\theta = \pi, 2\pi$ ) and points  $P_{1,4}$  (correspondingly,  $\theta = 0, 3\pi$ ) have different nature. So,  $P_{2,3}$  and  $P_{1,4}$  one shall call branching points and monotonic points (in the sense that function  $\bar{R}$  is monotonic in the vicinity of these points), respectively.

Now, the fitting of the various solution branches can be performed as follows (see Fig. 4.22). Let us start with the branch  $\Gamma_1 := (R_+ \leq \bar{R} \leq +\infty, X_{min} < X < +\infty)$ . Moving in on this branch from  $X \approx +\infty$  one is working in the one-solution sector  $Q > 0$  with

$$\bar{R}(\Gamma_1; Q) = \left[ r + Q^{1/2} \right]^{1/3} + \left[ r - Q^{1/2} \right]^{1/3} \quad (4.51)$$

until  $Q = 0$  is hit at  $X = X_{max}$ . At this point  $P_1 := (\Gamma_1, X = X_{max}) \in \Gamma_1$  one has to perform the first fitting. Due to  $r > 0$  the following may be chosen

$$\bar{R}(\Gamma_1; Q = 0) = 2r^{1/3} = 2|b|^{1/3} \quad (4.52)$$

so that as simplest parameter choice in (2.58) comes

$$P_1 = (\Gamma_1, X = X_{max}, Q = 0) \mapsto \vartheta = 0, k = 0. \quad (4.53)$$

Hence, the parametrization for  $(\Gamma_1, Q < 0)$  will be given as

$$\bar{R}(\Gamma_1, Q < 0) = 2|b|^{1/3} \cos(\theta/3). \quad (4.54)$$

For later convenience, the  $\vartheta$  from the equations (2.57), (2.58) is replaced by  $\theta$ . The reason will become clear from the subsequent discussion. It should be noted that on this  $\Gamma_1$ -segment one may set  $\vartheta = \theta$ . Let us further move on  $\Gamma_1$  until its end at  $X_{min}$ , where again  $Q = 0$ . Because there was no other point with  $Q = 0$  on this path, the smoothly changing  $\theta$  can at this local minimum  $P_2 = \Gamma_1 \cap \Gamma_2 = (X = X_{min}, \bar{R} = \bar{R}_+)$  only take one of the values  $\theta = \pm\pi$ . For definiteness  $\theta(P_2) = \pi$  is chosen. Hence, it holds

$$\begin{aligned}\bar{R}(P_2) &= 2|b|^{1/3} \cos(\pi/3) = |b|^{1/3} \\ &= \sqrt{-q} = \sqrt{-\alpha/(6\gamma)} = \bar{R}_+\end{aligned}\tag{4.55}$$

as it should hold. For convenience, let us parameterize the movement on the cubic curve by simply further increasing  $\theta$ . This gives for moving on  $\Gamma_2 = (\bar{R}_+ \geq \bar{R} \geq \bar{R}_-, X_{min} \leq X \leq X_{max})$  from the local minimum at  $P_2$  to the local maximum at  $P_3 = \Gamma_2 \cap \Gamma_3 = (X = X_{max}, \bar{R} = \bar{R}_-)$  a further increase of  $\theta$  by  $\pi$  up to  $\theta(P_3) = 2\pi$ . Accordingly, the complete consistency condition looks as

$$\begin{aligned}\bar{R}(P_3) &= 2|b|^{1/3} \cos(2\pi/3) = -|b|^{1/3} \\ &= -\sqrt{-q} = -\sqrt{-\alpha/(6\gamma)} = \bar{R}_-.\end{aligned}\tag{4.56}$$

By further increasing  $\theta$  up to  $\theta = 3\pi$  the point  $P_4 = (X = X_{min}, Q = 0) \in \Gamma_3$  can be reached with

$$\bar{R}(P_4) = 2|b|^{1/3} \cos(3\pi/3) = -2|b|^{1/3} = -2|r|^{1/3}.\tag{4.57}$$

Because of  $r < 0$  it can be smoothly fitted it to the one-solution branch

$$\bar{R}(\Gamma_4, Q) = \left[r + Q^{1/2}\right]^{1/3} + \left[r - Q^{1/2}\right]^{1/3}\tag{4.58}$$

by setting trivially

$$\bar{R}(P_4) = 2(-|r|)^{1/3} = -2|r|^{1/3}.\tag{4.59}$$

Summarizing, a very simple and transparent branch fitting picture is achieved, where all the movement in the three-solution sector can be parameterized by choosing the effective angle as  $\theta \in [0, 3\pi]$ . Finally, this picture have to be

fitted in terms of smoothly varying  $\theta \in [0, 3\pi]$  with the three-solutions  $\bar{R}_k$  from (2.58). For this purpose let us note that the single value  $\vartheta \in [0, \pi]$  in (2.58) is a projection of the smoothly varying  $\theta \in [0, 3\pi]$ . Fixing an arbitrary  $\vartheta$  one easily finds the following correspondences

$$\theta(\Gamma_1, \vartheta) = \vartheta, \quad \theta(\Gamma_2, \vartheta) = 2\pi - \vartheta, \quad \theta(\Gamma_3, \vartheta) = 2\pi + \vartheta \quad (4.60)$$

and hence

$$\begin{aligned} \bar{R}[\theta(\Gamma_1, \vartheta)] &= 2|b|^{1/3} \cos\left(\frac{\vartheta}{3}\right) = \bar{R}_{(k=0)} = \bar{\mathcal{R}}_3, \\ \bar{R}[\theta(\Gamma_2, \vartheta)] &= 2|b|^{1/3} \cos\left(\frac{2\pi - \vartheta}{3}\right) \\ &= 2|b|^{1/3} \cos\left(\frac{\vartheta - 2\pi}{3}\right) = \bar{R}_{(k=-1)} = \bar{\mathcal{R}}_2, \\ \bar{R}[\theta(\Gamma_3, \vartheta)] &= 2|b|^{1/3} \cos\left(\frac{2\pi + \vartheta}{3}\right) \\ &= \bar{R}_{(k=1)} = \bar{\mathcal{R}}_1. \end{aligned} \quad (4.61)$$

Analogically, the rules for fitting procedure can be obtained in the case  $\gamma < 0, \alpha > 0$ . So, all the fitting mechanism is clear now and can be used in further considerations.

#### 4.4.2. Dynamics of the Universe and scalaron in $R^2 + R^4$ model

To study the dynamics of the Universe in given model, let us assume that the four-dimensional metric  $g$  in (2.6) is spatially flat Friedmann-Robertson-Walker one:

$$g = -dt \otimes dt + a^2(t) d\vec{x} \otimes d\vec{x}. \quad (4.62)$$

Thus, scalar curvatures  $R$  and  $\bar{R}$  and scalaron  $\phi$  are functions of time. Therefore, Eq. (2.35) for homogeneous field  $\phi$  reads

$$\ddot{\phi} + 3H\dot{\phi} + \frac{dU}{d\phi} = 0, \quad (4.63)$$

where the Hubble parameter  $H = \dot{a}/a$  and the dotes denote the differentiation with respect to time  $t$ . Potential  $U$  is defined by Eq. (2.5). Because  $U$

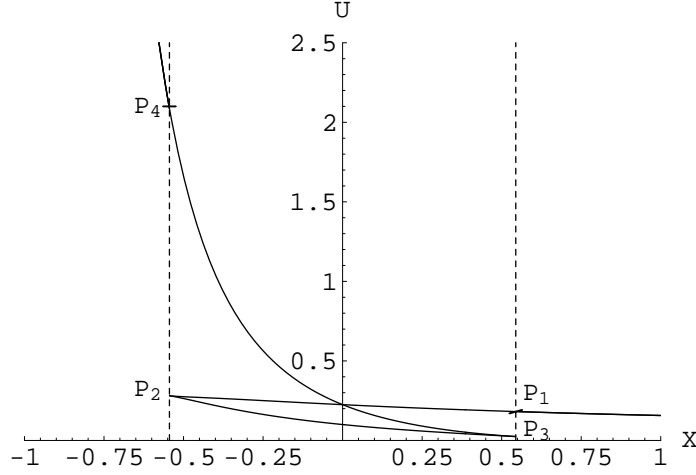


Figure 4.23: The form of the potential (3.8) as a multi-valued function of  $X = e^{A\phi} - 1$  in the case  $D = 4$ ,  $\Lambda_4 = 0.1$ ,  $\gamma = 1$  and  $\alpha = -1$ . Points  $P_{1,2,3,4}$  are defined in Fig. 4.22.

depends on  $\bar{R}$  which is a multi-valued function of  $\phi$  (or, equivalently, of  $X$ ), the potential  $U$  is also a multi-valued function of  $X$  (see Fig. 4.23)<sup>24</sup>. However, previous analysis shows that this problem can be avoided by making  $X$  and  $\bar{R}$  single-valued functions of a new field  $\theta$  (one would remind that the particular case of  $\alpha\gamma < 0$  is considered when  $\alpha < 0$ ,  $\gamma > 0$ ):

$$X(\theta) = \begin{cases} \sqrt{(1/\gamma) (2|\alpha|/3)^3} \cosh(\theta) & , \theta < 0 \\ \sqrt{(1/\gamma) (2|\alpha|/3)^3} \cos(\theta) & , 0 \leq \theta \leq 3\pi \\ -\sqrt{(1/\gamma) (2|\alpha|/3)^3} \cosh(\theta - 3\pi) & , \theta > 3\pi \end{cases} \quad (4.64)$$

and

$$\bar{R}(\theta) = \begin{cases} 2\sqrt{|\alpha|/(6\gamma)} \cosh(\theta/3) & , \theta < 0 \\ 2\sqrt{|\alpha|/(6\gamma)} \cos(\theta/3) & , 0 \leq \theta \leq 3\pi \\ -2\sqrt{|\alpha|/(6\gamma)} \cosh[(\theta/3) - \pi] & , \theta > 3\pi \end{cases} \quad (4.65)$$

The function  $X = X(\theta)$  is schematically given in Fig. 4.24. It is necessary to keep in mind that the case under consideration is  $f' > 0 \rightarrow X > -1$ . If condition  $X_{min} > -1$  is imposed (in opposite case the graphic  $X(\theta)$  will be cut into two disconnected parts) then the parameters  $\alpha$  and  $\gamma$  should satisfy

<sup>24</sup>In spite of the divergency of  $d\bar{R}/dX$  in the branching points  $P_{2,3}$ , the derivatives  $dU/dX$  are finite in these points. Moreover,  $\bar{R}$  and  $X$  have the same values in branching points for different branches. Therefore, the branches arrive at the branching points with the same values of  $dU/dX$  and Fig. 4.23 clearly shows it.

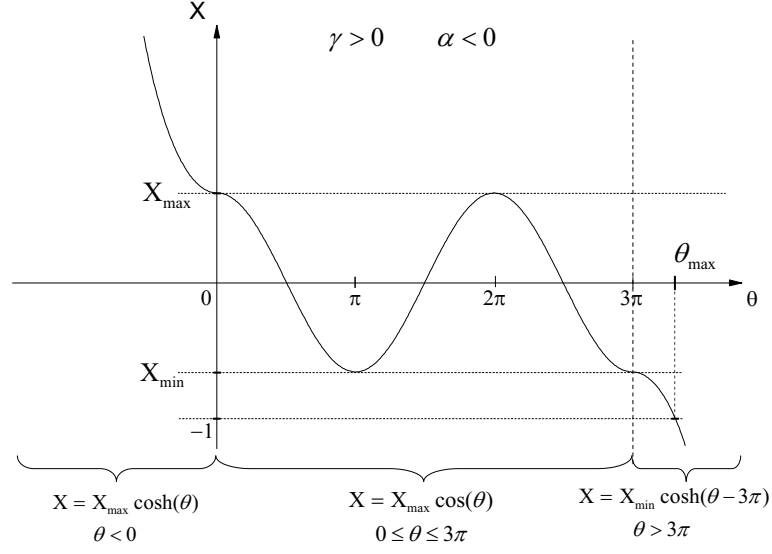


Figure 4.24: The schematic drawing of Eq. (4.64) in the case  $X_{min} > -1$ . Here,  $X_{max} = \sqrt{(1/\gamma) (2|\alpha|/3)^3}$ ,  $X_{min} = -\sqrt{(1/\gamma) (2|\alpha|/3)^3}$  and  $\theta_{max}$  is defined by Eq. (4.67).

the inequality:

$$X_{min} = -\sqrt{(1/\gamma) (2|\alpha|/3)^3} > -1 \Rightarrow |\alpha| \leq \frac{3}{2}\gamma^{1/3}. \quad (4.66)$$

The maximal value of  $\theta$  (which is greater than  $3\pi$  in the case  $X_{min} > -1$ ) is defined from the transcendental equation

$$\begin{aligned} & \frac{1}{2} \left[ \left( c + \sqrt{c^2 - 1} \right)^{1/3} + \left( c - \sqrt{c^2 - 1} \right)^{1/3} \right] = \\ & = \cosh[(\theta_{max}/3) - \pi], \end{aligned} \quad (4.67)$$

where  $c := \left( \sqrt{(1/\gamma) (2|\alpha|/3)^3} \right)^{-1}$ . The limit  $X \rightarrow -1$  corresponds to the limit  $\theta \rightarrow \theta_{max}$ . With the help of Eq. (4.64) and formula

$$\frac{d\phi}{d\theta} = \frac{1}{A(X+1)} \frac{dX}{d\theta} \quad (4.68)$$

the following useful expressions can be also obtained:

$$\left. \frac{d\phi}{d\theta} \right|_{\theta=0,\pi,2\pi,3\pi} = \left. \frac{dX}{d\theta} \right|_{\theta=0,\pi,2\pi,3\pi} = 0. \quad (4.69)$$

It can be easily verified that field  $\theta$  satisfies the equation:

$$\ddot{\theta} + 3H\dot{\theta} + \Gamma(\theta)\dot{\theta}^2 + G(\theta)\frac{dU}{d\theta} = 0. \quad (4.70)$$

Here,  $G(\theta) \equiv G^{11} = (G_{11})^{-1} = (d\phi/d\theta)^{-2}$  is the one dimensional metric on the moduli space with the corresponding Christoffel symbol  $\Gamma(\theta) \equiv \Gamma_{11}^1 = (1/2)G^{11}(G_{11})_{,\theta} = (d^2\phi/d\theta^2)/(d\phi/d\theta)$ .

#### 4.4.3. Properties of the potential $U(\theta)$

As it was mentioned above, in current case the potential (2.5) as a function of  $\theta$  is a single-valued one. Now, let us investigate analytically some general properties of  $U(\theta)$ . In this section,  $D$  is an arbitrary number of dimensions and signs of  $\alpha$  and  $\gamma$  are not fixed if it is not specified particularly.

First, let us consider the extrema of the potential  $U(\theta)$ . To find the extremum points the equation have to be solved

$$\frac{dU}{d\theta} = \frac{dU}{d\phi} \frac{d\phi}{d\theta} = \frac{dU}{d\phi} \frac{1}{A(X+1)} \frac{dX}{d\theta} = 0. \quad (4.71)$$

Therefore, the extrema correspond either to the solutions of the equation (2.30)  $dU/d\phi = 0$  for finite  $dX/d\theta$  ( $X > -1$ ) or to the solutions of the equation  $dX/d\theta = 0$  ( $X > -1$ ) for finite  $dU/d\phi$ . The form of the potential  $U$  (see Eq. (2.5)) shows that this potential and its derivative  $dU/d\phi$  is finite for  $X > -1$ . Thus, as it follows from Eq. (4.69), the potential  $U(\theta)$  has extrema at the matching points  $\theta = 0, \pi, 2\pi, 3\pi$ . Additional extremum points are real solutions of the equation (2.69). For the given model (2.43) this equation reads:

$$\bar{R}^4 \gamma \left( \frac{D}{2} - 4 \right) + \bar{R}^2 \alpha \left( \frac{D}{2} - 2 \right) + \bar{R} \left( \frac{D}{2} - 1 \right) - D\Lambda_D = 0. \quad (4.72)$$

The form of this equation shows that there are two particular cases:  $D = 8$  and  $D = 4$ . The  $D = 8$  case was considered previously. Let us consider now the case  $D = 4$ :

$$\bar{R}^4 - \frac{1}{2\gamma} \bar{R} + \frac{2\Lambda_4}{\gamma} = 0. \quad (4.73)$$

It is worth of noting that parameter  $\alpha$  disappeared from this equation. Thus  $\alpha$  has no an influence on a number of additional extremum points. To solve this quartic equation, one should consider an auxiliary cubic equation

$$u^3 - \frac{8\Lambda_4}{\gamma} u - \frac{1}{4\gamma^2} = 0. \quad (4.74)$$



The analysis of this equation can be performed in similar manner as it was done it for the cubic equation (2.45). Let us introduce the notations:

$$\begin{aligned}\bar{q} &:= -\frac{8}{3} \frac{\Lambda_4}{\gamma}, \bar{r} := \frac{1}{8} \frac{1}{\gamma^2}, \\ \bar{Q} &:= \bar{r}^2 + \bar{q}^3 = \frac{1}{\gamma^4} \left( \frac{1}{8^2} - \gamma \left( \frac{8\Lambda_4}{3} \right)^3 \right).\end{aligned}\quad (4.75)$$

It make sense to consider two separate cases.

$$1. \text{ sign } \gamma = -\text{sign } \Lambda_4 \quad \Rightarrow \quad \bar{Q} > 0.$$

In this case only one real solution of Eq. (4.74) is needed:

$$u_1 = \left[ \bar{r} + \bar{Q}^{1/2} \right]^{1/3} + \left[ \bar{r} - \bar{Q}^{1/2} \right]^{1/3} > 0. \quad (4.76)$$

Then, solutions of the quartic (4.73) are the real roots of two quadratic equations

$$\bar{R}^2 \pm \sqrt{u_1} \bar{R} + \frac{1}{2} \left( u_1 \pm \epsilon \sqrt{u_1^2 + 3q} \right) = 0, \quad \epsilon = \text{sign } \gamma. \quad (4.77)$$

Simple analysis shows that for any sign of  $\gamma$  two real solutions can be obtained:

$$\gamma < 0 \Rightarrow \bar{R}_{1,2}^{(+)} = -\frac{1}{2} u_1^{1/2} \pm \sqrt{-\frac{1}{4} u_1 + \frac{1}{2} (u_1^2 + 3q)^{1/2}}, \quad (4.78)$$

$$\gamma > 0 \Rightarrow \bar{R}_{1,2}^{(-)} = \frac{1}{2} u_1^{1/2} \pm \sqrt{-\frac{1}{4} u_1 + \frac{1}{2} (u_1^2 + 3q)^{1/2}}.$$

$$2. \text{ sign } \gamma = \text{sign } \Lambda_4 \quad \Rightarrow \quad \bar{Q} \geq 0.$$

It is not difficult to show that in this case the real solutions of the form of (4.78) (where the evident substitution is done  $u_1^2 + 3q \rightarrow u_1^2 - 3|q|$ ) takes place if

$$\bar{Q} > 0 \quad \Rightarrow \quad |\gamma|^{1/3} < \frac{3}{32|\Lambda_4|}. \quad (4.79)$$

Now, let us investigate zeros of the potential  $U$ . For  $f' \neq 0 \Rightarrow X \neq -1$ , the condition of zeros of the potential (2.5) is:

$$\bar{R}f' - f = 0 \quad \Rightarrow \quad 3\gamma\bar{R}^4 + \alpha\bar{R}^2 + 2\Lambda_D = 0. \quad (4.80)$$

Therefore, zeros are defined by equation:

$$\bar{R}^2 = -\frac{\alpha}{6\gamma} \pm \left[ \left( \frac{\alpha}{6\gamma} \right)^2 - \frac{2\Lambda_D}{3\gamma} \right]^{1/2}. \quad (4.81)$$

Obviously, the necessary conditions for zeros are:

$$\begin{aligned}\gamma > 0 &\Rightarrow \Lambda_D \leq \alpha^2/(24\gamma), \\ \gamma < 0 &\Rightarrow \Lambda_D \geq -\alpha^2/(24|\gamma|).\end{aligned}\tag{4.82}$$

Additionally, the positiveness of the r.h.s. of the equation (4.81) should be checked.

Let us consider now asymptotical behavior of the potential  $U(\theta)$ . Here, the limits  $\theta \rightarrow \theta_{max}$  and  $\theta \rightarrow -\infty$ . In the former case it appears:

$$\theta \rightarrow \theta_{max} \Rightarrow U(\theta) \rightarrow -\text{sign}(f(\theta_{max})) \times \infty.\tag{4.83}$$

In the latter case:

$$\begin{aligned}\theta \rightarrow -\infty &\Rightarrow \\ U(\theta) \sim \exp\left(\frac{8-D}{D-2}\theta\right) &\rightarrow \begin{cases} +\infty, & D > 8; \\ \text{const} > 0, & D = 8; \\ +0, & 2 < D < 8; \end{cases}\end{aligned}\tag{4.84}$$

where Eqs. (4.64) and (4.65) have been used. This result coincides with conclusions of appendix 1 in [59].

To illustrate the described above properties, let us draw the potential  $U(\theta)$  in Fig. 4.25 for the following parameters:  $D = 4$ ,  $\Lambda_4 = 0.1$ ,  $\gamma = 1$  and  $\alpha = -1$ . These parameters contradict to the inequalities (4.79) and (4.82). Therefore,  $\theta = 0, \pi, 2\pi, 3\pi$  are the only extremum points of the potential  $U(\theta)$  and zeros are absent. These parameters are also satisfy the condition (4.66). The absence of zeros means that all minima of the potential  $U(\theta)$  are positive.

For the subsequent investigations, it is useful also to consider an effective force and mass squared of the field  $\theta$ . As it follows from Eq. (4.70), the effective force:

$$F = -G(\theta)\frac{dU}{d\theta}.\tag{4.85}$$

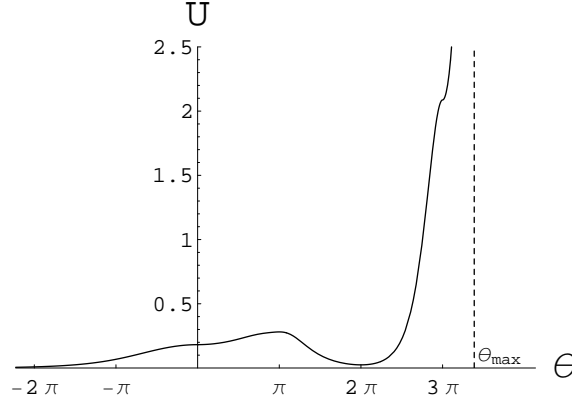


Figure 4.25: The form of the potential (2.5) as a function of  $\theta$  in the case  $D = 4$ ,  $\Lambda_4 = 0.1$ ,  $\gamma = 1$  and  $\alpha = -1$ . For these values of the parameters, all extrema correspond to the matching points  $\theta = 0, \pi, 2\pi, 3\pi$ . In the branching points  $\theta = \pi, 2\pi$  the potential has local maximum and local non-zero minimum, respectively, and the monotonic points  $\theta = 0, 3\pi$  are the inflection ones. Potential tends asymptotically to  $+\infty$  when  $\theta$  goes to  $\theta_{max}$  and to zero when  $\theta \rightarrow -\infty$ .

Varying Eq. (4.70) with respect to field  $\theta$  one obtains dynamical equation for small fluctuation  $\delta\theta$  where mass squared reads:

$$m_\theta^2 = G(\theta) \frac{d^2 U}{d\theta^2} + \frac{dG(\theta)}{d\theta} \frac{dU}{d\theta}. \quad (4.86)$$

In Fig. 4.26 the effective force and the mass squared are presented as functions of  $\theta$  for the potential drawn in Fig. 4.25. These figures indicate that field

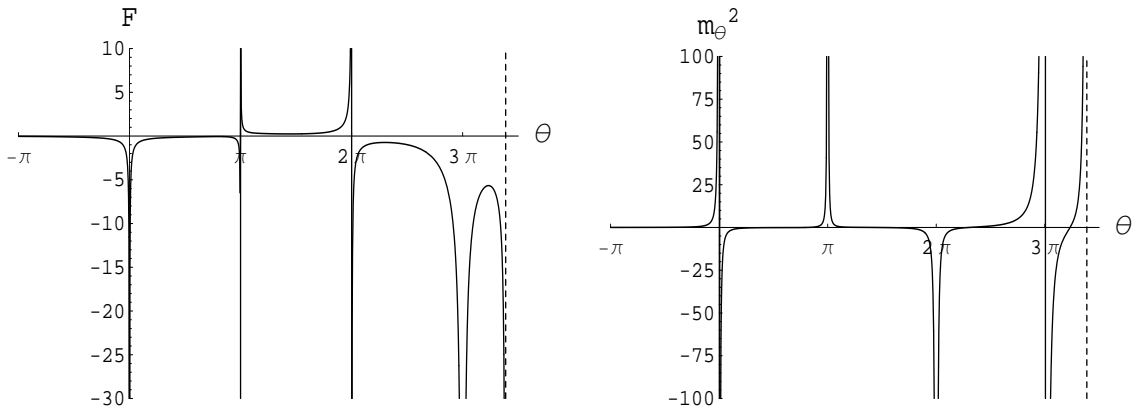


Figure 4.26: The effective force (4.85) (left panel) and the mass squared (4.86) (right panel) for the potential  $U(\theta)$  drawn in Fig. 4.25. These pictures clearly show singular behavior of  $F$  and  $m_\theta^2$  in the matching points  $\theta = 0, \pi, 2\pi, 3\pi$ .

$\theta$  may have very nontrivial behavior. This non-triviality follows from two

reasons. First, the field  $\theta$  has non-canonical kinetic term which result in appearing of non-flat moduli space metric  $G(\theta)$  and derivative of  $G(\theta)$  in Eq. (4.70). Second, the function  $G(\theta)$  has singular behavior at the matching points  $\theta = 0, \pi, 2\pi, 3\pi$ . Thus, the given intuition does not work when one wants to predict dynamical behavior of fields with equations of the form of (4.70) with potential drawn in Fig. 4.25, especially when field approaches the matching points. It is necessary to solve equations analytically or to investigate them numerically. Such analysis for the given model is performed in the next section where the concentration is focused on the case, where all extrema correspond to the matching points  $\theta = 0, \pi, 2\pi, 3\pi$ .

#### 4.4.4. Dynamical behavior of the Universe and field $\theta$

Let us investigate dynamical behavior of scalar field  $\theta$  and the scale factor  $a$  in more detail. There are no analytic solutions for considered model. So, numerical calculations are used. To do it, a Mathematica package proposed in [120] is applied and adjusted to the given models and notations in appendix 3 of the paper [61]. According to these notations, all dimensional quantities in the graphics are given in the Planck units. Additionally, one should remember that metric on the moduli space is not flat and defined in Eq. (4.70). For example, the canonical momenta and the kinetic energy read:

$$P_\theta = \frac{a^3}{\kappa_4^2} G_{11} \dot{\theta} = \frac{a^3}{\kappa_4^2} \left( \frac{d\phi}{d\theta} \right)^2 \dot{\theta}, \quad (4.87)$$

$$E_{kin} = \frac{1}{2\kappa_4^2} G_{11} \dot{\theta}^2 = \frac{\kappa_4^2}{2a^6} G^{11} P_\theta^2 = \frac{1}{2\kappa_4^2} \left( \frac{d\phi}{d\theta} \right)^2 \dot{\theta}^2,$$

where  $8\pi G \equiv \kappa_4^2$  and  $G$  is four-dimensional Newton constant. To understand the dynamics of the Universe, one shall also draw the Hubble parameter:

$$3 \left( \frac{\dot{a}}{a} \right)^2 \equiv 3H^2 = \frac{1}{2} G_{11} \dot{\theta}^2 + U(\theta) \quad (4.88)$$

and the acceleration parameter:

$$q \equiv \frac{\ddot{a}}{H^2 a} = \frac{1}{6H^2} \left( -4 \times \frac{1}{2} G_{11} \dot{\theta}^2 + 2U(\theta) \right). \quad (4.89)$$

Fig. 4.26 shows that the effective force changes its sign and the mass squared preserves the sign when  $\theta$  crosses the branching points  $\pi, 2\pi$  and vice versa, the effective force preserves the sign and the mass squared changes the sign when  $\theta$  crosses the monotonic points  $0, 3\pi$ . Therefore, it make sense to consider these cases separately.

#### 4.4.5. Branching points $\theta = \pi, 2\pi$

First, the dynamical behavior of the Universe and scalaron is considered in the vicinity of the branching point  $\theta = 2\pi$  which is the local minimum of the potential in Fig. 4.25. The time evolution of scalaron field  $\theta$  and its kinetic energy  $E_{kin}$  are drawn in Fig. 4.27. Here and in all pictures below, the same parameters are used as in Fig. 4.25. The time  $t$  is measured in the Planck times and classical evolution starts at  $t = 1$ . For the initial value of  $\theta$  it is taken that  $\theta_{initial} = 3.5$ . In Fig. 4.28 the evolution of the

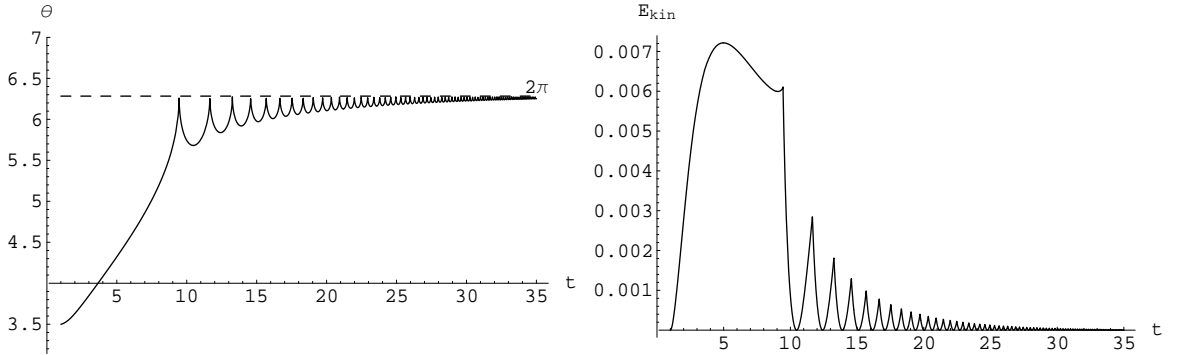


Figure 4.27: Dynamical behavior of scalar field  $\theta(t)$  (left panel) and its kinetic energy  $E_{kin}(t)$  (right panel) in the vicinity of the branching point  $\theta = 2\pi$ .

logarithms of the scale factor  $a(t)$  (left panel) and the evolution of the Hubble parameter  $H(t)$  (right panel) is plotted. and in Fig. 4.29 the evolution of the parameter of acceleration  $q(t)$  (left panel) and the equation of state parameter  $\omega(t) = [2q(t) + 1]/3$  (right panel).

Fig. 4.27 demonstrates that scalar field  $\theta$  bounces an infinite number of times with decreasing amplitude in the vicinity of the branching point  $\theta = 2\pi$ .  $\theta$  cannot cross this point. From Figs. 4.28 and 4.29 it can be

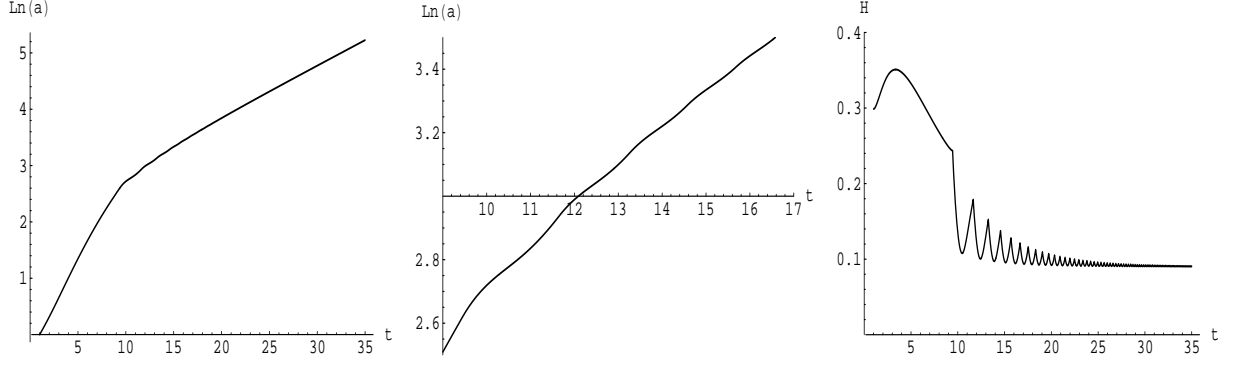


Figure 4.28: The time evolution of the logarithms of the scale factor  $a(t)$  (left panel) and the Hubble parameter  $H(t)$  (right panel) for the trajectory drawn in Fig. 4.27. A slightly visible oscillations of  $\ln(a)$  (caused by bounces) can be seen by magnification of this picture (middle panel).

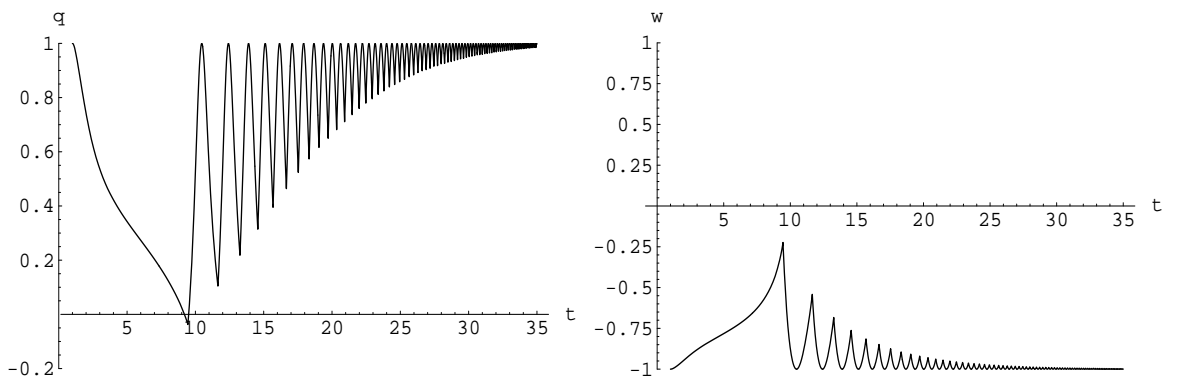


Figure 4.29: The parameter of acceleration  $q(t)$  (left panel) and the equation of state parameter  $\omega(t)$  (right panel) for the scale factor in Fig. 4.28.

seen that the Universe asymptotically approaches the de Sitter stage:  $H \rightarrow \text{const}$ ,  $q \rightarrow +1$ , and  $\omega \rightarrow -1$ . Such accelerating behavior can be called *bouncing inflation*.

Concerning the dynamical behavior in the vicinity of the branching point  $\theta = \pi$ , the analysis (similar performed above) shows that the scalaron field  $\theta$  cannot cross this local maximum regardless of the magnitude of initial velocity in the direction of  $\theta = \pi$ . It bounces back from this point.

#### 4.4.6. Monotonic points $\theta = 0, 3\pi$

Now, let us investigate the dynamical behavior of the model in the vicinity of the monotonic points  $\theta = 0, 3\pi$  which are the points of inflection of the potential in Fig. 4.25. Figs. 4.25 and 4.26 show that for both of these points the model has the similar dynamical behavior. Therefore, for definiteness, let us consider the point  $\theta = 3\pi$ . To investigate numerically the crossing of the monotonic point  $3\pi$ , it is necessary to take very small value of a step  $\Delta t$ . It can be achieved if very large value of the maximum number of steps is chosen. Thus, for the given value of the maximum number of steps, the closer to  $3\pi$  the initial value  $\theta_{\text{initial}}$  is taken the smaller step  $\Delta t$  is obtained. For current calculation let us choose  $\theta_{\text{initial}} = 9.513$ . Fig. 4.30 demonstrates that scalar field  $\theta$  slowly crosses the monotonic point  $3\pi$  with nearly zero kinetic energy<sup>25</sup>. Then, just after the crossing, the kinetic energy has its maximum value and starts to decrease gradually when  $\theta$  moves to the direction  $2\pi$ .

Figs. 4.31 and 4.32 demonstrate the behavior of the Universe before and after crossing  $3\pi$ . The vicinity of the branching point  $2\pi$  is not shown because when  $\theta$  approaches  $2\pi$  the Universe has the bouncing inflation described above. Hence, there are 3 phases sequentially: the short de Sitter-like stage during slow rolling in the vicinity of the inflection point before crossing, then decelerating expansion just after the crossing with gradual transition to the accelerating stage again when  $\theta$  approaches the branching point  $2\pi$ . Clearly

---

<sup>25</sup>The derivative  $d\theta/dt$  goes to  $-\infty$  when  $\theta \rightarrow 3\pi$  (with different speed on different sides of  $3\pi$ ) but  $d\phi/d\theta = 0$  at  $3\pi$  and kinetic energy is finite (see Eq. (4.87)).

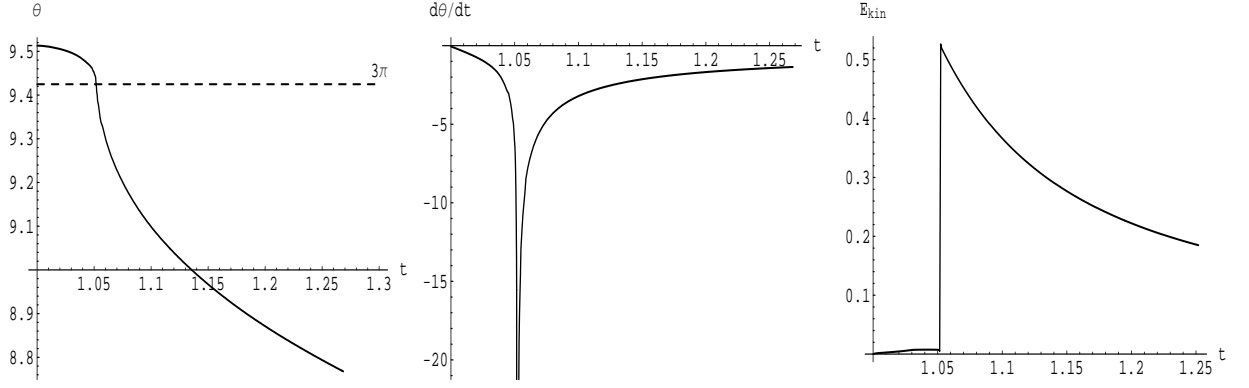


Figure 4.30: Dynamical behavior of scalar field  $\theta(t)$  (left panel) and its time derivative  $d\theta/dt$  (middle panel) and kinetic energy  $E_{kin}(t)$  (right panel) for the case of crossing of the inflection point  $\theta = 3\pi$ .

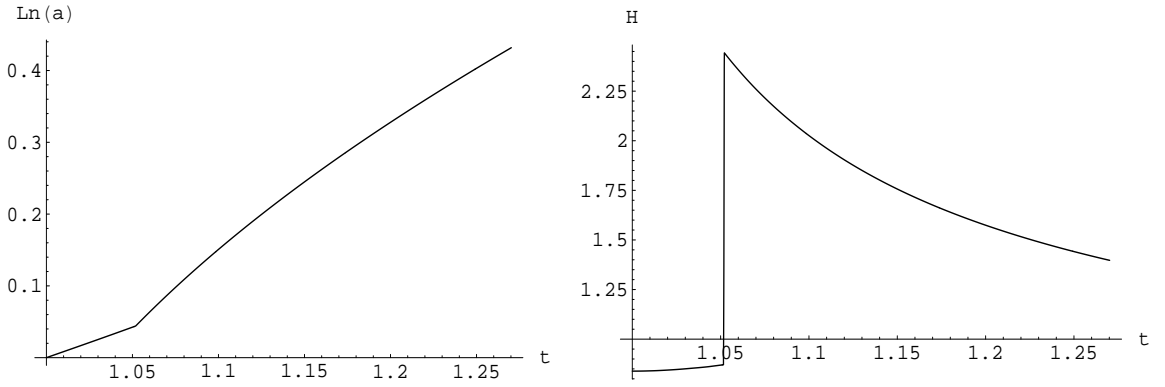


Figure 4.31: The time evolution of the logarithms of the scale factor  $a(t)$  (left panel) and the Hubble parameter  $H(t)$  (right panel) for the trajectory drawn in Fig. 4.30.

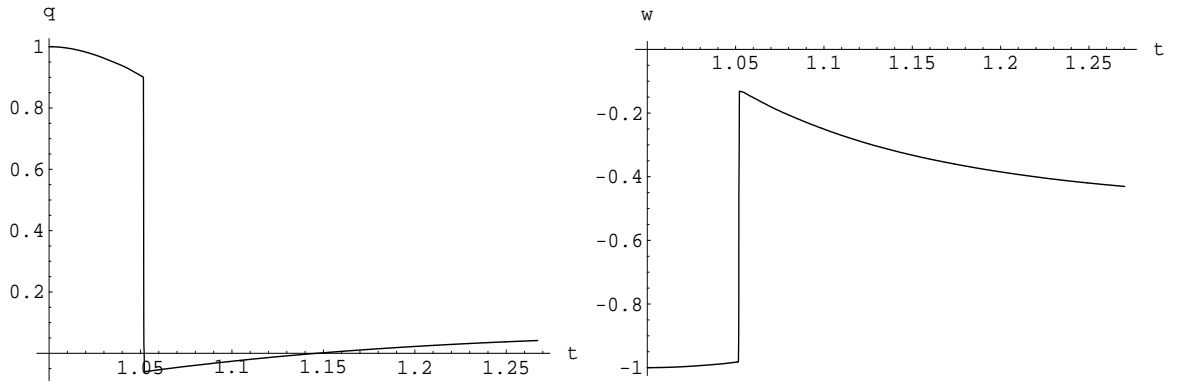


Figure 4.32: The parameter of acceleration  $q(t)$  (left panel) and the equation of state parameter  $\omega(t)$  (right panel) for the scale factor in Fig. 4.31.



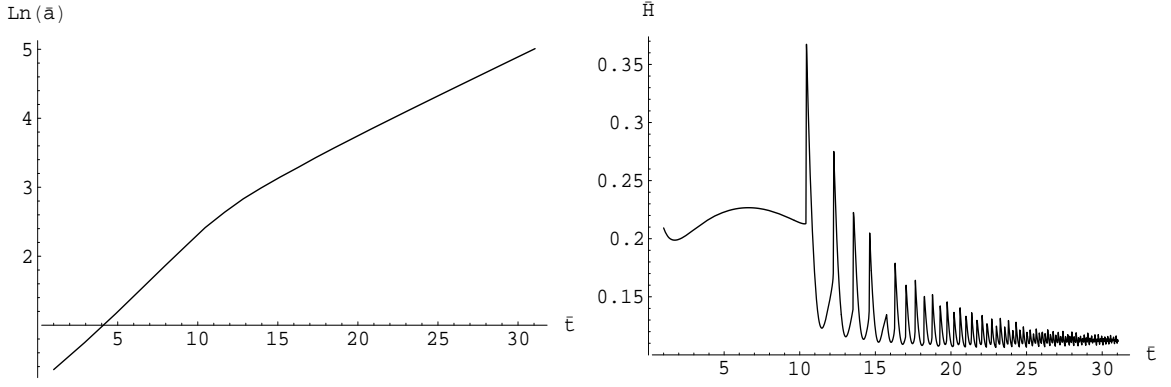


Figure 4.33: The time evolution of the logarithms of the scale factor  $\bar{a}(\bar{t})$  (left panel) and the Hubble parameter  $\bar{H}(\bar{t})$  (right panel) for the trajectory drawn in Fig. 4.27 in the Brans-Dicke frame.

that for another monotonic point  $\theta = 0$  the similar crossing behavior (without the bouncing stage when  $\theta \rightarrow -\infty$ ) can be reached. Therefore, the monotonic points  $\theta = 0$  and  $\theta = 3\pi$  are penetrable for the scalaron field  $\theta$ .

In appendix 4, it is shown that bouncing inflation in the vicinity of the branching point takes place also in the Brans-Dicke frame.

### Summary

A possibility of inflation in multidimensional cosmological models has been investigated. The main attention was paid to nonlinear (in scalar curvature) models with quadratic  $\bar{R}^2$  and quartic  $\bar{R}^4$  lagrangians. These models contain two scalar fields. One of them corresponds to the scale factor of the internal space and another one is related with the nonlinearity of the original models. The effective four-dimensional potentials in these models are fully determined by the geometry and matter content of the models. The geometry is defined by the direct product of the Ricci-flat external and internal spaces. As a matter source, a monopole form field, D-dimensional bare cosmological constant and tensions of branes located in fixed points have been included into consideration. The exact form of the effective potentials depends on the relation between parameters of the models and can take rather complicated view with a number of extrema points.

First of all, it was found that a range of parameters which insures the

existence of zero minima of the effective potentials. These minima provide sufficient condition to stabilize the internal space and, consequently, to avoid the problem of the fundamental constant variation. Zero minima correspond to the zero effective four-dimensional cosmological constant. In general, one can also consider positive effective cosmological constant which corresponds to the observable now dark energy. However, it usually requires extreme fine tuning of parameters of models.

Then, for corresponding effective potentials, the possibility of the external space inflation was investigated. It have been shown that for some initial conditions in the quadratic and quartic models can be achieve up to 10 and 22 e-folds, respectively. An additionally bonus of the considered model is that  $R^4$  model can provide conditions for the eternal topological inflation.

Obviously, 10 and 22 e-folds are not sufficient to solve the homogeneity and isotropy problem but big enough to explain the recent CMB data. To have the inflation which is long enough for modes which contribute to the CMB, it is usually supposed that  $\Delta N \geq 15$  [123]. Moreover, 22 e-folds is rather big number to encourage the following investigations of the nonlinear multidimensional models to find theories where this number will approach 50-60. It can be seen that the increase of the nonlinearity (from quadratic to quartic one) results in the increase of  $\Delta N$  in more that two times. So, there is a hope that more complicated nonlinear models can provide necessary 50-60 e-folds. Besides, this number is reduced in models where long matter dominated (MD) stage followed inflation can subsequently decay into radiation [127,128]. Precisely this scenario takes place for given models. It also have been shown for quadratic and quartic nonlinear models, that MD stage with the external scale factor  $a \sim t^{2/3}$  takes place after the stage of inflation. It happens when scalar fields start to oscillate near the position of zero minimum of the effective potential.

For the investigation of the dynamical behavior of the scalaron field  $\phi$  and the Universe in nonlinear model with curvature-squared and curvature-quartic correction terms: , the parameters  $\alpha$  and  $\gamma$  are chosen in such a way that the scalaron potential  $U(\phi)$  is a multi-valued function consisting of a

number of branches. These branches are fitted with each other either in the branching points (points  $P_{2,3}$  in Fig. 4.23) or in the monotonic points (points  $P_{1,4}$  in Fig. 4.23). The potential  $U$  was optimized so that a way that it becomes the one-valued function of a new field variable  $\theta = \theta(\phi)$  (see Fig. 4.25). This has enabled to consider the dynamical behavior of the system in the vicinity of the branching and monotonic points in  $(D = 4)$ -dimensional space-time. This investigation shows that the monotonic points are penetrable for scalaron field (see Figs. 4.30-4.32) while in the vicinity of the branching points scalaron has the bouncing behavior and cannot cross these points. Moreover, there are branching points where scalaron bounces an infinite number of times with decreasing amplitude and the Universe asymptotically approaches the de Sitter stage (see Figs. 4.27-4.29). Such accelerating behavior is called bouncing inflation. It should be noted that for this type of inflation there is no need for original potential  $U(\phi)$  to have a minimum or to check the slow-roll conditions. A necessary condition is the existence of the branching points. This is a new type of inflation. It is shown that this inflation takes place both in the Einstein and Brans-Dicke frames. It is found that this type of inflation for the model with the curvature-squared and curvature-quartic correction terms which play an important role during the early stages of the Universe evolution. However, the branching points take also place in models with  $\bar{R}^{-1}$ -type correction terms [129]. These terms play an important role at late times of the evolution of the Universe.

There is no need for fine tuning of the initial conditions to get the bouncing inflation. In Figs. (4.27)-(4.29), for definiteness the initial conditions are chosen as  $\theta = 3.5$  and  $E_{kin} = 0$ . However, the calculations show that these figures do not qualitatively change if one takes arbitrary  $\theta \in (\pi, 2\pi)$  and non-zero  $E_{kin}$ . Fig. 4.26 indicates that the minimum at  $\theta = 2\pi$  is stable with respect to tunneling through the barrier at this point. The situation is similar to the quantum mechanical problem with infinitely high barrier. It has been stressed already that the form of the potential Fig. 4.25 is not sufficient to predict the dynamical behavior of  $\theta$ . This field has very non-trivial behavior because of non-canonical kinetic term and singular (at the matching points)

non-flat moduli space metric  $G(\theta)$ . Therefore, it is impossible to "jump" quantum mechanically from one branch to another. It is impossible to apply to given dynamical system the standard tunneling approach (e.g., in [130]). This problem needs a separate investigation. It is worth of noting that the Universe with a bounce preceding the inflationary period was considered in [131] where it was shown that due to a bounce the spectrum of primordial perturbations has the characteristic features. It indicates that the similar effect can take place in this model.

## CONCLUSION

Several nonlinear multidimensional gravitational models are studied in this Thesis from the point of freezing stabilization and compactification of additional dimensions; and possibility of inflation. The main results may be constituted as follows.

Two separate branches of the four-dimensional spaces are produced for multidimensional nonlinear models with the scalar curvature of type  $\bar{R}^{-1}$  after dimensional reduction. For these type of models, simultaneous compactification and late-time acceleration is unreachable, due to branching of potential.

The pure gravitational model with curvature-quadratic and curvature-quartic correction terms allows too the stable compactification of the internal space for certain interval of the parameters (regions of stability). Assuming the scale factor of the stabilized internal space to be in order of the Fermi length:  $b_{(0)1} \sim L_F \sim 10^{-17}\text{cm}$ , one arrive that  $\alpha \sim L_F^2$  and for the effective cosmological constant and masses folds:  $-\Lambda_{eff} \sim m_1^2 \sim m_\phi^2 \sim 1\text{TeV}^2$ .

Adding forms to the model of  $\bar{R}^{-1}$  gives possibility to obtain positive minimum of the effective potential. In this model the freezing stabilization of the internal spaces is provided. This allows to avoid the problem of the fundamental constant variation in multidimensional models [95, 96]. At the same time, the stage of the cosmic acceleration is achieved too. However, fine tuning is required to get parameters of the present-day accelerating expansion.

Additionally the existence of domain walls was found for this model, which separates regions with different vacua in the Universe without providing of inflation, because the effective potential is not flat enough around the saddle point. In case of parameter  $z < 2$  the minimums of the potential is metastable, i.e. the quantum tunneling is possible both in  $\phi$  and in  $\varphi$  directions. For  $z \geq 2$ , tunneling in  $\varphi$  direction is still possible due to  $U_{eff}(\varphi, \phi_0) \approx e^{b\varphi}U(\phi_0) \rightarrow 0$  for  $\varphi \rightarrow -\infty$  which is less than any positive

$\Lambda_{eff}$ . This could result in the materialization of bubbles of the new phase in the metastable one (see e.g. [97]). Hence, late-time acceleration is possible only if characteristic lifetime of the metastable stage is greater than the age of the Universe. For this model the global negative minimum is also possible. This minimum is stable both in classical and quantum limits. However, the acceleration is absent because of its negativity.

Another feature of this model consists in multi-valued form of the effective potential, which was two branches for each choice of parameter  $\mu$ . This gives possibility for investigation of transitions from one branch to another one by analogy with catastrophe theory or similar to the phase transitions in statistical theory. In this particular model the point  $\phi = 0$  corresponds to the singularity  $\bar{R}, R \rightarrow \pm\infty$ . Indicating that the analog of the second order smooth phase transition through the point  $\phi = 0$  is impossible in this model. The analog of the first order transition via quantum jumps is possible too.

The inflation has been investigated in the models with nonlinearities of type  $\bar{R}^2$  and  $\bar{R}^4$  with a monopole form field, D-dimensional bare cosmological constant and tensions of branes located in fixed points as source. As result, the equivalent linear model has two scalar fields: one corresponds to the scale factor of the internal space and another the nonlinearity of the original models. Up to 10 and 22 e-folds can be achieved for  $\bar{R}^2$  and  $\bar{R}^4$  respectively, although it is not sufficient to solve the problems of homogeneity and isotropy in recent CMB data, where 50-60 e-folds are needed. This number is reduced in case if inflation, followed by long matter dominated stage, can subsequently decay into radiation [127, 128]. This scenario takes place for given models, as have been shown for  $\bar{R}^2$  and  $\bar{R}^4$  models: matter dominated stage with the external scale factor  $a \sim t^{2/3}$  occurs after the stage of inflation. It happens when scalar fields start to oscillate near the position of zero minimum of the effective potential. Another significant problem for these models consists in the spectral index. For example, in the case of  $\bar{R}^4$  model, the spectral index:  $n_s \approx 1 + 2\eta|_{\chi_{2(+)}} \approx 0.61$  which is less than observable now  $n_s \approx 1$ . As possible solution of this problem, more complicated function  $f(\bar{R})$  can be used. For example, in [56] it is shown that quadratic and quartic nonlinearities lead to

increase of  $n_s$ .

As next step, the dynamical behavior of the scalaron field  $\phi$  and the Universe in quadratic and quartic nonlinear model was investigated. In this case, the scalaron potential  $U(\phi)$  can be a multi-valued function consisting of a number of branches, being connected in the branching points or in the monotonic points. Further reparametrization of the potential  $U$  to the one-valued function of a new field variable  $\theta = \theta(\phi)$ , enables consideration of the dynamical behavior of the system in the vicinity of the branching and monotonic points. It appears that the monotonic points are penetrable for scalaron field while in the vicinity of the branching points scalaron has the bouncing behavior and cannot cross these points. Also branching points were found, where scalaron bounces an infinite number of times with decreasing amplitude, approaching asymptotically de Sitter stage. This kind of accelerating behavior is called bouncing inflation. For this type of inflation there is no need for original potential  $U(\phi)$  to have a minimum or to check the slow-roll conditions, i.e. no need for fine tuning. The existence of the branching points is only condition imposed. The minimum at  $\theta = 2\pi$  is stable for tunneling through the barrier at this point.

This represents a new type of inflation, which takes place both in the Einstein and Brans-Dicke frames and play an important role during the early stages of the Universe evolution. In the model of nonlinearity  $\bar{R}^{-1}$  [129] the branching points also take place, playing an important role at late times of the evolution of the Universe. Therefore, bouncing inflation may be responsible for the late-time accelerating expansion of the Universe.

## APPENDIXES

### Appendix 1. The critical dimensions in $f(\bar{R})$ theories

The existence of a critical dimension (in this case  $D = 8$ ) is a rather general feature of gravitational theories with polynomial scalar curvature terms (see, e.g., Refs. [42, 132, 133]). Following the paper [37], it can be easily demonstrated for a model with curvature nonlinearity of the type

$$f(\bar{R}) = \sum_{k=0}^N a_k \bar{R}^k \quad (\text{A1.1})$$

for which the ansatz

$$e^{A\phi} = f' = \sum_{k=0}^N k a_k \bar{R}^{k-1} \quad (\text{A1.2})$$

leads, similar like (2.5), to a potential

$$U(\phi) = \frac{1}{2} (f')^{-D/(D-2)} \sum_{k=0}^N (k-1) a_k \bar{R}^k. \quad (\text{A1.3})$$

The condition of extremum (2.30) for this potential reads:

$$Df - 2\bar{R}f' = \sum_{k=0}^N (D-2k) a_k \bar{R}^k = 0. \quad (\text{A1.4})$$

Thus, at the critical dimension  $D = 2N$  the degree of this equation is reduced from  $N$  to  $N-1$ . In this case the search of extrema is considerably simplified.

In the limit  $\phi \rightarrow +\infty$  the curvature will behave like  $\bar{R} \approx ce^{h\phi}$  where  $h$  and  $c$  can be defined from the dominant term in (A1.2):

$$e^{A\phi} \approx N a_N \bar{R}^{N-1} \approx N a_N c^{N-1} e^{(N-1)h\phi}. \quad (\text{A1.5})$$



Here the requirement  $f' > 0$  allows for the following sign combinations of the coefficients  $a_N$  and the curvature asymptotics  $\bar{R}(\phi \rightarrow \infty)$ :

$$\begin{aligned} N = 2l : & \quad \text{sign}[a_N] = \text{sign}[\bar{R}(\phi \rightarrow \infty)] \\ N = 2l + 1 : & \quad a_N > 0, \quad \text{sign}[\bar{R}(\phi \rightarrow \infty)] = \pm 1. \end{aligned} \quad (\text{A1.6})$$

The other combinations,  $N = 2l : \text{sign}[a_N] = -\text{sign}[\bar{R}(\phi \rightarrow \infty)]$ ,  $N = 2l + 1 : a_N < 0, \text{sign}[\bar{R}(\phi \rightarrow \infty)] = \pm 1$ , would necessarily correspond to the  $f' < 0$  sector, so that the complete consideration should be performed in terms of the extended conformal transformation technique of Ref. [50]. Such a consideration is out of the scope currently and the focus is restricted to the cases (A1.6). The coefficients  $h$  and  $c$  are then easily derived as  $h = A/(N-1)$  and  $c = \text{sign}(a_N) |Na_N|^{-\frac{1}{N-1}}$ . Plugging this into (A1.3) one obtains

$$U(\phi \rightarrow +\infty) \approx \text{sign}(a_N) \frac{(N-1)}{2N} |Na_N|^{-\frac{1}{N-1}} e^{-\frac{D}{D-2}A\phi} e^{\frac{N}{N-1}A\phi} \quad (\text{A1.7})$$

and that the exponent

$$\frac{D-2N}{(D-2)(N-1)}A \quad (\text{A1.8})$$

changes its sign at the critical dimension  $D = 2N$ :

$$U(\phi \rightarrow +\infty) \rightarrow \text{sign}(a_N) \frac{(N-1)}{2N} |Na_N|^{-\frac{1}{N-1}} \times \begin{cases} \infty & \text{for } D > 2N, \\ 1 & \text{for } D = 2N, \\ 0 & \text{for } D < 2N. \end{cases} \quad (\text{A1.9})$$

This critical dimension  $D = 2N$  is independent of the concrete coefficient  $a_N$  and is only defined by the degree  $\deg_{\bar{R}}(f)$  of the scalar curvature polynomial  $f$ . From the asymptotics (A1.9) follows that in the high curvature limit  $\phi \rightarrow +\infty$ , within given oversimplified classical framework, the potential  $U(\phi)$  of the considered toy-model shows asymptotical freedom for subcritical dimensions  $D < 2N$ , a stable behavior for  $a_N > 0$ ,  $D > 2N$  and a catastrophic instability for  $a_N < 0$ ,  $D > 2N$ . It should be noted that this general behavior suggests a way how to cure a pathological (catastrophic) behavior of polynomial  $\bar{R}^{N_1}$ -nonlinear theories in a fixed dimension  $D > 2N_1$ : By including higher order corrections up to order  $N_2 > D/2$  the theory gets shifted into

the non-pathological sector with asymptotical freedom. More generally, one is even led to conjecture that the partially pathological behavior of models in supercritical dimensions could be an artifact of a polynomial truncation of an (presently unknown) underlying non-polynomial  $f(\bar{R})$  structure at high curvatures — which probably will find its resolution in a strong coupling regime of  $M$ -theory or in loop quantum gravity.

## Appendix 2. Self-similarity condition

Due to the zero minimum conditions  $U(\phi_{min}) = f_1^2 = \lambda/2$ , the effective potential (4.13) can be written in the form:

$$U_{eff}(\varphi, \phi) = U(\phi_{min}) e^{-\sqrt{\frac{2d_1}{d_1+2}} \varphi} \times \left[ \frac{U(\phi)}{U(\phi_{min})} + e^{-2\sqrt{\frac{2d_1}{d_1+2}} \varphi} - 2e^{-\sqrt{\frac{2d_1}{d_1+2}} \varphi} \right]. \quad (\text{A2.1})$$

Exact expressions for  $U(\phi)$  (4.20) and (4.26) indicate that the ratio

$$\frac{U(\phi)}{U(\phi_{min})} = F(\phi, k, d_1) \quad (\text{A2.2})$$

depends only on  $\phi, k$  and  $d_1$ . Dimensionless parameter  $k = \xi \Lambda_D$  for the quadratic model and  $k = \gamma \Lambda_D^3$  for the quartic model. In Eq. (A2.2) one have to take into account that  $\phi_{min}$  is a function of  $k$  and  $d_1$ :  $\phi_{min} = \phi_{min}(k, d_1)$ . Then,  $U(\phi_{min})$  defined in Eqs. (4.20) and (4.26) reads:

$$U(\phi_{min}) = \Lambda_D \tilde{F}(\phi_{min}(k, d_1), k, d_1). \quad (\text{A2.3})$$

Therefore, parameters  $k$  and  $d_1$  determine fully the shape of the effective potential, and parameter  $\Lambda_D$  serves for conformal transformation of this shape. This conclusion is confirmed with the fact that all extrema depend only on  $k$  and  $d_1$ . Thus, figures 4.10, and 4.15 for contour plots are defined by  $k$  and  $d_1$  and will not change with  $\Lambda_D$ . From the definition of the slow roll parameters it is clear that they also do not depend on the hight of potentials and in the given model depend only on  $k$  and  $d_1$  (see figures 4.16 and 4.47). Similar dependence takes place for difference  $\Delta\phi = \phi_{max} - \phi_{min}$  drawn in Fig. 4.21.

Thus the conclusions concerning the slow roll and topological inflations are fully determined by the choice of  $k$  and  $d_1$  and do not depend on the height of the effective potential, in other words, on  $\Lambda_D$ . So, for fixed  $k$  and  $d_1$  parameter  $\Lambda_D$  can be arbitrary. For example, one can take  $\Lambda_D$  in such a way that the height of the saddle point  $\chi_{2(+)}$  will correspond to the restriction on the slow roll inflation potential (see e.g. [134])  $U_{eff} \lesssim 2.2 \times 10^{-11} M_{Pl}^4$ , or in the notations  $U_{eff} \lesssim 5.5 \times 10^{-10} M_{Pl}^2$ .

Above, the figure is indicated which (for given  $k$  and  $d_1$ ) do not depend on the height of the effective potential (on  $\Lambda_D$ ). What will happen with dynamical characteristics drawn in figures 4.18, 4.19 and 4.20 (and analogous ones for the quadratic model) if keeping fixed  $k$  and  $d_1$ , will change  $\Lambda_D$ ? In other words, the positions of the extrema points (in  $(\varphi, \phi)$ -plane) are kept, but the height of extrema experience change. One can easily answer this question using the self-similarity condition of the Friedmann equations. Let the potential  $U$  in Eqs. (A3.2) and (A3.3) be transformed conformally:  $U \rightarrow cU$  where  $c$  is a constant. Next, let us introduce a new time variable  $\tau := \sqrt{c}t$ . Then, from Eqs. (A3.2)-(A3.5) follows that the Friedmann equations have the same form as for the model with potential  $U$  where time  $t$  is replaced by time  $\tau$ . This condition one may call the self-similarity. Thus, if in the model one changes the parameter  $\Lambda_D$  :  $\Lambda_D \rightarrow c\Lambda_D$ , it results (for fixed  $k$  and  $d_1$ ) in rescaling of all dynamical graphics (e.g. Figures 4.18 - 4.20) along the time axis in  $1/\sqrt{c}$  times (the decrease of  $\Lambda_D$  leads to the stretch of these figures along the time axis and vice versa the increase of  $\Lambda_D$  results in the shrink of these graphics). Numerical calculations confirm this conclusion. The property of the conformal transformation of the shape of  $U_{eff}$  with change of  $\Lambda_D$  for fixed  $k$  and  $d_1$  can be also called as the self-similarity.

### Appendix 3. Multi-component scalar field model

Let us consider  $n$  scalar fields minimally coupled to gravity in four dimen-

sions. The effective action of this model reads

$$S = \frac{1}{16\pi G} \int d^4x \sqrt{|\tilde{g}^{(0)}|} \left( R[\tilde{g}^{(0)}] - G_{ij} \tilde{g}^{(0)\mu\nu} \partial_\mu \varphi^i \partial_\nu \varphi^j - 2U(\varphi^1, \varphi^2, \dots) \right) \quad (\text{A3.1})$$

where the kinetic term is taken in the canonical form:  $G_{ij} = \text{diag}(1, 1, \dots)$  (flat  $\sigma$  model). Such multi-component scalar fields originate naturally in multidimensional cosmological models (with linear or nonlinear gravitational actions) [57, 110, 115]. Here, the usual conventions  $c = \hbar = 1$  is used, i.e.  $L_{Pl} = t_{Pl} = 1/M_{Pl}$  and  $8\pi G = 8\pi/M_{Pl}^2$ . Here, scalar fields are dimensionless and potential  $U$  has dimension  $[U] = \text{length}^{-2}$ .

Because the aim is to investigate dynamical behavior of our Universe in the presence of scalar fields, let us suppose that scalar fields are homogeneous:  $\varphi^i = \varphi^i(t)$  and four-dimensional metric is spatially-flat Friedmann-Robertson-Walker one:  $\tilde{g}^{(0)} = -dt \otimes dt + a^2(t) d\vec{x} \otimes d\vec{x}$ .

For energy density and pressure follows:

$$\begin{aligned} \rho &= \frac{1}{8\pi G} \left( \frac{1}{2} G_{ij} \dot{\varphi}^i \dot{\varphi}^j + U \right), \\ P &= \frac{1}{8\pi G} \left( \frac{1}{2} G_{ij} \dot{\varphi}^i \dot{\varphi}^j - U \right); \end{aligned} \quad (\text{A3.2})$$

$$\Rightarrow \begin{cases} \frac{1}{2} G_{ij} \dot{\varphi}^i \dot{\varphi}^j = 4\pi G(\rho + P), \\ U = 4\pi G(\rho - P). \end{cases} \quad (\text{A3.3})$$

The Friedmann equations for considered model are

$$3 \left( \frac{\dot{a}}{a} \right)^2 \equiv 3H^2 = 8\pi G\rho = \frac{1}{2} G_{ij} \dot{\varphi}^i \dot{\varphi}^j + U, \quad (\text{A3.4})$$

and

$$\dot{H} = -4\pi G(\rho + P) = -\frac{1}{2} G_{ij} \dot{\varphi}^i \dot{\varphi}^j. \quad (\text{A3.5})$$

From these two equations, one obtains the following expression for the acceleration parameter:

$$\begin{aligned} q &\equiv \frac{\ddot{a}}{H^2 a} = 1 - \frac{4\pi G}{H^2}(\rho + P) = -\frac{8\pi G}{6H^2}(\rho + 3P) \\ &= \frac{1}{6H^2} \left( -4 \times \frac{1}{2} G_{ij} \dot{\varphi}^i \dot{\varphi}^j + 2U \right). \end{aligned} \quad (\text{A3.6})$$

It can be easily seen that the equation of state (EoS) parameter  $\omega = P/\rho$  and parameter  $q$  are linearly connected:

$$q = -\frac{1}{2}(1 + 3\omega). \quad (\text{A3.7})$$

From the definition of the acceleration parameter, it follows that  $q$  is constant in the case of the power-law and De Sitter-like behavior:

$$q = \begin{cases} (s-1)/s; & a \propto t^s, \\ 1; & a \propto e^{Ht}. \end{cases} \quad (\text{A3.8})$$

For example,  $q = -0.5$  during the matter dominated (MD) stage where  $s = 2/3$ .

Because the minisuperspace metric  $G_{ij}$  is flat, the scalar field equations are:

$$\ddot{\varphi}^i + 3H\dot{\varphi}^i + G^{ij}\frac{\partial U}{\partial \varphi^j} = 0. \quad (\text{A3.9})$$

For the action (A3.1), the corresponding Hamiltonian is

$$\mathcal{H} = \frac{8\pi G}{2a^3} G^{ij} P_i P_j + \frac{a^3}{8\pi G} U, \quad (\text{A3.10})$$

where

$$P_i = \frac{a^3}{8\pi G} G_{ij} \dot{\varphi}^j \quad (\text{A3.11})$$

are the canonical momenta and equations of motion have also the canonical form

$$\dot{\varphi}^i = \frac{\partial \mathcal{H}}{\partial P_i}, \quad \dot{P}_i = -\frac{\partial \mathcal{H}}{\partial \varphi^i}. \quad (\text{A3.12})$$

It can be easily seen that the latter equation (for  $\dot{P}_i$ ) is equivalent to the eq. (A3.9).

Thus, the Friedmann equations together with the scalar field equations

can be replaced by the system of the first order ODEs:

$$\dot{\varphi}^i = \frac{8\pi G}{a^3} G^{ij} P_j, \quad (\text{A3.13})$$

$$\dot{P}_i = -\frac{a^3}{8\pi G} \frac{\partial U}{\partial \varphi^i}, \quad (\text{A3.14})$$

$$\dot{a} = aH, \quad (\text{A3.15})$$

$$\begin{aligned} \dot{H} &= \frac{\ddot{a}}{a} - H^2 \\ &= \frac{1}{6} \left( -4 \times \frac{1}{2} G_{ij} \dot{\varphi}^i \dot{\varphi}^j + 2U \right) - H^2 \end{aligned} \quad (\text{A3.16})$$

with Eq. (A3.4) considered in the form of the initial conditions:

$$H(t=0) = \sqrt{\frac{1}{3} \left( \frac{1}{2} G_{ij} \dot{\varphi}^i \dot{\varphi}^j + U \right)} \Big|_{t=0}. \quad (\text{A3.17})$$

One can make these equations dimensionless:

$$\begin{aligned} \frac{d\varphi^i}{M_{Pl} dt} &= \frac{8\pi}{M_{Pl}^3 a^3} G^{ij} P_j, \\ \Rightarrow \frac{d\varphi^i}{dt} &= \frac{8\pi}{a^3} G^{ij} P_j; \end{aligned} \quad (\text{A3.18})$$

$$\begin{aligned} \frac{dP_i}{M_{Pl} dt} &= -\frac{a^3 M_{Pl}^3}{8\pi} \frac{\partial(U/M_{Pl}^2)}{\partial \varphi^i}, \\ \Rightarrow \frac{dP_i}{dt} &= -\frac{a^3}{8\pi} \frac{\partial U}{\partial \varphi^i}. \end{aligned} \quad (\text{A3.19})$$

That is to say the time  $t$  is measured in the Planck times  $t_{Pl}$ , the scale factor  $a$  is measured in the Planck lengths  $L_{Pl}$  and the potential  $U$  is measured in the  $M_{Pl}^2$  units.

The system of dimensionless first order ODEs together with the initial condition (A3.17) is used for numerical calculation of the dynamics of considered models with the help of a Mathematica package [120].

#### Appendix 4. Bouncing inflation in the Brans-Dicke frame

According to Eq. (2.6), the four-dimensional FRW metrics in the Einstein frame (4.62) and in the Brans-Dicke frame are related as follows:

$$-dt \otimes dt + a^2(t) d\vec{x} \otimes d\vec{x} = f' \left[ -d\bar{t} \otimes d\bar{t} + \bar{a}^2(\bar{t}) d\vec{x} \otimes d\vec{x} \right], \quad (\text{A4.1})$$

where  $f' = X + 1 > 0$  and  $X$  is parameterized by Eq. (4.64). Therefore, for the synchronous times and scale factors in both frames one obtains, correspondingly:

$$d\bar{t} = dt / \sqrt{f'(t)}, \quad (\text{A4.2})$$

$$\bar{a}(\bar{t}) = a(t(\bar{t})) / \sqrt{f'(t(\bar{t}))}, \quad (\text{A4.3})$$

which lead to the following equations:

$$\bar{t} = \int_1^t \frac{dt}{\sqrt{X(t) + 1}} + 1, \quad (\text{A4.4})$$

where the constant of integration is chosen in such a way that  $\bar{t}(t = 1) = 1$ , and

$$\begin{aligned} \bar{H}(\bar{t}) &= \frac{d\bar{a}}{d\bar{t}} \frac{1}{\bar{a}} = \sqrt{X(t(\bar{t})) + 1} \left[ H(t(\bar{t})) \right. \\ &\quad \left. - \frac{1}{2(X(t(\bar{t})) + 1)} \frac{dX}{dt}(t(\bar{t})) \right]. \end{aligned} \quad (\text{A4.5})$$

From the latter equation follows the relation between the Hubble parameters in both frames. In Fig. 4.33 the logarithms of the scale factor  $\bar{a}(\bar{t})$  and the Hubble parameter  $\bar{H}(\bar{t})$  are depicted for the trajectory drawn in Fig. 4.27. These pictures clearly demonstrate that in the Brans-Dicke frame the Universe has also asymptotical de Sitter stage when the scalaron field approaches the branching point  $\theta = 2\pi$ . It is not difficult to verify that because  $X(t \rightarrow +\infty) \rightarrow X_{max}$  and  $dX/dt(t \rightarrow +\infty) \rightarrow 0$ , one obtains the following relation for the asymptotic values of the Hubble parameters in both frames:

$$\bar{H} = H \sqrt{X_{max} + 1}. \quad (\text{A4.6})$$

## LITERATURE

- [1] Green M.B. Superstring theory / Green M.B., Schwarz J.H., Witten E. // Cambridge University Press. – 1987.
- [2] Polchinski J. String theory / Polchinski J. // Cambridge University Press. – 1998.
- [3] Wang L. Cosmic Concordance and Quintessence / Wang L., Caldwell R.R., Ostriker J.P., Steinhardt P.J. // Astrophys. J. – 2000. – V. 530. – P. 17–35.
- [4] Arkani-Hamed N. Stabilization of submillimeter dimensions: The new guise of the hierarchy problem / Arkani-Hamed N., Dimopoulos S., March-Russell G.J. // Phys. Rev. D. – 2000. – V. 63. – 064020, 13 p.
- [5] Banks T. Constraints on theories with large extra dimensions / Banks T., Dine M., Nelson A.E. // JHEP. – 1999. – V. 014. – 9906, 32 p.
- [6] Arkani-Hamed N. Rapid asymmetric inflation and early cosmology in theories with sub-millimeter dimensions / Arkani-Hamed N., Dimopoulos S., Kaloper N., March-Russell J. // Nucl. Phys. B. – 2000. – V. 567. – P. 189–228.
- [7] Carroll S.M. Classical stabilization of homogeneous extra dimensions / Carroll S.M., Geddes J., Hoffman M.B., Wald R.M. // Phys. Rev. D. – 2002. V. 66 – 024036, 25 p.
- [8] Geddes J. The Collapse of Large Extra Dimensions / Geddes J. // Phys. Rev. D. – 2002. – V. 65. – 104015, 12 p.
- [9] Demir D.A. Flavordynamics with Conformal Matter and Gauge Theories on Compact Hyperbolic Manifolds in Extra Dimensions / Demir D.A., Shifman M. // Phys. Rev. D. – 2002. – Vo. 65. – 104002, 16 p.



- [10] Nasri S. Radion stabilization in compact hyperbolic extra dimensions / Nasri S., Silva P.J., Starkman G.D., Trodden M. // Phys. Rev. D. – 2002, V. 66. – 045029, 16 p.
- [11] Perivolaropoulos L. Cosmological effect of radion oscillations / Perivolaropoulos L., Sourdis C. // Phys. Rev. D. – 2002. – V. 66. – 084018, 7 p.
- [12] Capozziello S. A Bird's Eye View of  $f(R)$ -Gravity / Capozziello S., De Laurentis M., Faraoni V. // The Open Astronomy J. – 2009. – V. 3. – 2009. – P. 49–72.
- [13] Spergel D.N. Wilkinson Microwave Anisotropy Probe (WMAP) Three Year Results: Implications for Cosmology / Spergel D.N. // Astrophys. J. Suppl. – 2007. – V. 170. – 377, 91 p.
- [14] Riess A.G. Type Ia Supernova Discoveries at  $z > 1$  From the Hubble Space Telescope: Evidence for Past Deceleration and Constraints on Dark Energy Evolution / Riess A.G. // Astrophys. J. – 2004. – V. 607. – P. 665–687.
- [15] Astier P. The Supernova Legacy Survey / Astier P. // Astron. Astrophys. – 2006. – V. 447. – P. 31–48.
- [16] Eisenstein D.J. Sloan Digital Sky Survey (SDSS) / Eisenstein D.J. // Astrophys. J. – 2005. – V. 633. – P. 560–574.
- [17] Sotiriou T.P.  $f(R)$  theories of gravity / Sotiriou T.P., Faraoni V. // Rev. Mod. Phys. – 2010. – V. 82. – P. 451–497.
- [18] Wald R.M. General Relativity / Wald R.M. // University of Chicago Press. – 1984.
- [19] Guth A.H. Inflationary universe: A possible solution to the horizon and flatness problems / Guth A.H. // Phys. Rev. D. – 1981. – V. 23. – P. 347–356.

- [20] Kolb E.W. The Early Universe / Kolb E.W., Turner M.S. // Addison-Wesley. – 1992.
- [21] Linde A. Particle Physics and Inflationary Cosmology / Linde A. // Harwood Academic Publishers. – 1990.
- [22] Nojiri S. Unified cosmic history in modified gravity: from  $F(R)$  theory to Lorentz non-invariant models / Nojiri S., Odintsov S.D. // E Print arXiv.org: 1011.0544v3.
- [23] Carroll S.M. The Cosmological Constant / Carroll S.M. // Living Rev. Rel. – 2001. – V. 4, 50 p.
- [24] Bondi H. Cosmology / Bondi H. // Cambridge University Press: Cambridge. – 1952.
- [25] Brans C.H. Mach's Principle and a Relativistic Theory of Gravitation / Brans C.H., Dicke R.H. // Phys Rev. – 1961. – V. 124. – P. 92–935.
- [26] Capozziello S. Noether Symmetries in Cosmology / Capozziello S., de Ritis R., Rubano C., Scudellaro P. // Riv Nuovo Cimento. – 1996. – V. 19. 114 p.
- [27] Sciama D.W. On the Origin of Inertia / Sciama D.W. // Mon Not R Ast Soc. – 1953. – V. 113. – P. 34–42.
- [28] Birrell N.D. Quantum Fields in Curved Space / Birrell N.D., Davies P.C.W. // Cambridge University Press. – 1982.
- [29] Nojiri S. Where new gravitational physics comes from: M-theory? / Nojiri S., Odintsov S.D. // Phys. Lett. B. – 2003. – V. 576. – P. 5–11.
- [30] Woodard R.P. Leading Log Solution for Inflationary Yukawa / Woodard R.P. // Lect. Notes Phys. – 2007. – V. 720. – 044019, 35 p.
- [31] Nojiri S. Introduction to Modified Gravity and Gravitational Alternative for Dark Energy / Nojiri S., Odintsov S.D. // Int. J. Geom. Meth. Mod. Phys. – 2007. – V. 4. – P. 115–146.

- [32] Sotiriou T.P.  $f(R)$  Theories Of Gravity / Sotiriou T.P., Faraoni V. // Rev. Mod. Phys. – 2010. – V. 82. – P. 451–497.
- [33] Kolb E.W. Time variation of fundamental constants, primordial nucleosynthesis, and the size of extra dimensions / Kolb E.W., Perry M.J., Walker T.P. // Phys. Rev. D. – 1986. – V. 33. – P. 869–871.
- [34] Gunther U. Gravitational excitons from extra dimensions / Gunther U., Zhuk A. // Phys. Rev. D. – 1997. – V. 56. – P. 6391–6402.
- [35] Gunther U. Stabilization of internal spaces in multidimensional cosmology / Gunther U., Zhuk A. // Phys. Rev. D. – 2000. – V. 61. – 124001, 11p.
- [36] Gunther U. Asymptotical AdS from non-linear gravitational models with stabilized extra dimensions / Gunther U., Moniz P., Zhuk A. // Phys. Rev. D. – 2002. – V. 66. – 044014, 12 p.
- [37] Gunther U. AdS and stabilized extra dimensions in multidimensional gravitational models with nonlinear scalar curvature terms  $1/R$  and  $R^4$  / Gunther U., Zhuk A., Bezerra V.B., Romero C. // Class. Quant. Grav. – 2005. – V. 22. – 3135, 28 p.
- [38] Kerner R. Cosmology without singularity and non-linear gravitational lagrangians / Kerner R. // GRG. – 1982. – V. 14. – P. 453–469.
- [39] Barrow J.D. The stability of general relativistic cosmological theory / Barrow J.D., Ottewill A.C. // J. Phys. A. – 1983. – V. 10. – P. 2757–2776.
- [40] Duruisseau J.P. Non-Einsteinian lagrangians assuring non-singular cosmological solutions / Duruisseau J.P., Kerner R. // GRG. – 1983. – V. 15. – P. 797–807.
- [41] Whitt B. Fourh-order gravity as general relativity plus matter / Whitt B. // Phys. Lett. B. – 1984. – V. 145. – P. 176–178.

- [42] Barrow J.D. Inflation and the conformal structure of higher-order gravity theories / Barrow J.D., Cotsakis S. // Phys. Lett. B. – 1988. – V. 214. – P. 515–518.
- [43] Maeda K. Chaotic inflationary scenario of the Universe with a nonminimally coupled “inflaton” field / Maeda K., Stein–Schabes J.A., Futamase T. // Phys. Rev. D. – 1989. – V. 39. – P. 2848–2853.
- [44] Magnano G. On Physical Equivalence between Nonlinear Gravity Theories / Magnano G., Sokolowski L.M. // Phys. Rev. D. – 1994. – V. 50. – P. 5039–5059.
- [45] Wands D. Extended Gravity Theories and the Einstein-Hilbert Action / Wands D. // CQG. – 1994. – V. 11. – P. 269–279.
- [46] Ellis J. Topological  $R^4$  Inflation / Ellis J., Kaloper N., Olive K.A., Yokoyama J. // Phys. Rev. D. – 1999. – V. 59. – 103503, 54 p.
- [47] Nojiri S. Dark energy, inflation and dark matter from modified  $F(R)$  gravity / Nojiri S., Odintsov S.D. // E Print arXiv.org: 0807.0685.
- [48] Witt B. Fourth-order gravity as general relativity plus matter / Witt B. // Phys. Lett. B. – 1984. – V. 145. – P. 176–178.
- [49] Muller V. The stability of the de Sitter space-time in fourth order gravity / Muller V., Schmidt H.J., Starobinsky A.A. // Phys. Lett. B. – 1988. – V. 202. – P. 198–200.
- [50] Maeda K. Towards the Einstein-Hilbert action via conformal transformation // Phys. Rev. D. – 1989. – V. 39. – P. 3159–3162.
- [51] Kaneda S. Fourth-order gravity as the inflationary model revisited / Kaneda S., Ketov S.V., Watanabe N. // Mod. Phys. Lett. A. – 2010. – V. 25. – P. 2753–2762.
- [52] Kaneda S. Slow-roll inflation in  $(R + R^4)$  gravity / Kaneda S., Ketov S.V., Watanabe N. // Class. Quantum Grav. – 2010. – V. 27. – 145016, 12 p.

- [53] Starobinsky A.A. A new type of isotropic cosmological model without singularity / Starobinsky A.A. // Phys. Lett. B. – 1980. – V. 91. – 99, 4 p.
- [54] Saidov T.  $1/R$  multidimensional gravity with form-fields: Stabilization of extra dimensions, cosmic acceleration, and domain walls / Saidov T., Zhuk. A. // Phys. Rev. D. – 2007. – V. 75. – 084037, 10 p.
- [55] Carroll S.M. The Cosmology of Generalized Modified Gravity Models / Carroll S.M., De Felice A., Duvvuri V., Easson D.A., Trodden M., Turner M.S. // Phys.Rev. D. – 2005. – V. 71. – 063513, 27 p.
- [56] Ellis J. Topological  $R^4$  Inflation / Ellis J., Kaloper N., Olive K.A., Yokoyama J. // J. Phys. Rev. D. – 1999. – V. 59. – 103503, 25 p.
- [57] Gunther U. Asymptotical AdS from non-linear gravitational models with stabilized extra dimensions / Gunther U., Moniz P., Zhuk A. // Phys. Rev. D. – 2002. – V. 66. – 044014, 12 p.
- [58] Gunther U. Nonlinear multidimensional cosmological models with form fields: stabilization of extra dimensions and the cosmological constant problem / Gunther U., Moniz P., Zhuk A. // Phys. Rev. D. – 2003. – V. 68. – 044010, 21 p.
- [59] Saidov T. AdS Nonlinear Curvature-Squared and Curvature-Quartic Multidimensional (D=8) Gravitational Models with Stabilized Extra Dimensions / Saidov T., Zhuk. A. // Gravitation and Cosmology. – 2006. – V. 12. – P. 253–261.
- [60] Bronnikov K.A. Abilities of multidimensional gravity / Bronnikov K.A., Rubin S.G. // Grav. and Cosmol. – 2007. – V. 13. – 253, 6 p.
- [61] Saidov T. Problem of inflation in nonlinear multidimensional cosmological models / Saidov T., Zhuk A. // Phys. Rev. D. – 2009. – V. 79. – 024025, 18 p.
- [62] Arkani-Hamed N. Phenomenology, Astrophysics and Cosmology of Theories with Sub-Millimeter Dimensions and TeV Scale Quantum Gravity /

- Arkani-Hamed N., Dimopoulos S., Dvali G. // Phys. Rev. D. – 1999. – V. 59. – 086004, 52 p.
- [63] Gunther U. Multidimensional cosmological models: cosmological and astrophysical implications and constraints / Gunther U., Starobinsky A., Zhuk A. // Phys. Rev. D. – 2004. – V. 69. – 044003, 16 p.
- [64] Srianand R. Aracil B. Limits on the time variation of the electromagnetic fine-structure constant in the low energy limit from absorption lines in the spectra of distant quasars / Srianand R., Chand H., Petitjean P., Aracil B. // Phys. Rev. Lett. – 2004. – V. 92. – 121302, 4 p.
- [65] Hannestad S. Possible Constraints on the Time Variation of the Fine Structure Constant from Cosmic Microwave Background Data / Hannestad S. // Phys. Rev. D. – 1999. – V. 60. – 023515, 5 p.
- [66] Kaplinghat M. Constraining Variations in the Fine-Structure Constant with the Cosmic Microwave Background / Kaplinghat M., Scherrer R.J., Turner M.S. // Phys. Rev. D. – 1999. – V. 60. – 023516, 9 p.
- [67] Webb J.K. Further Evidence for Cosmological Evolution of the Fine Structure Constant / Webb J.K. // Phys. Rev. Lett. – 2001. – V. 87. – 091301, 5 p.
- [68] Ivashchuk V.D. On Wheeler-De Witt equation in multidimensional cosmology / Ivashchuk V.D., Melnikov V.N., Zhuk A.I. // Nuovo Cimento B. – 1989. – V. 104. – P. 575–582.
- [69] Rainer M. Tensor-multi-scalar theories from multidimensional cosmology / Rainer M., Zhuk A. // Phys. Rev. D. – 1996. – V. 54. – P. 6186–6192.
- [70] Capozziello S. Quintessence without scalar field / Capozziello S., Carloni S., Troisi A. // Recent Res. Dev. Astron. Astrophys. – 2003. – V. 1. – 625, 46 p.

- [71] Carrol S.M. Is Cosmic Speed-Up Due to New Gravitational Physics? / Carrol S.M., Duvvuri V., Trodden M., Turner M.S. // Phys. Rev. D. – 2004. – V. 70. – 043528, 4 p.
- [72] Vollick D.N.  $1/R$  Curvature Corrections as the Source of the Cosmological Acceleration / Vollick D.N. // Phys. Rev. D. – 2003. – V. 68. – 063510, 7 p.
- [73] Dick R. On the Newtonian Limit in Gravity Models with Inverse Powers of  $R$  / Dick R. // Gen. Rel. Grav. – 2004. – V. 36. – 217, 8 p.
- [74] Dolgov A.D. Can modified gravity explain accelerated cosmic expansion? / Dolgov A.D., Kawasaki M. // Phys. Lett. B. – 2003. – V. 573. – P. 1–4.
- [75] Nojiri S. Modified gravity with negative and positive powers of the curvature: unification of the inflation and of the cosmic acceleration / Nojiri S., Odintsov S.D. // Phys. Rev. D. – 2003. – V. 68. – 123512, 23 p.
- [76] Nojiri S. Modified gravity with  $\ln R$  terms and cosmic acceleration / Nojiri S., Odintsov S.D. // Gen. Rel. Grav. – 2004. – V. 36. – P. 1765–1780.
- [77] Chiba T.  $1/R$  gravity and Scalar-Tensor Gravity / Chiba T. // Phys. Lett. B. – 2003. – V. 575, 4 p.
- [78] Meng X. Modified Friedmann Equations in  $R^{-1}$ -Modified Gravity / Meng X., Wang P. // Class. Quant. Grav. – 2003. – V. 20. – P. 4949–4962.
- [79] Gunther U. Multidimensional Cosmology and Asymptotical AdS / Gunther U., Moniz P., Zhuk A. // Astrophysics and Space Science. – 2003. – V. 283. – P. 679–684.
- [80] Freund P.G.O. Dynamics of dimensional reduction / Freund P.G.O., Rubin M.A. // Phys. Lett. B. – 1980. – V. 97. – P. 233–235.
- [81] Gunther U. Multidimensional perfect fluid cosmology with stable compactified internal dimensions / Gunther U., Zhuk A. // Class. Quant. Grav. – 1998. – V. 15. – 2025, 10 p.

- [82] Ivashchuk V.D. Billiard Representation for Multidimensional Cosmology with Multicomponent Perfect Fluid near the Singularity / Ivashchuk V.D., Melnikov V.N. // *Class. Quant. Grav.* – 1995. – V. 12. – 809, 16 p.
- [83] Zhuk A. Integrable scalar field multi-dimensional cosmologies / Zhuk A. // *Class. Quant. Grav.* – 1996. – V. 13. – 2163, 17 p.
- [84] Bousso R. Quantization of Four-form Fluxes and Dynamical Neutralization of the Cosmological Constant / Bousso R., Polchinski J. // *JHEP.* – 2000. – V. 006. – 0006, 30 p.
- [85] Schwartz-Perlov D. Probabilities in the Bousso-Polchinski multiverse / Schwartz-Perlov D., Vilenkin A. // *JCAP.* – 2006. – V. 010. – 0606, 22 p.
- [86] Zhuk A. Conventional cosmology from multidimensional models / Zhuk A. // E Print arXiv.org: hep-th/0609126.
- [87] Linde A. Monopoles as big as a universe / Linde A. // *Phys. Lett. B.* – 1994. – V. 327. – P. 208–213.
- [88] Vilenkin A. Topological inflation / Vilenkin A. // *Phys. Rev. Lett.* – 1994. – V. 72. – P. 3137–3140.
- [89] Sakai N. Dynamics of Topological Defects and Inflation / Sakai N., Shinkai H., Tachizawa T., Maeda K. // *Phys.Rev. D.* – 1996. – V. 53. – 655, 15 p.
- [90] Hindawi A. Higher-Derivative Gravitation and a New Mechanism for Supersymmetry Breaking in Four-Dimensions / Hindawi A., Ovrut B.A., Waldram D. // *Prog. Theor. Phys. Suppl.* – 1996. – V. 123. – P. 397–410.
- [91] Kiritsis E. On  $R^4$  threshold corrections in IIB string theory and (p,q) string instantons / Kiritsis E., Pioline B. // *Nucl. Phys. B.* – 1997. – V. 508. – P. 509–534.
- [92] Green M.B. One loop in eleven dimensions / Green M.B., Gutperle M., Vanhove P. // *Phys. Lett. B.* – 1997. – V. 409. – P. 177–184.



- [93] Bachas C.P. Curvature terms in D-brane actions and their M-theory origin / Bachas C.P., Bain P., Green M.B. // JHEP. – 1999. – V. 011. – 9905, 32 p.
- [94] Nojiri S. Finite gravitational action for higher derivative and stringy gravities / Nojiri S., Odintsov S. // Phys. Rev. D. – 2000. – V. 62. – 064018, 21 p.
- [95] Zhuk A. Restrictions on dilatonic brane-world models / Zhuk A. // Int. Journ. Mod. Phys. D. – 2002. – V. 11. – 1399, 10 p.
- [96] Baukh V. Sp-brane accelerating cosmologies / Baukh V., Zhuk A. // Phys. Rev. D. – 2006. – V. 73. – 104016, 17 p.
- [97] Rubakov V.A. Large and infinite extra dimensions / Rubakov V.A. // Phys. Usp. – 2001. – V. 44. – P. 871–893.
- [98] Appelquist T. Bounds on Universal Extra Dimensions / Appelquist T. , Cheng H.C., Dobrescu B.A. // Phys.Rev. D. – 2001. – V. 64. – 035002, 22 p.
- [99] Ponton E. Casimir Energy and Radius Stabilization in Five and Six Dimensional Orbifolds / Ponton E., Poppitz E. // JHEP. – 2011. – V. 019. – 0106, 38 p.
- [100] Cheng H.C. Schmaltz M. Radiative Corrections to Kaluza-Klein Masses / Cheng H.C., Matchev K.T., // Phys. Rev. D. – 2002. – V. 66. – 036005, 33 p.
- [101] Servant G. Is the Lightest Kaluza-Klein Particle a Viable Dark Matter Candidate? / Servant G., Tait T.M.P. // Nucl.Phys. B. – 2003. – V. 650. – 391, 32 p.
- [102] Bergstrom L. Gamma Rays from Kaluza-Klein Dark Matter / Bergstrom L., Bringmann T., Eriksson M., Gustafsson M. // Phys. Rev. Lett. – 2005. – V. 94. – 131301, 14 p.

- [103] Townsend P.K. Four lectures on M-theory / Townsend P.K. // E Print arXiv.org: hep-th/9612121.
- [104] Moffat J.W. M-theory on a supermanifold / Moffat J.W. // E Print arXiv.org: hep-th/0111225.
- [105] Kundu A. Universal Extra Dimension / Kundu A. // E Print arXiv.org: 0806.3815.
- [106] Ratra B. Cosmological consequences of a rolling homogeneous scalar field / Ratra B., Peebles P.J. // Phys. Rev. D. – 1988. – V. 37. – P. 3406–3427.
- [107] Ellis G.F.R. Exact scalar field cosmologies / Ellis G.F.R., Madsen M.S. // Class. Quant. Grav. – 1991. – V. 8. – 667, 11 p.
- [108] Ratra B. Inflation in an exponential-potential scalar field model / Ratra B. // Phys. Rev. D. – 1992. – V. 45. – P. 1913–1952.
- [109] Stornaiolo C. Cosmological fluids with general equations of state / Stornaiolo C. // Phys. Let. A. – 1994. – V. 189. – P. 351–360.
- [110] Gunther U. Gravitational excitons from extra dimensions / Gunther U., Zhuk A. // Phys. Rev. D. – 1997. – V. 56. – 6391, 20 p.
- [111] Arkani-Hamed N. Stabilization of Sub-Millimeter Dimensions: The New Guise of the Hierarchy Problem / Arkani-Hamed N., Dimopoulos S., March-Russell J. // Phys.Rev. D. – 2001. – V. 63. – 064020, 30 p.
- [112] Cho Y.M. Dilatonic dark matter and unified cosmology: a new paradigm / Cho Y.M., Keum Y.Y. // Class. Quant. Grav. – 1998. – V. 15. – 907, 16 p.
- [113] Cho Y.M. Dilaton as a Dark Matter Candidate and its Detection / Cho Y.M., Kim J.H. // Phys. Rev. D. – 2009. – V. 79. – 023504, 23 p.
- [114] Martin J. The precision of slow-roll predictions for the CMBR anisotropies / Martin J., Schwarz D. // Phys. Rev. D. – 2000. – V. 62. – 103520, 15 p.

- [115] Gunther U. Stabilization of internal spaces in multidimensional cosmology / Gunther U., Zhuk A. // Phys. Rev. D. – 2000. – V. 61. – 124001, 11 p.
- [116] Deruelle N. "Detuned"  $f(R)$  gravity and dark energy / Deruelle N., Sasaki M., Sendouda Y. // Phys. Rev. D. – 2008. – V. 77. – 124024, 10 p.
- [117] Nakamura T.T. The spectrum of cosmological perturbations produced by a multi-component inflaton to second order in the slow-roll approximation / Nakamura T.T., Stewart E.D. // Phys. Lett. B. – 1996. – V. 381. – P. 413–419.
- [118] Gong J.O. The Power Spectrum for a Multi-Component Inflaton to Second-Order Corrections in the Slow-Roll Expansion / Gong J.O., Stewart E.D. // Phys. Lett. B. – 2002. – V. 538. – P. 213–222.
- [119] Nibbelink S.G. Density perturbations arising from multiple field slow-roll inflation / Nibbelink S.G., Tent B.J.W. // E Print arXiv.org: hep-ph/0011325v2.
- [120] Kallosh R. SuperCosmology / Kallosh R., Prokushkin S. // E Print arXiv.org: hep-th/0403060.
- [121] Lyth D.H. Particle Physics Models of Inflation and the Cosmological Density Perturbation / Lyth D.H., Riotto A. // Phys. Rept. – 1999. – V. 314, 155 p.
- [122] Efstathiou G. The Lyth Bound Revisited / Efstathiou G., Mack K.J. // JCAP. – 2005. – V. 008. – 0505, 8 p.
- [123] Peiris H.V. Primordial Black Holes, Eternal Inflation, and the Inflationary Parameter Space after WMAP5 / Peiris H.V., Easter R. // JCAP. – 2008. – V. 024. – 0807, 24 p.
- [124] Bronnikov K.A. Abilities of multidimensional gravity / Bronnikov K.A., Rubin S.G. // Grav and Cosmol. – 2007. – V. 13. – 253, 6 p.

- [125] Linde A. Monopoles as Big as a Universe / Linde A. // Phys. Lett. B. – 1994. – V. 327. – P. 208–213.
- [126] Vilenkin A. Topological Inflation / Vilenkin A. // Phys.Rev.Lett. – 1994. – V. 72. – P. 3137–3140.
- [127] Liddle A.R. The Cold Dark Matter Density Perturbation / Liddle A.R., Lyth D.H. // Phys. Rept. – 1993. – V. 231, 105 p.
- [128] Barenboim G. About a (standard model) universe dominated by the right matter / Barenboim G., Vives O. // Phys. Rev. D. – 2009. – V. 79. – 033007, 15 p.
- [129] Frolov A.V. A Singularity Problem with  $f(R)$  Dark Energy / Frolov A.V. // Phys. Rev. Lett. – 2008. – V. 101. – 061103, 5 p.
- [130] Coleman S. Gravitational effects on and of vacuum decay / Coleman S., De Luccia F. // Phys. Rev. D. – 1980. – V. 21. – P. 3305–3315.
- [131] Cai Y. A Model Of Inflationary Cosmology Without Singularity / Cai Y., Qiu T., Xia J., Zhang X. // Phys. Rev. D. – 2009. – V. 79. – 021303, 4 p.
- [132] Paul B.C. Singular instantons in higher derivative theories / Paul B.C., Mukherjee S., Tavakol R.K. // Phys. Rev. D. – 2002. – V. 65. – 064020, 14 p.
- [133] Biswas T. Bouncing Universe in string-inspired gravity / Biswas T., Mazumdar A., Siegel W. // JCAP. – 2006. – V. 009. – 0603, 28 p.
- [134] Lyth D.H. Large-scale energy-density perturbations and inflation / Lyth D.H. // Phys. Rev. D. – 1985. – V. 31. – P. 1792–1798.

## ACKNOWLEDGMENT

First of all, I would like to thank my parents, especially my mother, who instilled in me a love for science.

With my greatest pleasure I would like to thank my supervisor Prof. Alexander Ivanovich Zhuk, who has opened for me the multidimensional cosmology, for his strong support in the research, fruitful discussions and many of very interesting walk tours we had around Sevastopol and Odessa. His capability for elegant solutions in very complex theoretical tasks will always amaze me.

I would like to address my warmest gratitude to professors of the Department of Theoretical Physics ONU: Prof. V.M. Adamyan, Prof. N.P. Malomuzh and Prof. A.V. Zatovskiy, Dr. V.P. Olyiynik, Dr. M.Ya. Sushko and Dr. V.L. Kulinskiy; their lectures allowed me to enter the world of theoretical physics.

Then I like to thank my **T**eacher of physics (deserving capital T) Vadim Leonidovich Manakin, whose impact on my life is impossible to overestimate. There are people gifted with ability to kindle a passion to knowledge and science. I was lucky to meet such a person - Vadim Leonidovich.

And last, but definitely not least, I would like to acknowledge my close friend Volodymyr Volodymyrovych Nemertsalov for his great help in preparation of promotion ceremony.

Thank you all!

## CURRICULUM VITAE

Tamerlan Adamovich Saidov was born in Grozny (Chechen Republic) in October 1, 1982. In 1999 he graduated with the certificate of merit the Riche-lieu Lyceum (Department of Chemistry and Biology) in Odessa, Ukraine.

In 2003 he received the Bachelor degree in Theoretical Physics with Excellence at the Faculty of Physics (Department of Theoretical Physics) of the Odessa I.I. Mechnikov National University (Odessa, Ukraine). The study of the bachelor report was focused on Navier-Stokes equations in cylindrical coordinates.

In period of 2003 - 2004, Tamerlan Saidov has obtained the Master degree in Theoretical Physics with Excellence at the same department. The work of the master program was dedicated to the properties of fermions fields in models of charged leptons, and was performed under supervision of Dr. V.P. Olyiynik.

Simultaneously with studying of physics, in 2005 Tamerlan Saidov graduated the Faculty of Economy and Law (Department of Administrative Law) of Odessa I.I. Mechnikov National University (Odessa, Ukraine) and received Master degree in Law. The master thesis was written on the administrative right and obligations with the focus on the specifics of their origin and prosecuting.

In the period of 2004 - 2008, Tamerlan Saidov was appointed as phd-student at the Department of Theoretical Physics of the Odessa I.I. Mechnikov National University (Odessa, Ukraine), where under the supervision of Prof. A.I. Zhuk, he has undertaken the theoretical study on multidimensional cosmology: the compactification of extra dimensions and accelerated expansion of the Universe. The results of this work are described in this Thesis.

Starting from 2007 to 2011, he did his second phd-research, in the Department of Applied Physics of Eindhoven University of Technology (Eindhoven, The Netherlands). Where under the supervision of Dr. L. Pel, the crystallization and ion transport of salts was studied in porous media by Nuclear

Magnetic Resonance technique.

From 2011, Tamerlan Saidov is working on the cancer detection by contrast ultrasound imaging in the Signals Processing Systems group at the Department of Electrical Engineering of Eindhoven University of Technology (Eindhoven, The Netherlands).